
Electronic Thesis and Dissertation Repository

11-2-2022 1:00 PM

Tracing the Fate of Cytokeratin 19+ Cells During Beta Cell Regeneration Stimulated by Multipotent Stromal Cell-Secreted Effectors

Nazihah Rasiwala, *The University of Western Ontario*

Supervisor: Hess, David A., *The University of Western Ontario*

A thesis submitted in partial fulfillment of the requirements for the Master of Science degree in Physiology and Pharmacology

© Nazihah Rasiwala 2022

Follow this and additional works at: <https://ir.lib.uwo.ca/etd>



Part of the [Cell Biology Commons](#)

Recommended Citation

Rasiwala, Nazihah, "Tracing the Fate of Cytokeratin 19+ Cells During Beta Cell Regeneration Stimulated by Multipotent Stromal Cell-Secreted Effectors" (2022). *Electronic Thesis and Dissertation Repository*. 8944. <https://ir.lib.uwo.ca/etd/8944>

This Dissertation/Thesis is brought to you for free and open access by Scholarship@Western. It has been accepted for inclusion in Electronic Thesis and Dissertation Repository by an authorized administrator of Scholarship@Western. For more information, please contact wlsadmin@uwo.ca.

Abstract

Human bone marrow-derived multipotent stromal cells expanded under Wnt pathway stimulation (Wnt+) secrete beta cell-regenerative factors that can be collected as conditioned media (CdM). Herein, we used the cytokeratin 19 (CK19)-CreERT Rosa26-mTomato lineage tracing mouse to observe CK19+ cell conversion to insulin+ beta cells following intra-pancreatic injection of Wnt+ CdM. 8-week-old mice were given tamoxifen to label CK19+ ductal and acinar cells with fluorescent reporter tdTomato and STZ to induce hyperglycemia. Injection of Wnt+ CdM increased beta cell mass and islet number in the pancreas, reduced non-fasted blood glucose levels, and improved glucose tolerance over a 28-day period compared to controls. Flow cytometry on dissociated pancreas tissue revealed insulin+/tdTomato+ cells were increased in mice given Wnt+ CdM, suggesting a small percentage (<5%) of regenerated beta cells originated from CK19+ ductal or acinar cells. Our results suggest CK19+ cells showed a minor contribution to Wnt+ CdM-induced beta cell regeneration.

Keywords

Diabetes, Multipotent Stromal Cell, Beta Cell Regeneration, Beta Cell Progenitor, Cytokeratin 19, Pancreatic Ductal Cell, Lineage Tracing

Summary for Lay Audience

Diabetes mellitus is characterized by a loss of insulin-producing beta cells that reside in the pancreatic islets of Langerhans resulting in high blood glucose levels, or hyperglycemia. Residual beta cell function has been found in patients living with diabetes for over 50 years. Thus, the induction of beta cell regeneration may be a promising approach to replenish lost beta cells in individuals with diabetes. Multipotent stromal cells (MSC), isolated from human bone marrow, secrete a mixture of proteins that can aid in repairing and regenerating damaged cells. Pro-regenerative factors released by MSC in the lab can be collected as conditioned media and can be used to regenerate beta cells that were destroyed during diabetes. Our lab has previously shown that direct injection of conditioned media collected from MSC into the pancreas of hyperglycemic mice induced beta cell regeneration and lowered blood glucose levels. The mechanism by which MSC conditioned media stimulated beta cell regeneration was unclear, although new beta cells formed adjacent to pancreatic ductal structures.

We hypothesized that pancreatic ducts contain precursor or parent cells that can be activated to form new beta cells. Thus, the goal of this project was to track the offspring of pancreatic ductal cells during beta cell regeneration stimulated by MSC conditioned media. To achieve this goal, we used a 'lineage tracing' mouse model that permanently labelled ductal cells and their offspring with a red fluorescent tag. Hyperglycemic mice that were intrapancreatic-injected with MSC conditioned media showed reduced blood glucose levels and an improved ability to regulate a glucose meal compared to control mice not given conditioned media. The pancreas of mice treated with MSC conditioned media had an increased number of beta cells compared to controls, indicating islet regeneration had occurred. A small percentage of these beta cells were labelled with the red tag, suggesting some newly formed beta cells may have originated from a ductal cell. By documenting the role of pancreatic ductal cells during beta cell regeneration, the work outlined in this thesis has contributed to the development of cell-free and protein-based regenerative therapies for diabetes.

Co-Authorship Statement

The following thesis contains material from a manuscript in preparation co-authored by Nazihah Rasiwala, Brianna Ananthan, Charlette James, Gillian Bell, and Dr. David Hess.

Nazihah Rasiwala performed all experimental work and data analysis/interpretation presented in this thesis in the lab of Dr. David Hess. Gillian Bell and Brianna Ananthan assisted with technique training, experimental conceptualization, and animal care. Charlette James assisted with immunofluorescence imaging and image quantification for islet-duct association and EdU+ beta cell analyses. Dr. David Hess contributed to the design and interpretation of all experiments included in this thesis.

Acknowledgments

First of all, I would like to thank Dr. David Hess for all of your support and guidance as my mentor during the 2 years of my Master's degree. Thank you for seeing my potential. I was an undergraduate student with no prior experience and it's safe to say that you have helped excel my abilities as a researcher and a scientist far beyond what I had ever thought possible. Thank you for believing in me and helping to propelling my career forward. The lessons I have learned from you are invaluable.

Thank you to Gillian Bell and Brianna Ananthan for your assistance with training and animal care. You both made me feel welcome to the lab during a time with so much uncertainty and gave me the confidence to start my path as a graduate researcher. Thank you to Kristin Chadwick at the London Regional Flow Cytometry Facility for assistance with running the flow cytometer and flow cytometric data analysis. Thank you to Stephanie Milkovich at the London Regional Microscopy Facility for training and assistance with confocal microscopy.

Thank you to Drs. David Hill, Samuel Asfaha, and Andrew Watson for serving as the members of my Advisory Committee. I am grateful for your expertise and recommendations that enhanced the quality and depth of my research project.

Thank you to all the past and previous members of the Hess lab for being the best teammates and lending your support over the last 2 years. A special thanks to Yehia Moharrem and Fiona Serack for teaching me how to be a better scientist, and providing me with advice and motivation whenever I needed it.

Finally, thank you to my family, friends, and my partner John for your tremendous amounts of support and love throughout my graduate school journey. I couldn't have been successful without all of you by my side.

Table of Contents

Abstract.....	ii
Summary for Lay Audience.....	iii
Co-Authorship Statement.....	iv
Acknowledgments	v
Table of Contents	vi
List of Tables	x
List of Figures	xi
List of Abbreviations	xiii
List of Appendices	xvi
1.0 Introduction.....	1
1.1 Diabetes Mellitus.....	1
1.1.1 Diabetes Epidemiology and Etiology	1
1.1.2 Diabetes Pathology	2
1.1.3 Current Diabetes Treatments	3
1.2 Approaches to Restore Pancreatic Beta Cells.....	5
1.2.1 Beta Cell Replacement	5
1.2.2 Beta Cell Regeneration	7
1.3 Multipotent Stromal Cells.....	12
1.3.1 MSC Function and Therapeutic Potential.....	12
1.3.3 Wnt Pathway Upregulation in BM-MSc	19
1.4 Beta Cell Progenitors in the Pancreas	21
1.4.1 Pancreatic Plasticity during Development and Metabolic Challenge	22
1.4.2 Beta Cell Replication.....	23
1.4.3 Alpha-to-Beta Cell Conversion	23

1.4.4	Acinar-to-Beta Cell Conversion	25
1.4.5	A Resident Progenitor Located in the Ductal Epithelium	25
1.4.6	Rare Pancreatic Populations with Progenitor-like Characteristics	27
1.5	Rationale and Project Overview	32
1.6	Hypothesis and Objectives	33
2.0	Materials and Methods	34
2.1	BM-MSC Culture and Conditioned Media Collection	34
2.1.1	Primary BM-MSC Isolation	34
2.1.2	Preparation of BM-MSC Conditioned Media	34
2.2	Flow Cytometry on BM-MSC	35
2.2.1	Cell Surface Marker Analysis	35
2.2.2	Total Intracellular Beta-Catenin Analysis	35
2.3	BM-MSC Nuclear Beta-Catenin Quantification	36
2.4	Mouse Treatments and Monitoring	37
2.4.1	CK19-CreERT Rosa26-mTomato Model	37
2.4.2	Tamoxifen Dose Optimization	37
2.4.3	Streptozotocin (STZ) Dose Optimization	37
2.4.4	Intrapancreatic (iPAN) injection of CdM and Lineage Tracing Experiments	38
2.4.5	EdU Injections	38
2.4.6	Insulin Treatments	39
2.4.7	Glucose Tolerance Test (GTT)	39
2.5	Flow Cytometry on Pancreas Tissue	39
2.6	Immunohistochemistry and Immunofluorescence Microscopy	39
2.6.1	Pancreas Tissue Preparation and Sectioning	39

2.6.2 Immunohistochemistry (IHC) for Beta Cell Mass and Islet Number Quantification.....	40
2.6.3 Immunofluorescence (IF) Staining, Imaging, and Quantification.....	40
2.7 Statistical Analysis	41
3.0 Results.....	42
3.1 Treatment with CHIR99021 increased nuclear beta-catenin levels and did not alter BM-MSC cell surface phenotype.	42
3.2 Tamoxifen administration in CK19-CreERT Rosa26-mTomato mice resulted in dose-dependent labelling of CK19+ pancreatic ductal cells.	44
3.3 STZ treatment of 50 mg/kg/day for 5 days resulted in hyperglycemia, glucose intolerance, and decreased beta cell mass.	48
3.4 iPAN injection of Wnt+ CdM preserved beta cell mass and islet number, but did not significantly reduce hyperglycemia 11 days following injection.	52
3.5 iPAN injection of Wnt+ CdM increased tdTomato and insulin co-expression at Day 21.....	54
3.6 Regenerated insulin+ cells of STZ-treated mice iPAN-injected with CdM were devoid of a high side-scatter population.	59
3.7 iPAN injection of Wnt+ CdM followed by a 7-day insulin treatment regimen did not improve hyperglycemia, glucose tolerance, or beta cell mass.	61
3.8 iPAN injection of Wnt+ CdM reduced hyperglycemia and improved glucose tolerance over a 28-day period.	64
3.9 Increased insulin+ cell labelling with tdTomato observed at Day 21 following iPAN injection of Wnt+ and Untreated CdM is decreased by Day 42.....	68
3.10 Regenerated tdTomato+/insulin+ cells may have originated from tdTomato+ ductal, acinar, or beta cells.	71
3.11 iPAN injection of CdM did not alter islet-duct association or the frequency of islets with CK19+ cells.	73
3.12 Islets from mice treated with Wnt+ CdM and Untreated CdM demonstrated improved beta cell/alpha cell ratio.	76
3.13 Treatment with STZ followed by Wnt+ CdM delivery increased levels of beta cell proliferation compared to healthy mice.	76
4.0 Discussion	79

4.1 Summary of Findings.....	79
4.2 Wnt+ CdM delivery in hyperglycemic mice preserved beta cell mass at Day 21, although did not lower hyperglycemia.	80
4.3 Insulin treatment following iPAN injection of Wnt+ CdM did not permit enhanced beta cell regeneration.....	81
4.4 Wnt pathway stimulation of BM-MSc may be involved in improved glucose homeostasis.....	82
4.5 Differences in glycemia reduction were discerned in female mice, but not male mice, treated with Wnt+ CdM once analyzed separately.	83
4.6 Increased beta cell mass following Wnt+ CdM delivery may be confounded by regeneration occurring as a result of STZ-mediated beta cell ablation.	84
4.7 Wnt+ CdM-stimulated beta cell regeneration in CK19-CreERT Rosa26-mTomato mice was not as strong as in the NOD/SCID model.....	85
4.8 Tamoxifen administration in CK19-CreERT Rosa26-mTomato lineage tracing mice resulted the labelling of pancreatic ductal, acinar, and beta cells.....	87
4.9 Pancreatic ductal cells as the origin of regenerated beta cells?	89
4.10 Other mechanisms of Wnt+ CdM-induced beta cell regeneration may be at play.....	92
4.11 Limitations	93
4.12 Significance.....	95
References.....	96
Appendices	115
Appendix 1. Supplementary Figures	115
Appendix 2. Human Ethics Approval.....	116
Appendix 3. Animal Ethics Approval	117
Curriculum Vitae	118

List of Tables

Table 1.1. Summary of lineage tracing studies investigating various pancreatic cell types and their conversion to beta cells in the adult mouse pancreas.	30
Table 2.1. Antibody specifications for flow cytometry experiments.	36
Table 2.2. Antibody specifications for IHC/IF staining.....	41
Table 3.1. The frequency of cells that co-expressed tdTomato and insulin was increased in mice injected with Wnt+ CdM compared to basal media.	57
Table 3.2. Frequencies of cells that co-expressed tdTomato, insulin, and glucagon remained consistent following treatment with 12 mg of tamoxifen in healthy citric acid buffer (CAB) control mice.....	58

List of Figures

Figure 1.1. Overview of the pleiotropic mechanisms by which BM-MSC can treat T1DM and T2DM.....	14
Figure 1.2. Overview of BM-MSC “signal-receiving” cells in the pancreas and their progression towards regenerating beta cells.....	29
Figure 1.3. Overview of BM-MSC derived Wnt+ CdM-induced beta cell regeneration from a CK19+ ductal cell origin.....	33
Figure 2.1. Generation of concentrated Wnt+ and Untreated CdM from BM-MSC.....	35
Figure 2.2. STZ dose optimization timeline.....	38
Figure 3.1. CHIR-treated MSC upregulated beta-catenin and retained expression of stromal cell markers.....	43
Figure 3.2. Tamoxifen treatment (12 mg) in CK19-CreERT Rosa26-mTomato mice increased the proportion of tdTomato+/CK19+ cells.....	46
Figure 3.3. tdTomato expression was observed in pancreatic acinar and beta cells following tamoxifen treatment.....	47
Figure 3.4. STZ treatment (50 and 60 mg/kg/day for 5 days) in CK19-CreERT Rosa26-mTomato mice resulted in hyperglycemia (≥ 12 mmol/L) by Day 14.....	50
Figure 3.5. Beta cell mass and islet number were reduced in CK19-CreERT Rosa26-mTomato mice treated with STZ at Day 14.....	51
Figure 3.6. Beta cell mass and islet number were preserved following iPAN injection of Wnt+ CdM.....	53
Figure 3.7. tdTomato co-expression with insulin was increased following iPAN injection of Wnt+ CdM.....	56

Figure 3.8. High side scatter insulin+ cells were depleted in STZ- and CdM-treated mice compared to healthy CAB control mice.	60
Figure 3.9. Glucose levels and beta cell mass were unchanged following iPAN injection of CdM and 7-day treatment with insulin.	63
Figure 3.10. iPAN injection of Wnt+ CdM decreased non-fasted blood glucose levels and improved glucose tolerance at Day 42.	66
Figure 3.11. iPAN injection of Wnt+ CdM did not change beta cell mass or insulin+ islet number at Day 42.	67
Figure 3.12. iPAN injection of Wnt+ and Untreated CdM increased the frequency of tdTomato+/insulin+ co-expressing cells at Day 21.....	70
Figure 3.13. Three mechanisms were traced in CK19-CreERT Rosa26-mTomato mice.	73
Figure 3.14. Islet-duct association and islets with CK19+ cells were not changed following iPAN injection of Wnt+ CdM.	75
Figure 3.15. The beta cell/alpha cell ratio of islets at Day 21 was increased in mice iPAN-injected with Wnt+ and Untreated CdM.	77
Figure 3.16. The frequency of proliferating beta cells at Day 17 was not changed following iPAN injection of Wnt+ CdM.	78

List of Abbreviations

AD – Adipose

Arx – Aristaless-related homeobox

AUC – Area under the curve

BM – Bone marrow

BMI – Body mass index

CAII – Carbonic anhydrase II

CAB – Citric acid buffer

CD – Cluster of differentiation

CdM – Conditioned media

CK19 – Cytokeratin 19

Cre – Cre recombinase

DYRK1A – Dual-specificity tyrosine-regulated kinase 1A

EdU – 5-Ethynyl-2'-deoxyuridine

EGF – Epidermal growth factor

ELISA – Enzyme-linked immunosorbent assay

ERT – Tamoxifen-inducible estrogen ligand-binding domain

FoxO1 or FoxA2 – Forkhead box protein O1 or A2

GABA – Gamma-aminobutyric acid

GCG – Glucagon

GFP – Green fluorescent protein

GLP-1 – Glucagon-like peptide 1

GLUT2 or GLUT4 – Glucose transporter 2 or 4

GSK3 – Glycogen synthase kinase-3

GTT – Glucose tolerance test

HbA1c – Hemoglobin A1c (glycated hemoglobin)

hESC – Human embryonic stem cell

HLA-DR – Human leukocyte antigen-DR isotype

IDO – Indoleamine 2,3-dioxygenase

IF – Immunofluorescence

IFIH1 – Interferon induced with helicase C domain 1

IHC – Immunohistochemistry

IL2RA – Interleukin 2 receptor A

IL – Interleukin

INS – Insulin

i.p. – Intraperitoneal

iPAN – Intra-pancreatic

iPSC – Induced pluripotent stem cell

ISCT – International Society for Cell and Gene Therapy

i.v. – Intravenous

MafA – MAF BZIP Transcription Factor A

MafB – MAF BZIP Transcription Factor B

MHC – Major histocompatibility complex

M.F.I. – Mean fluorescence intensity

MSC – "Multipotent stromal cell" or "Mesenchymal stem cell"

NFBG – Non-fasted blood glucose

Ngn3 – Neurogenin 3

NOD/SCID – Non-obese diabetic/severe combined immunodeficiency

Pax4 – Paired box 4

PDL – Pancreatic ductal ligation

Pdx1 – Pancreatic and duodenal homeobox 1

Procr – Protein C receptor

Px – Pancreatectomy

SD – Standard deviation

Sox9 – Sex-determining region Y-box 9

SST – Somatostatin

STZ – Streptozotocin

T1DM – Type 1 diabetes mellitus

T2DM – Type 2 diabetes mellitus

tdT – tdTomato

TGF-beta – Transforming growth factor beta

TIMP-1 – Tissue inhibitors of matrix metalloproteinase 1

UC – Umbilical cord

Ucn3 – Urocortin 3

Wnt+ – Wnt pathway stimulated

List of Appendices

Appendix 1. Supplementary Figures	115
Appendix 2. Human Ethics Approval	116
Appendix 3. Animal Ethics Approval	117

1.0 Introduction

1.1 Diabetes Mellitus

Diabetes mellitus (DM) is a group of metabolic disorders characterized by a loss of blood glucose homeostasis resulting in hyperglycemia¹. Type 1 diabetes mellitus (T1DM) is a chronic, autoimmune disorder caused by T-cell mediated destruction of insulin-producing beta cells in the pancreas. Type 2 diabetes mellitus (T2DM) involves diminishing insulin secretion by pancreatic beta cells and is often a consequence of insulin resistance, the inability of peripheral tissues to respond to insulin and uptake glucose². Gestational DM, defined as glucose intolerance diagnosed during pregnancy, is the third general category of DM. Women diagnosed with gestational diabetes may be at risk for developing T2DM and are recommended to receive life-long screening³. Other forms of diabetes mellitus arise from pathologies distinct from T1DM and T2DM, such as cystic fibrosis-related DM, post-transplantation DM, and monogenic disorders that result in beta cell dysfunction (ex. maturity-onset diabetes of the young)³.

1.1.1 Diabetes Epidemiology and Etiology

Diabetes is considered a global epidemic. As of March 2022, it was estimated that there were 11.7 million individuals living with diabetes or prediabetes in Canada⁴. Diabetes is costly to both the person suffering from the disease and the health care system. In 2019, diabetes-related treatments costed the Canadian health care system just under \$30 billion⁵. Seventy percent of individuals in Ontario that have diabetes report they are burdened by their health care bills and 1/3 pay out-of-pocket for their required medications⁵, costs that could prevent adherence to prescribed treatments. In 2018, it was estimated that individuals with T1DM diagnosed prior to 10 years of age had a decreased life expectancy of 16 years and those diagnosed after 20 years of age had a decreased life expectancy of about 10 years⁶.

Diabetes represents an accelerating, “silent” epidemic driven primarily by increases in T2DM cases, although rates of T1DM are also steadily climbing.

Epidemiological studies from multiple countries have reported an increase in the prevalence and incidence of T1DM in their young over the past 2 decades⁷⁻¹⁰. Amongst youths aged 19 or younger in the United States, the relative increases in T1DM and T2DM prevalence from 2001 to 2017 were 45.1% and 95.3% respectively¹¹.

Genetic and environmental factors interact to play a role in the development of both T1DM and T2DM. T1DM is associated with inheritance of the human leukocyte antigen (HLA)-DR3/4 genotype¹². Other predispositions include genetic mutations in the HLA-B39, insulin, interleukin 2 receptor A (IL2RA), and interferon induced with helicase C domain 1 (IFIH1) loci¹³. Environmental factors such as diet during infancy and childhood¹⁴, human enteroviruses¹⁵, and socioeconomic status⁹ have also been correlated with T1DM incidence. These environmental stressors may accelerate the onset of disease in those with a genetic predisposition. It is generally accepted that the primary risks for developing T2DM are environmental and lifestyle factors such as energy-dense diets, lack of exercise, sleep quality, and socioeconomic status¹⁶. Interestingly, genome-wide association studies of multiple populations have linked 250 genetic loci to predisposition for T2DM¹⁷. One report of 336 individuals with genetic predispositions to T2DM or obesity found that, irrespective of obesity, genetic predisposition for T2DM was associated with abnormal expansion of adipose cell volume and a more pro-atherogenic lipid profile in lean individuals (BMI<25 kg/m²)¹⁸. Thus, the interplay of genetics and the environment engender the complexity of T1DM and T2DM etiology.

1.1.2 Diabetes Pathology

Pancreatic beta cells, the primary cell type that comprises about 70% of the islet of Langerhans, are involved in regulating post-prandial glucose homeostasis via secretion of the hormone insulin. Following a meal, blood glucose levels rise and this increase is 'sensed' by glucose transporter 1 (GLUT1) on the membrane of beta cells¹⁹. Beta cells then release insulin into the circulation to allow for the uptake and utilization of glucose by peripheral tissues like skeletal muscle and adipose. During periods of fasting or low glucose levels, alpha cells, the second most common cells inhabiting about 20% of the islet, release glucagon that signals to the liver to release glucose from glycogen stores.

Both T1DM and T2DM result in the loss of pancreatic beta cells. In T1DM, autoimmune attack results in a decline of beta cell function and mass over time². Beta cell-specific antigens are presented on dendritic cells and autoantibodies are produced causing T-lymphocyte activation and infiltration into the islets of Langerhans, a process known as insulinitis²⁰. A combination of cytotoxic T-lymphocyte-mediated cell death and prolonged exposure to inflammatory cytokines produced by infiltrating leukocytes and islet cells leads to the destruction of beta cells by apoptosis or necrosis^{21,22}. In T2DM, insulin resistance and hyperglycemia lead to increased insulin demand and functional beta cell compensation, leading to beta cell stress, de-differentiation, and increased beta cell death^{2,23}. In both disorders, the depletion of pancreatic beta cells causes insulin deficiency, producing constantly elevated blood glucose levels or hyperglycemia.

Sustained hyperglycemia can have serious consequences for individuals with diabetes. Elevated blood glucose levels lead to increased protein kinase C-dependent activation of NADPH oxidase and the production of hydroxyl radicals in vascular smooth muscle and endothelial cells, resulting in endothelial damage and vascular complications^{24,25}. Acute complications of diabetes include diabetic ketoacidosis and non-ketonic hyperosmolar coma, and chronic complications include coronary and peripheral artery disease, diabetic neuropathy, and diabetic retinopathy²⁶. Long-standing diabetes is also a risk factor for cognitive decline in later life²⁷. North America, Europe, and high-income Asia-Pacific countries have seen a downward trend in the prevalence of diabetic comorbidities, although, having diabetes still poses a significantly higher risk for developing these complications compared to those without diabetes²⁸. One study of a Swedish cohort including 7409 patients with T1DM diagnosed between 0 and 10 years old found, compared to age-matched controls, patients had hazard ratios of 11.44 for cardiovascular disease, 30.50 for coronary heart disease, and 12.90 for heart failure⁶.

1.1.3 Current Diabetes Treatments

In 1921, breakthrough research done by Drs. Frederick Banting and Charles Best led to the discovery of insulin, the 51-amino acid peptide hormone secreted by pancreatic beta cells²⁹. The administration of exogenous insulin was transformative for diabetes care

and allowed survival of the previously fatal disease. Nowadays insulin is the cornerstone of diabetes treatment as all T1DM patients and most late-stage T2DM patients require insulin therapy to lower their blood glucose levels. Those in the earlier stages of T2DM can control their hyperglycemia with exercise and diet and have other therapeutic options targeted at increasing insulin release (ex. sulfonylureas) and enhancing peripheral insulin sensitivity (ex. biguanides)³⁰. Additionally, sodium glucose co-transporter 2 inhibitors and glucagon-like peptide 1 receptor agonists are new classes of drugs that increase renal excretion of glucose, and increase glucose-dependent insulin secretion and reduce food intake, respectively³⁰. These novel glucose-lowering agents have changed the landscape of T2DM treatment and can improve the cardiovascular health of T2DM patients³¹.

There have been many advancements in insulin therapy since its inception in 1921, such as the development of ultralong basal insulin analogues, glucose-responsive insulin systems, and insulin patch-pump systems³². Although improvements in insulin formulations and delivery modalities have improved T1DM care, patients still have a heightened risk for the complications mentioned above^{6,33}. Data from the T1D Exchange Registry collected from 2016 to 2018 reported only 17% of youths and 21% of adults achieved hemoglobin A1c (HbA1c) goals set by the American Diabetes Association, with an increase in mean HbA1c levels seen in the 2016-2018 cohort compared to the 2010-2012 cohort³⁴. This indicates that glycemic control had not improved in the Registry cohort over time despite a substantial increase in the proportion of participants using continuous glucose monitoring. Accordingly, diabetic ketoacidosis was still common amongst participants less than 26 years old and severe hypoglycemia was most frequent in participants greater than 50 years old³⁴.

Exogenous insulin therapy, especially with the use of an insulin pump, can extend the lives of individuals with T1DM and lower the risk of complications, although glucose variability is unremitting in diabetes patients and has been linked to a lower quality of life³². Diabetes management should encompass quality of life, overall health and well-being, and a reduced burden of disease. Thus, a curative therapy for diabetes is still required given the diverse challenges faced by affected individuals.

1.2 Approaches to Restore Pancreatic Beta Cells

The optimal treatment for T1DM would eliminate the immense burden of disease and stress faced by patients due to the constant monitoring their blood glucose levels. To replicate the fine-tuned glucose-sensing insulin secretory mechanism that has evolved in pancreatic beta cells is a technological feat³². Hence replenishing or replacing human beta cells themselves is the best approach to treat diabetes.

1.2.1 Beta Cell Replacement

The Edmonton protocol for islet transplantation, published in 2000 by Shapiro and colleagues, involved infusing human islets from cadaveric donor pancreata into the portal vein of the liver of T1DM patients³⁵. The islets lodged in the portal sinusoidal capillaries and secreted insulin in response to glucose. The initial 7 Edmonton protocol patients received 2 separate infusions for a cumulative islet mass of over 11 000 islet equivalents per kg. The transplant corrected HbA1c levels and patients were insulin independent for over 1 year with sustained C-peptide production³⁵. All patients encountered side effects associated with the immunosuppressive regimen required to prevent rejection of the transplanted islets. A 5-year follow-up of the 7 patients showed 80% had persistent C-peptide secretion although only 10% remained insulin independent, possibly due to auto- or allo-immune destruction and/or poor long-term engraftment of the transplanted islets³⁶. An international trial of the Edmonton protocol on 36 patients demonstrated 21% of patients reached insulin independence at 1 year post-infusion and this dropped to 13% by the 2-year follow up³⁷. Progress in islet preparation as well as improvements in anti-inflammatory interventions have been made, however a recent report from the Collaborative Islet Transplant Registry showed 73% of 1300 allogenic islet recipients required reinfusion of islets at an average of 13 ± 22 months, only 50% of patients were insulin independent at 1-year following their last infusion, and prevalence of insulin independence steadily declined over 5-years of follow-up³⁸. Lastly, up to 4 donor pancreata were needed per recipient, therefore the shortage of donor islets currently limits the widespread use of this procedure.

In 1998, Thompson et al. propagated the inner cell mass of a human blastocyst on a mouse embryonic fibroblast feeder layer with plasma components, synthetic fetal bovine serum, and fibroblast growth factor to establish the first known human embryonic stem cell (hESC) line³⁹. hESC are pluripotent stem cells that can differentiate into any specialized cell type of the 3 germ layers. In 2008, Takahashi and Yamanaka discovered that the ectopic expression of 4 transcription factors, Oct3/4, Klf4, Sox2, and c-Myc, in terminally differentiated adult cells can reprogram them to a pluripotent state, thus rendering these transformed cells induced pluripotent stem cells (iPSC)⁴⁰. The advent of hESC and iPSC technologies started a revolution of cell replacement therapies and *in vitro* modelling strategies for various human disorders.

Initial stepwise differentiation protocols to derive insulin-producing cells from pluripotent stem cells were generated based on cellular signalling in the embryonic pancreas^{41,42} and have been refined since to produce functional beta cells with the ability to attenuate hyperglycemia following transplantation into mice^{43,44}. Most protocols still result in a heterogeneous mix of beta-like, alpha-like, and enterochromaffin-like endocrine cells as well as a heterogeneous population of Sox9+ ductal cells⁴⁵, although groups are currently working on deriving islets from hESC or iPSC that closely resemble the composition, cytoarchitecture, and cellular metabolism of human islets^{46,47}.

In 2014, ViacYTE led the first in-human clinical trial involving hESC-derived pancreatic endoderm progenitor cells macro-encapsulated in a semi-permeable, immune-protective device that was implanted subcutaneously for the treatment of T1DM. The trial endpoint was not reached and was terminated due to a fibrotic host response to the graft and the inability of the cells to survive in the device⁴⁸. In 2017, a second trial by ViaCyte was launched to improve pancreatic progenitor engraftment and survival using a non-immune-protective encapsulation device that allowed for direct access from host vasculature⁴⁹. Stimulated C-peptide was detected in 35% of participants, although most patients did not have a greater than 50% reduction in insulin requirements and none of the participants achieved insulin independence^{50,51}. Upon explanting the devices, there was vast heterogeneity in the pancreatic cell types detected and the endocrine cell population was enriched for glucagon+ cells that were not insulin+⁵¹. Last year, Vertex

Pharmaceuticals launched a clinical trial for their curative T1DM therapy, VX-880, involving portal vein infusion of hESC-derived fully differentiated islets. Preliminary results from 2 patients given half the target dose were released. Patient 1 was insulin independent and had 99.9% time-in-range for blood glucose at 270 days post-infusion and patient 2 had 51.9% time-in-range for blood glucose with 30% reduced insulin use at 150 days post-infusion⁵². While these initial results look promising, there are clear hurdles to overcome with stem cell-based beta cell replacement therapies and the cost and accessibility of these therapies is unknown. Thus, the search for a safe and renewable source of beta cells remains an active area of vigorous research.

1.2.2 Beta Cell Regeneration

In 2010, the Joslin 50-Year Medalist Study was conducted using a cohort of 411 T1DM patients that have been managing their diabetes by taking insulin for over 50 years. A shocking finding was that 67.4% of participants had residual C-peptide secretion⁵³. Histological analysis of post-mortem pancreata obtained from 9 T1DM patients with varying C-peptide production showed small clusters of insulin+ cells in all patients⁵³. More recent evidence provided by Lam et al. in a study of 47 T1DM pancreata showed 64% of T1DM pancreata had residual beta cells located within islet clusters and a few samples from both recent-onset and long-standing T1DM individuals had wide-spread insulin+ islets⁵⁴. This supports the concept that, even after >50 years of autoimmune attack, beta cells can be replenished by endogenous processes.

Direct evidence of beta cell regeneration has been provided in each of the following rodent models of pancreatic damage: (1) partial pancreatectomy (surgical removal of 50-90% of the pancreas; Px), (2) pancreatic ductal ligation (surgical ligation of the main pancreatic duct that results in obstructive pancreatitis; PDL), and (3) specific ablation of beta cells using cytotoxic glucose analogs streptozotocin or alloxan.

1.2.2.1 Pancreatectomy (Px)

Px in adult rodents has shown that the pancreas has the capacity to regenerate entire lobes via cellular replication and neogenesis. In studies of 90% Px in rats, the

pancreas remnant demonstrated upregulated beta cell and exocrine cell proliferation from 7-14 days following surgery⁵⁵ and increased endocrine hormone content 8-10 weeks following surgery⁵⁶. Mice that underwent a 40% Px and were subsequently treated with parathyroid hormone-related protein showed transiently improved glucose tolerance and increased beta cell mass and proliferation compared to untreated mice⁵⁷. Long-acting glucagon-like peptide 1 (GLP-1) agonist exendin-4 lowered blood glucose, improved glucose tolerance, increased beta cell mass following 90-95% Px in 4-5 week old rats⁵⁸. Treatment with gastrin following 95% Px in rats has also shown to induce beta cell regeneration⁵⁹, although this was lost by 12 months of age⁶⁰. Therefore, beta cell regeneration can be aptly studied following partial or near total loss of pancreatic content.

1.2.2.2 Pancreatic Ductal Ligation (PDL)

PDL serves as a beneficial model to study regeneration since injury is limited to the portion of the pancreas distal to the ligation, allowing for the proximal portion to serve as an internal control. Pioneering work done by Wang et al. in 1995 found that regeneration of beta and alpha cells was pronounced following PDL in rats, and could not be accounted for by beta cell proliferation alone⁶¹. Rather, an increased number of insulin+ cell clusters and single insulin+ cells suggested that a neogenic mechanism of regeneration from a non-beta cell may have occurred⁶¹. In the decades following, other groups have provided evidence of beta cell regeneration from resident progenitor cells using PDL⁶²⁻⁶⁴. Hao et al. found that one week following extreme beta cell ablation induced by PDL and alloxan treatment in adolescent mice, reversal of ligation led to regeneration of both exocrine and endocrine tissue⁶⁵. Islet cells co-expressed alpha and beta cell markers early on but not at late timepoints that showed a large increase in beta cell proliferation following reversal of PDL⁶⁵. In contrast Cavelti-Welder et al. found extensive regeneration of the exocrine pancreas with no evidence of beta cell regeneration in adult rats that underwent PDL and treatment with streptozotocin (STZ)⁶⁶. Beta cell and islet frequencies remained low both 5 and 10 months following PDL and STZ with no distinct increase in small, extra-islet clusters of endocrine cells⁶⁶ indicating reversal of PDL may be crucial to investigating beta cell regenerative processes.

1.2.2.3 Chemical Ablation

Streptozotocin (STZ) and alloxan are structurally similar to glucose and are able to specifically accumulate in and ablate beta cells via selective uptake by the GLUT2 glucose transporter⁶⁷. Depending on the dose administered, a partial or near absolute loss of beta cells can be obtained, resulting in varying levels of hyperglycemia. Thus, the amount of regeneration seen in this model is affected by the extent of beta cell damage elicited by a given dose of STZ or alloxan. Adaptive beta cell proliferation has been seen in mice and rats following both multiple low doses and a single high dose of STZ^{68–72}, although similar to partial Px, this regenerative response was diminished in older animals^{69,70}. Treatment with alloxan in adult rodents has shown to stimulate endocrine regeneration within 2 weeks^{73,74}. When long-term glycemic control was provided, either via insulin therapy or islet transplantation, beta cell regeneration in mice following high dose STZ treatment was more robust⁷⁵.

1.2.2.4 Beta Cell Regeneration in Humans

While rodent models of beta cell regeneration are vital for deciphering underlying mechanisms, studying regeneration in adult humans is critical for the development of regenerative medicines. Physiological increases in beta cell mass that occur during pregnancy and obesity exhibit the capacity for adult human islets to regenerate via beta cell proliferation and/or neogenesis^{76–79}. Neogenesis from ductal cells has been proposed as a mechanism of beta cell regeneration in humans. Insulin+ ductal cells have been observed in obese individuals⁸⁰ and ductal cells displaying immature beta cell markers were detected in pregnant women and in individuals with T2DM⁷⁶, indicating neogenesis may serve as a compensatory mechanism to expand beta cell mass in humans.

There is a decline in the rate of beta cell proliferation following the first 2 years of life in humans, however a pool of proliferating beta cells can persist into adulthood at a frequency below 0.5% in healthy individuals⁸¹. Mature beta cells are thought to be post-mitotic and unable to replicate, although it is possible cyclins and cyclin-dependent kinases are localized to the cytoplasm rather than the nucleus of the cell and have the potential for nuclear re-location, allowing the cells to initiate cell cycle entry⁸². In 2001,

Tyrberg et al. provided evidence that 3H-thymidine was incorporated in transplanted adult human islets and proliferation, indicated by the percentage of 3H-thymidine-labelled cells, was increased 1.7-fold in beta and 2.2-fold in ductal cells upon transplantation into hyperglycemic obese mice compared to lean mice⁸³, indicating regeneration via increased proliferation is possible in human beta cells.

In a study of 47 T1DM pancreata, Lam et al. found that children with T1DM had beta cell proliferation rates of up to 1.33%, significantly higher than that of the age-matched control population, whereas this percentage dropped to 0-0.08% in adults with T1DM, significantly lower than the control population⁵⁴. A study of 10 recent onset T1DM pancreata showed a marked increase in the percentage of proliferating alpha and beta cells compared to controls and proliferating cells were increased in islets with insulinitis⁸⁴. Thus, if diagnosed with T1DM early enough, beta cell regeneration could be stimulated and may counteract beta cell destruction.

Px is used for the treatment of pancreatic cancer or pancreatitis, thus tissue samples from patients that have undergone Px can be used to study regeneration in humans. It has been reported that young children and infants demonstrate regeneration of the pancreas head and body following 90-95% Px⁸⁵. One study of individuals with pancreatitis or pancreatic carcinoma that had undergone partial Px on two separate occasions showed no changes in beta cell area, islets per mm², or the percentage of proliferating beta and ductal cells⁸⁶. The study concluded that regeneration following Px does not occur in adult humans, although the patients' underlying disease could have affected the capacity for regeneration.

1.2.2.5 Agents to Induce Beta Cell Regeneration

Various stimuli have been evaluated for their anti-diabetic and beta cell-regenerative potential. Many plant based extracts such as that of *Opuntia megacantha* leaves⁸⁷, *Spergularia purpurea*⁸⁸, *Agaricus bisporus* lectins⁸⁹, *Coccinia grandis*⁹⁰ and *Momordica charantia* fruits⁹¹ have been tested for glucose-lowering capability, as a proxy for endogenous beta cell recovery, following pancreatic damage in rodents. Mangiferin is a plant xanthonoid that has been shown to improve fasting blood glucose and glucose

tolerance, and to stimulate increased beta cell volume in mice that underwent Px^{92,93}. Pseudo-pregnant mice given exogenous estrogen and placental lactogen have shown to recapitulate pregnancy-induced beta cell replication⁷⁷, although hormonal mechanisms inducing cell proliferation should be rigorously assessed for off-target tumorigenic effects.

Beta cell replication has been increased to frequencies of 2% in adult human islets by inhibiting dual-specificity tyrosine-regulated kinase 1A (DYRK1A) using harmine and harmine analogs alone^{94–96} or in combination with transforming growth factor-beta (TGF-beta) signalling inhibitors,^{97,98} 5-iodotubercidin⁹⁹, or aminopyrazine compounds¹⁰⁰. Recently, Ackeifi et al. showed that combining harmine and GLP-1 increased the proportion of replicating beta cells to 5-8%¹⁰¹. The combination of harmine with GLP-1 yielded two unique advantages: (1) a higher frequency of beta cell replication that is required to restore the large portion of beta cells lost during diabetes, and (2) a specified target for increased replication as beta cells express the GLP-1 receptor¹⁰¹.

Beta cell differentiation via direct reprogramming from an endocrine cell precursor within the islets has been shown in rodent models. For example, mice treated with gamma-aminobutyric acid (GABA) for 2 months showed robust alpha-to-beta cell conversion, regenerating beta cells lost during STZ treatment¹⁰². One-week treatment with epidermal growth factor (EGF) and gastrin delivered via mini-osmotic pumps stimulated beta cell regeneration, possibly via neogenesis from a ductal origin, in alloxan-treated mice¹⁰³. Transient expression of Pdx1, MafA, and Ngn3, delivered to the pancreas of 8-week-old adult mice, resulted in stable conversion of pancreatic exocrine cells to insulin-producing cells over a 10-day period¹⁰⁴. Altogether, induction of differentiation from related cell types may provide an additional source of beta cells.

Whether these agents will proceed to clinical trials, pass safety regulations with minimal off-target effects, and be able to induce regeneration substantial enough to out-compete ongoing autoimmune-mediated beta cell destruction or insulin resistance-induced beta cell exhaustion remains unknown. Achieving endogenous beta cell regeneration in diabetes patients will require dampening autoimmunity or increasing insulin sensitivity combined with provision of a potent stimulus for regeneration.

1.3 Multipotent Stromal Cells

Multipotent stromal cells (MSC), also known as mesenchymal stem cells, are mesodermal progenitor cells found amongst the perivascular population of several tissues¹⁰⁵. In Dominici et al., the International Society for Cell and Gene Therapy (ISCT) define MSC as having 3 distinct characteristics: (1) MSC grow adherent to plastic in culture, (2) MSC express the stromal markers CD73 (ecto-5'-nucleotidase), CD90 (Thy-1), and CD105 (endoglin) on at least 95% of cells and express hematopoietic markers CD45, CD34, CD14 or CD11b, CD79a or CD19, and HLA-DR on less than 2% of cells, and (3) MSC have the potential to differentiate into bone, cartilage, and fat *in vitro*¹⁰⁶. MSC can be prospectively isolated from the stromal fraction of multiple tissues using the pericyte marker CD146. Once expanded *ex-vivo*, MSC upregulate CD105, CD73, and CD90 and, unlike pericytes, are able to differentiate into osteoblasts, chondrocytes, adipocytes, and myocytes¹⁰⁵. Recently, lineage tracing and single-cell RNA sequencing have revealed MSC are diverse in phenotype and function and distinct types of MSC exist even within the same tissue¹⁰⁷. The work done in this thesis studies human bone marrow-derived MSC (BM-MSC)^{108,109}, which meet the criteria outlined by the ISCT.

1.3.1 MSC Function and Therapeutic Potential

MSC have the potential to differentiate into various mesenchymal lineages, although this is only relevant to a few tissues like bone, fat, and cartilage that already possess lineage-committed progenitors. The expansive clinical applications of MSC originate from their ability to modulate the local tissue environment via paracrine signalling of a diverse set of bioactive stimuli¹⁰⁷. Multifaceted actions on tissue regeneration, immunomodulation, stem and progenitor cell differentiation, innervation, and vascularization have been demonstrated by MSC *in vivo*¹¹⁰. MSC act as the “paramedics of the body”¹⁰⁷ and their perivascular location is advantageous for rapidly sensing and homing to areas of tissue damage to coordinate a reparative response. MSC response will depend on type of damage, pre-existing inflammatory state, and the regenerative capacity of the tissue.

The excitement for MSC as a therapeutic cell type is generated by their potential to modulate both innate and adaptive immune responses. An array of studies have shown that different types of MSC inhibit T- and B-cell proliferation, reduce inflammatory cytokine secretion, and promote differentiation into T-regulatory cells in the presence of inflammatory stimuli^{111–117}. MSC dampen innate immunity by inhibiting the maturation and antigen-presentation function of dendritic cells^{118,119}, and downregulating interferon production and cytotoxicity of natural killer cells¹²⁰. It is well known that MSC immunomodulatory action is elicited, in part, via the secretion of indoleamine 2,3-dioxygenase (IDO), prostaglandin E2, and TGF-beta and the cell surface expression of negative costimulatory molecule B7-H4^{114,117,120,121}.

According to the U.S. National Institute of Health ClinicalTrials.gov database, 416 clinical trials involving MSC have been recruiting, active, or completed from 2015 to 2022¹²². The majority of these trials were for brain and neurological disorders or diseases of the muscle, bone, and cartilage. These studies of MSC have shown a remarkable safety profile when transplanted in patients, although variability in the source, donor characteristics, expansion *ex-vivo*, and cryopreservation of these cells all limit the reported effectiveness of MSC-based therapies in the clinic¹²². Since MSC function via packaged and secreted cargo¹²³, MSC-derived exosomes have also been tested as a cell transplant-free option for regenerative therapies. MSC are currently under investigation for the treatment of a number of autoimmune diseases, including diabetes mellitus^{121,124,125}. The anti-inflammatory and regenerative properties of MSC may provide the ideal combination for endogenous beta cell recovery and insulin production in both T1DM and T2DM patients (Figure 1.1).

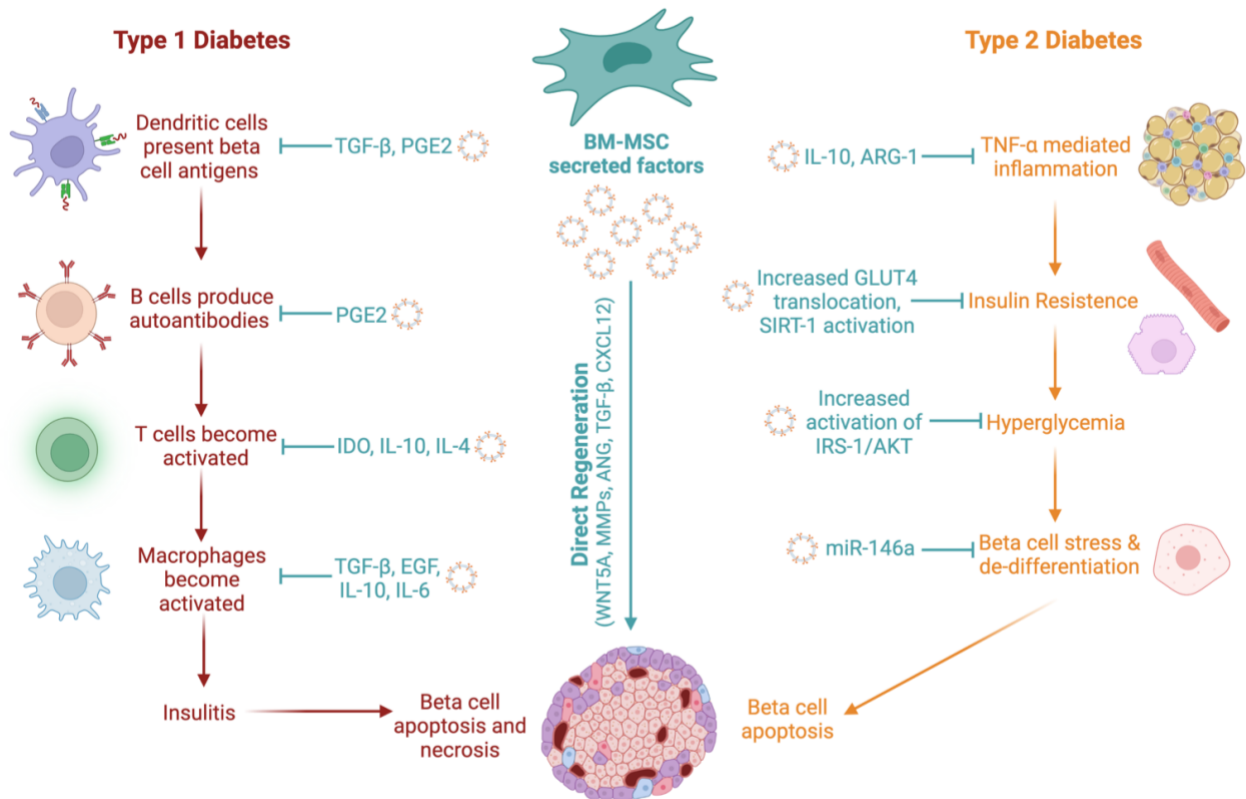


Figure 1.1. Overview of the pleiotropic mechanisms by which BM-MSC can treat T1DM and T2DM. In T1DM, autoimmune destruction of beta cells is mediated by multiple adaptive and innate immune cell types. In T2DM, hyperglycemia results from insulin resistance, which can be brought about by inflammation. Ultimately, an increased insulin demand leads to beta cell stress, de-differentiation, and apoptosis. BM-MSC secreted factors can: (1) dampen autoimmunity by inhibiting immune cell activation and pro-inflammatory cytokine secretion in T1DM; (2) can combat insulin resistance and hyperglycemia, and preserve beta cell identity in T2DM. Created with BioRender.com.

1.3.2 MSC for the Treatment of Diabetes

MSC have beneficial effects on beta cells *in vitro* and can ameliorate diabetes symptoms in both animals and humans. Early studies investigating MSC as a treatment for diabetes initially focused on manipulating the cells to differentiate into insulin-producing cells in culture prior to transplantation in STZ-treated mice. BM-MSC derived from humans and mice can be differentiated into insulin-producing cells that lower blood glucose when transplanted under the kidney capsule of hyperglycemic mice^{126,127}. Clear evidence on the maturity of MSC-derived beta cells was lacking and only up to 3% of MSC were capable of forming functional beta cells *in vivo*¹²⁸, thus their differentiation efficiency was limited compared to pluripotent stem cells. Upon the discovery that MSC function via paracrine signalling, co-culture studies of various types of MSC with beta cells demonstrated the ability of MSC to improve beta cell survival and insulin secretory function^{129–133}. Thus recent clinical trials using MSC for diabetes treatment focus on their ability to orchestrate tissue regeneration and dampen the host immune response (Figure 1.1) and investigation into MSC-derived beta cells as a treatment option for individuals with diabetes has receded.

1.3.2.1 Delivery of MSC in T1DM Models

Ground-breaking work done by Hess et al. in 2003 found that hyperglycemia in non-obese diabetic/severe combined immunodeficiency (NOD/SCID) mice treated with multiple low-dose STZ could be resolved by bone marrow transplantation. Specifically, sublethal irradiation of the mouse bone marrow followed by intravenous (i.v.) injection of green fluorescent protein (GFP)-labeled mouse bone marrow cells and isolated mouse c-kit⁺ hematopoietic stem/progenitor cells reduced blood glucose levels, increased serum insulin levels, and increased number of insulin⁺ islets over a one-month period¹³⁴. The transplanted GFP⁺ bone marrow cells surrounded islets to orchestrate pancreatic islet repair¹³⁴. These results were later recapitulated using cells with high aldehyde dehydrogenase activity from human bone marrow¹³⁵ and umbilical cord blood¹³⁶.

In 2006, Lee et al. found that 2 doses of 2.5 million human BM-MSC delivered via intracardiac infusion to NOD/SCID mice, previously treated with multiple low-dose STZ, reduced blood glucose, increased serum insulin, and increased islet number one month following transplantation¹³⁷. This indicated that the islet regeneration coordinated by whole bone marrow transplants in Hess et al. (2003) may be due to the actions of BM-MSC. Indeed, rat BM-MSC transplantation in combination with exendin-4, the long-acting GLP-1 agonist, normalized fasting blood glucose levels, increased beta cell mass and maturity, and restored beta cell function in STZ-treated Sprague Dawley rats over a one-month period¹³⁸. Furthermore, systemic delivery of human adipose-derived MSC (AD-MSC) lowered the incidence of anti-programmed cell death receptor ligand 1 antibody-induced diabetes male non-obese diabetic (NOD) mice¹³⁹. AD-MSC transplantation reduced blood glucose levels, preserved islet area and insulin content, and prevented CD3+ T cell and chemokine ligand 9+ macrophage accumulation in the islets¹³⁹.

In 2012, Bell et al. further established that tail vein injection human BM-MSC could ameliorate hyperglycemia, augment systemic insulin release, and increase beta cell mass and islet number over a 32-day period, although this regenerative induction showed bone marrow donor-dependent variability^{135,140}. Additionally, the i.v.-delivered MSC were difficult to locate in the pancreas¹³⁵, and subsequent studies have shown that MSC first engraft in the lung micro-vasculature when delivered systemically¹³⁹. It has been proposed that local delivery of MSC may improve survival and islet-regenerative function. Intra-pancreatic (iPAN) injection of 500 000 human AD-MSC further decreased blood glucose levels and islet number over a 30-day period in STZ-treated mice compared to i.v. injection of MSC¹⁴¹. iPAN transplantation of AD-MSC also increased transcription levels of anti-inflammatory cytokines epidermal growth factor and IL-10, but not pro-inflammatory cytokines IL-1beta or tumour necrosis factor-alpha in the pancreas¹⁴¹.

1.3.2.2 Delivery of MSC along with Islets

During islet transplantation, inflammation, poor engraftment, and sub-par vascularization can negatively affect islet cells such that they lose glucose responsiveness. It has been proposed that islet graft failure can be prevented by using

MSC to stimulate angiogenesis¹⁰⁸ and improve tissue engraftment^{131,132}. Co-culture of human BM-MSC with human islets improved glucose-induced insulin secretion and prevented apoptosis of islet beta cells in the presence of pro-inflammatory cytokines¹³². Transplantation of human AD-MSC with islets allowed for quicker blood glucose normalization and improved engraftment in STZ-treated immunodeficient mice compared to transplantation of islets alone¹³¹. Co-culture with MSC overexpressing tissue inhibitors of matrix metalloproteinase 1 (TIMP-1) increased cell viability and insulin secretion of normal and STZ-treated mouse islets. Infusion of 5 million umbilical cord-derived MSC (UC-MSC) overexpressing TIMP-1 also improved blood glucose levels and increased serum insulin over a 42-day period following tail vein injection into STZ-treated mice¹³⁰. In NOD mice that spontaneously develop autoimmune diabetes, co-encapsulation of UC-MSC and islet cells in sodium alginate reduced blood glucose levels and increased numbers of T regulatory cells¹⁴² and 8 injections of 1 million congenic mouse BM-MSC over 4 weeks reduced hyperglycemia over a 12 week period¹⁴³. Portal vein infusion of allogeneic islets along with autologous BM-MSC in STZ-treated cynomolgus monkeys showed that MSC co-transplantation enhanced islet engraftment, survival, and glucose-stimulated insulin release¹⁴⁴.

1.3.2.3 Delivery of MSC in T2DM Models

T2DM rodent models have been used to assess the effect of MSC on insulin resistance and insulin signalling. T2DM-like conditions can be induced in rats using a high-fat diet and STZ. I.v. infusion of MSC at 1-week and 3-weeks post-STZ injection lowered blood glucose for a 2-3 week period and protected islet architecture in T2DM-like rats¹⁴⁵. Furthermore, MSC treatment improved insulin sensitivity assessed via a hyperinsulinemic-euglycemic clamp, and restored membrane concentrations of GLUT4 in skeletal muscle and adipose tissue via activation of insulin receptor substrate 1¹⁴⁵. In line with these findings, exosomes collected from UC-MSC improved insulin sensitivity, promoted GLUT4 translocation in muscle tissue, and reduced STZ-induced beta cell apoptosis¹⁴⁶ and miR-146a+ exosomes from BM-MSC prevented diabetes-induced beta

cell dedifferentiation via Numb/beta-catenin signalling¹⁴⁷ in T2DM rodent models. Thus, MSC can halt multiple pathological processes underlying T2DM (Figure 1.1).

1.3.2.4 MSC Conditioned Media and Exosomes

Allogeneic MSC have shown to be relatively safe for transplantation, although they may still trigger an alloreactive response as MSC express varying levels of MHC class I molecules. From a clinical viewpoint, the use of conditioned media or exosomes collected from MSC as a cell-free alternative could circumvent complications associated with administering live allogeneic cells to patients¹⁴⁸. Conditioned media (CdM) can allow us to investigate the complex secretome of MSC and infusion of MSC CdM has shown to work just as well as the MSC themselves to modulate tissue repair. CdM generated from BM-MSCs increased the number of beta cells, proportion of live beta cells, and proportion of proliferating beta cells in human islet cultures¹⁴⁹. A meta-analysis of 20 islet and MSC co-culture studies found that viability and glucose responsiveness of islets were consistently improved when islets were co-cultured with MSC, although improvements in viability were higher for islets co-cultured indirectly with MSC rather than those in direct physical contact with MSC¹³³. Injection of rat BM-MSCs-derived exosomes showed effective glucose-lowering capability, equal to that of MSC themselves¹⁵⁰. Lastly, MSC native to the human pancreas (Panc-MSCs) can be isolated as vimentin+/nestin+ plastic adherent cells when culturing human islets. iPAN injection of concentrated CdM and isolated exosomes from Panc-MSCs reduced hyperglycemia over a month-long period in STZ-treated mice^{151,152}.

1.3.2.5 Clinical Trials of MSC-based Therapies for Diabetes

Meta-analyses of 8 MSC-based clinical trials for T1DM and 5 trials for T2DM over the last 10 years suggest that MSC have an islet-protective effect in T2DM but the extent of glycemic control achieved by MSC in T1DM patients remains inconsistent¹⁵³. The first randomized controlled trial using MSC to intervene early on in the course of T1DM was conducted by Carlsson et al. in 2015 in which 20 newly diagnosed (<3 weeks before enrollment) T1DM patients were given an i.v. injection of $2.1-3.6 \times 10^6$ BM-MSCs from

autologous bone marrow¹⁵⁴. Following transplantation, there were no differences in HbA1c levels, insulin requirements, and fasting and stimulated C-peptide measurements in the MSC-treated group compared to the placebo control¹⁵⁴. At the 1-year follow-up a mixed meal tolerance test showed a preserved or increased C-peptide response in MSC-treated patients compared to controls¹⁵⁴, suggesting that BM-MSC transplantation may preserve beta cell function in recent-onset T1DM patients.

Recently, the safety and efficacy of i.v. infusion of autologous BM-MSC was assessed in a trial of 21 recently diagnosed T1D patients¹⁵⁵. BM-MSC were isolated and expanded until passage 2 or 3 and delivered at 2 separate infusions of 1×10^6 cells per kg of body weight. No adverse events related to the MSC transplant were reported. Patients transplanted with MSC showed significantly lower numbers of hypoglycemic events and reduced HbA1c at 12 months post-transplant compared to placebo¹⁵⁵. No differences in fasting blood glucose levels, ability to lower glycemia following a meal, and requirements for exogenous insulin use were seen between MSC-transplanted and placebo participants. Lastly, BM-MSC transplantation significantly increased serum levels of anti-inflammatory cytokines IL-4 and IL-10 and reduced levels of pro-inflammatory marker tumour necrosis factor-alpha¹⁵⁵.

The first clinical study of portal vein infusion of islets along with autologous BM-MSC was conducted by Wang et al. in 2018. Three chronic pancreatitis patients underwent total pancreatectomy and subsequently received islet and MSC co-transplantation¹⁵⁶. During the 12 months following transplantation, the patients showed improved glycemic control and no direct adverse events associated with the therapy¹⁵⁶. Thus, infusion of autologous BM-MSCs during islet transplantation may have the potential to improve islet engraftment and glycemic control.

1.3.3 Wnt Pathway Upregulation in BM-MSC

MSC secrete a variety of growth factors, chemokines, and cytokines and the secretome of MSC appears to vary significantly, depending on the donor and niches where the cells reside^{149,151}. BM-MSC lines showed donor-dependent variability in their ability to induce islet regeneration in STZ-treated NOD/SCID mice^{135,157,158}. Studies from

our laboratory monitoring glucose levels for 42 days following multiple low-dose STZ injection and subsequent BM-MSC injection found that 25-33% of BM-MSC lines significantly reduced glycemia (highly regenerative), whereas 22-33% moderately reduced glycemia (moderately regenerative), and 42-44% did not reduce glycemia (non-regenerative)^{140,149}. Quantification of global mRNA expression of highly regenerative vs. non-regenerative BM-MSC found that highly regenerative BM-MSC upregulated transcription of canonical Wnt/beta-catenin signalling effectors¹⁴⁰, indicating this pathway was implicated in MSC-induced islet regeneration. Wnt/beta-catenin signalling in MSC has shown to promote cell proliferation and adhesion¹⁵⁹. Quantitative mass-spectrometry-based proteomics revealed that members of the Wnt signalling pathway, such as (Wnt1-inducible-signalling protein (WISP) 2, Wnt5a, Wnt5b, Spondin-2 and secreted frizzled-related protein 1, were upregulated in highly regenerative BM-MSC compared to non-regenerative BM-MSC^{149,158}, further confirming that activation of the Wnt pathway was central to BM-MSC regenerative function. BM-MSC lines can be accurately categorized as regenerative or non-regenerative by using proteomics to measure the relative secretion of Wnt signalling effectors¹⁵⁸.

The Wnt/beta-catenin signalling pathway can be upregulated in BM-MSC by the addition of glycogen synthase kinase-3 (GSK3)-inhibitor CHIR99021 to culture conditions¹⁴⁹. GSK3 is an intracellular kinase and is a part of the beta-catenin destruction complex that acts to phosphorylate beta-catenin and mark it for degradation¹⁶⁰. Inhibition of GSK3 allows the intracellular accumulation and nuclear translocation of beta-catenin resulting in the transcription of downstream Wnt pathway effectors. Compared to untreated BM-MSC, both regenerative and non-regenerative BM-MSC treated with CHIR99021 showed increased intracellular beta-catenin levels via flow cytometry¹⁴⁹. Moreover, BM-MSC expression of BCL9 and MYC, genes transcribed during active Wnt-signalling, was increased by treatment with CHIR99021¹⁶¹.

In 2019, Kuljanin et al. investigated the effect of intra-pancreatic (iPAN) injection of CdM from BM-MSC treated with CHIR99021 (Wnt+ CdM) in multiple low-dose STZ-treated NOD/SCID mice¹⁶¹. Compared to a basal media vehicle control, Wnt+ CdM consistently reduced non-fasted blood glucose levels, increased serum insulin levels, and

improved glucose tolerance in mice over 1 month post-CdM injection¹⁶¹. Furthermore, islet number, beta cell mass, and beta cell proliferation were increased in the pancreas of mice treated with Wnt+ CdM compared to controls. The proportion of beta cells expressing maturation markers Nkx6.1 and MafA was also increased after Wnt+ CdM injection¹⁶¹. This work demonstrated that Wnt+ CdM generated from BM-MSC could induce beta cell regeneration in a model of STZ-generated diabetes. However, the cellular mechanisms driving this beta cell regeneration remain uncharacterized to date.

1.4 Beta Cell Progenitors in the Pancreas

MSC modify their surrounding environment by signalling pro- or anti-apoptotic, proliferative, or differentiative factors to near-by cells. Communication with tissue-resident progenitor cells may also occur during times of damage when tissue repopulation and remodelling is required¹⁰⁷. Thus, the islet preservative and regenerative mechanisms conducted by BM-MSC in experimental models of T1DM and T2DM may occur via resident progenitor cell activation in the pancreas (Figure 1.2). Whether a non-insulin+ beta cell progenitor exists in the pancreas is a controversial query. Elegant genetic lineage tracing studies have allowed researchers in the field to trace various cell lineages in the pancreas and assess their contribution to other, distinct cell populations. Lineage tracing involves the permanent labelling of a specific cell type using the Cre recombinase/loxP system. Fusion of Cre recombinase (Cre) to the tamoxifen-inducible estrogen receptor (ERT) allows labelling in a spatially and temporally controlled manner. CreERT is knocked-in downstream of a cell type-specific promoter, and nuclear translocation permitting Cre-recombination can only occur upon administration of the estrogen receptor substrate tamoxifen. Cre-mediated removal of loxP sites surrounding a STOP codon downstream of a constitutively active promoter (ex. Rosa26) permanently labels cells and their progeny with a non-endogenous marker (ex. GFP or beta-galactosidase). Due to variability in experimental models and methodology of lineage tracing studies in the pancreas, the results to date have not converged on a prevailing hypothesis on the source of regenerated beta cells (Table 1.1).

Two competing viewpoints of the beta cell precursor debate are as follows^{162–164}: (1) Neogenesis/transdifferentiation: New beta cells are formed by differentiation from endocrine progenitor cells or direct conversion from a terminally differentiated non-insulin+ cell type. (2) Beta cell proliferation: Pre-existing beta cells undergo self-replication to form new beta cells. The field is slowly converging to the resolution that both proliferation and neogenesis contribute to the formation of new beta cells.

1.4.1 Pancreatic Plasticity during Development and Metabolic Challenge

The expansion of the embryonic pancreas occurs through a process called branching morphogenesis during E11.5-E13.5 in mice and 33-45 days post coitum in humans¹⁶⁵. During this process a tree-like epithelium undergoes successive rounds of cell division in a branching pattern, resulting in the lobular morphology of the pancreas containing both exocrine and endocrine compartments. The branching tree can be divided into the “trunk” cells that are Nkx6.1+/FoxA2+/Sox9+ and the branching “tip” cells that are Ptf1+/Cpa1+. The secondary transition of pancreatic specification occurs at E13.5-E16.5 in mice and 45-58 days post coitum in humans¹⁶⁵. Hnf1b+ trunk cells manifest a Hnf1b+/Sox9+/Hnf6+/CK19+ ductal fate controlled in part by high Notch signalling whereas an endocrine progenitor cell fate is determined via low Notch and the transient expression of Neurogenin 3 (Ngn3)¹⁶⁶. As endocrine cells acquire their specific fate, there is a gradual change towards cell type-specific gene expression profiles corresponding with the downregulation of Ngn3¹⁶⁷. For example, in rodents, Arx expression determines alpha and pancreatic polypeptide cell differentiation whereas Pax4 expression results in beta and delta cell specification^{168,169}. Until birth, Sox9+/Ptf1a+/Nkx6.1+/Hnf1b+ cells at the interface of the branching epithelium remains multipotent and can form cells of endocrine, acinar, and ductal lineages^{170,171}.

During post-natal development of the human pancreas, beta cell proliferation peaks within the first 2 years of life and then declines⁸¹. The notion that the adult pancreas has an extremely low turnover rate under physiological conditions^{81,172} and that only certain periods of high metabolic demand, like pregnancy or severe obesity, can expand beta cell mass¹⁷³ has now changed. Newer evidence has found that plasticity is retained

in the adult pancreas and disorders such as T1DM^{174–176}, and even viruses such as SARS-CoV-2¹⁷⁷, may result in dynamic changes in cell phenotypes.

1.4.2 Beta Cell Replication

Proponents of viewpoint that beta cell proliferation is the primary mechanism of beta cell expansion have not found any evidence for a source of beta cells other than pre-existing beta cells in adult mice under various conditions (Table 1.1). Furthermore, a stem-cell niche, such as those found in highly regenerative tissues like the intestinal tract or skin, has not yet been established in the adult pancreas¹⁷⁸.

In an early study tracing the progeny of beta cells using an insulin receptor (RIP)-CreERT model, Dor et al. found that the frequency of traced beta cells did not change during the course of 1 year of adult life nor after 70% Px. An increase in beta cell proliferation following Px indicated that regenerated beta cells were formed by self-duplication in this model¹⁷⁹. These findings were corroborated by Teta et al. who looked at DNA analog incorporation at a single-cell level and concluded that adult beta cell self-duplication was the only mechanism of beta cell expansion¹⁸⁰. Recently Zhao et al. used a dual-recombinase-mediated genetic lineage tracing system to trace insulin+ and insulin- cells simultaneously. They found that non-beta cells do not contribute to the beta cell population during adult homeostasis or pregnancy, and after STZ-induced beta cell ablation, Px, or PDL⁷⁸. Using the pulse-chase strategy done by Dor et al. with a super-efficiency tracing model (labels >99.9% of beta cells), they found the labelled beta cell population was not diluted by the contribution of non-beta cells over a 25-week period nor following Px, indicating that beta cell replication is the main source of beta cell regeneration. Only following extreme beta cell loss mediated by diphtheria toxin-mediated genetic ablation, were alpha and delta cells observed to regenerate new beta cells.⁷⁸.

1.4.3 Alpha-to-Beta Cell Conversion

Beta, alpha, delta, epsilon, and pancreatic polypeptide cells share a common Ngn3+ endocrine progenitor during development. These terminally differentiated cells may have similar transcriptomes and epigenetic patterns that would allow for plasticity

and transdifferentiation between related islet cell types¹⁸¹. In fact, treatment with a histone methyltransferase inhibitor in islet cultures resulted in the co-localization of glucagon and insulin¹⁸¹ and intraductal viral delivery of beta cell genes Pdx1 and MafA in alloxan-treated mice reversed hyperglycemia and allowed for alpha cell reprogramming into beta cells¹⁸². Ectopic Pax4 expression and Arx inactivation in alpha cells *in vivo* induced transdifferentiation into insulin+ cells^{168,169}. This conversion required the re-expression of developmental marker Ngn3 and lost alpha cell replacement seemed to occur from a ductal cell origin¹⁶⁸. It was later found that the alpha-to-beta transdifferentiation seen upon Arx inactivation was due to an upregulation of GABA signalling and GABA treatment in healthy and STZ-treated mice showed a dramatic increase in insulin+ cells originating from traced glucagon+ cells¹⁰². Islets from donors that had T1DM for 4-5 years showed glucagon+ cells that lacked Arx expression or displayed co-expression of beta cell markers such as Pdx1 and Nkx6.1¹⁷⁶, suggesting that alpha-to-beta cell conversion may occur following the loss of beta cells in T1DM.

Beta cell regeneration from an alpha cell origin has been traced in multiple models of beta cell ablation (Table 1.1). Lineage tracing of beta cells following diphtheria toxin-mediated ablation of over 99% of beta cells showed a 10-fold dilution of beta cell labelling as beta cell mass tripled. Subsequent glucagon+ cell tracing showed a 65% contribution of alpha cells to the regenerated beta cell population following 1 month¹⁸³. In a rodent model combining PDL and alloxan treatment, near complete ablation of beta cells permitted the investigation of putative neogenic mechanisms¹⁸⁴. Chung et al. discovered that 1 week following PDL + alloxan there was an increase in alpha cell replication and co-expression of beta cell markers. Further, an emergence of MafB+/insulin+ cells and insulin+ cells that co-expressed glucagon suggested that alpha-to-beta cell conversion may have occurred¹⁸⁴. This was later replicated in a rat model of STZ-induced beta cell ablation⁶⁸. Furthermore, alpha cells have contributed to beta cell regeneration during homeostasis via an intermediate immature beta cell stage that expresses insulin but not beta cell maturation marker urocortin 3 (Ucn3)¹⁸⁵. In human neonatal islets, Ucn3-negative beta cells are seen in between mature alpha and beta cells or at the islet

periphery. Residual Ucn3-negative beta cells are found in T1DM pancreata¹⁸⁵, although these cells could have either been regenerating or dedifferentiating beta cells.

1.4.4 Acinar-to-Beta Cell Conversion

The pancreas consists of >95% exocrine tissue and <5% endocrine tissue¹⁶⁶. In theory, if efficiency of conversion was equal in exocrine and endocrine cells, a larger number of beta cells could be derived from transdifferentiation of exocrine cells compared to that of the limited population of endocrine cells. Pancreatic acinar cells are abundant in the exocrine compartment of pancreas rendering them an attractive source of cells to replace lost beta cells (Figure 1.2). Indeed, acinar lineage tracing using the Ptf1a promoter showed that, following PDL alone or the combination of PDL and STZ, acinar cells gained expression of the multipotency factors Sox9 and Hnf1b and were able to regenerate ductal and endocrine cells, including mature insulin+ beta cells¹⁷¹.

In 2008, Zhou et al. first demonstrated acinar cells could be reprogrammed to beta cells, without an observable intermediate phenotype, upon viral delivery of beta cell genes Pdx1, MafA, and Ngn3 directly to the pancreas¹⁰⁴. The ectopic expression of the 3 genes recovered hyperglycemia in STZ-treated mice and induced beta cells were morphologically and phenotypically similar to non-induced beta cells¹⁰⁴. In a follow-up study conducted by Li et al., enhanced reprogramming efficiency using the same 3 genes allowed the regenerated beta cells to mature and form islet-like structures over a 13-month period via induction of an acinar-to-beta DNA methylation pattern, and suppression of acinar genes alongside expression of beta cell genes in a temporal manner¹⁸⁶. It was subsequently discovered that hyperglycemia had a negative effect on Pdx1/MafA/Ngn3-mediated reprogramming of acinar cells to beta cells as the frequency of induced beta cells during hyperglycemia dropped to half of that yielded during normoglycemia¹⁸⁷.

1.4.5 A Resident Progenitor Located in the Ductal Epithelium

Beta cell neogenesis from a ductal origin (Figure 1.2) has been suggested for over a century^{188,189} due to the fact that fetal beta cells were derived from the differentiation of human cytokeratin 19 (CK19)+ ductal cells¹⁹⁰, CK19+ ductal cells have shown to form

outgrowths of insulin+ islet buds over 3-4 weeks in culture^{191,192}, and cadaveric human pancreata have shown islet structures located within the ductal epithelium¹⁹³. CK19+ ductal cells have also demonstrated progenitor-like functions in other organs, replenishing Lgr5+ crypt-based columnar cells in the intestine¹⁹⁴ and hepatocytes in the liver¹⁹⁵.

Prior to the advent of lineage tracing, evidence for a ductal-to-beta neogenic mechanism was limited to the detection of insulin-positive cells within the ductal epithelium^{61,193,196}. Early studies using rodent models of 90% Px^{196,197} and PDL⁶¹ found that injury resulted in ductal cell hyperplasia and the emergence of hormone+ cells amongst the ducts. Pancreas biopsies from 9 simultaneous pancreas-kidney transplant recipients with T1DM displayed CK19+/insulin+ cells located in pancreatic ducts¹⁹⁸, indicating that ductal cells may be contributing to human beta cell regeneration in an inflammatory autoimmune setting. Diphtheria toxin-induced deletion of acinar and endocrine cells in adult mice resulted in ductal expression of Pdx1 and subsequent contribution to both regenerated acinar and endocrine cells¹⁹⁹. Lastly, Sox9+ centroacinar or terminal duct cells, positioned at the interface of acini and small ducts, were found to generate endocrine cells when injected into cultured fetal pancreatic buds²⁰⁰.

In 2008, back-to-back lineage tracing studies using the PDL model showed ductal cells frequently gave rise to regenerated beta cells^{62,64}. Since then a wealth of lineage tracing studies using ductal markers such as CK19, carbonic anhydrase II (CAII), Sox9, Hnf1b, and Ngn3 have yielded inconclusive results as to whether ductal cells contribute to beta cell neogenesis in the adult mouse pancreas (Table 1.1). Inada et al. were the first to use CAII+ ductal cell lineage tracing and observed that CAII+ cells contributed to beta cell regeneration during post-natal development and following PDL⁶⁴. CAII+ ductal cells have since shown to contribute to beta cell mass expansion during pregnancy and insulin resistance⁷⁶.

Upregulation of TGF-beta signalling paired with Sox9 genetic and viral lineage tracing elegantly showed neogenic islet formation from the ducts following 50-60% pancreatectomy²⁰¹. In contrast, Kopp et al. traced Sox9+ ductal cells and found they did not differentiate into insulin+ cells during post-natal development nor following PDL¹⁷⁰. Alternatively, Sox9+ ductal cells directly contributed to beta cell neogenesis triggered by

administration of EGF and gastrin following alloxan-induced beta cell ablation, although only under conditions of moderate hyperglycemia²⁰².

In 2009, an Hnf1b ductal lineage tracing study conducted by Solar et al. found, following PDL, ductal cells contributed to exocrine regeneration, but did not contribute to newly formed endocrine cells²⁰³. Furthermore, ductal cells did not contribute to the 9-fold increase in beta cell mass seen following treatment with EGF and gastrin in alloxan-treated mice²⁰³. The failure to detect neogenesis in the Hnf1b model may be due to only a fraction of ductal cells being traced. Recently, Gribben et al. used Hnf1b-CreERT mice to observe that ductal cells contributed to insulin+ cell expansion during homeostasis at a rate of 0.66% per week²⁰⁴.

As previously mentioned, during development, ductal and endocrine cells arise from a common progenitor located amongst the trunk cells of the branching epithelium^{203,205}. The transient expression of Ngn3 is necessary for determination of an endocrine fate^{165,205}. Following injury in the adult mouse pancreas, Ngn3 reactivation in the ducts has been shown to be critical for beta cell mass expansion⁶³. Thus, many ductal lineage tracing studies have utilized the Ngn3 promoter to elucidate a developmental mechanism of beta cell neogenesis from the ducts (Table 1.1). During Pax4 overexpression-mediated alpha-to-beta cell conversion¹⁶⁸, ductal cells re-expressed Ngn3, and these Ngn3+ cells repopulated lost alpha and beta cells²⁰⁶. Similarly, deletion of Fbw7, a master regulator of stem cell fate decisions and multipotency, in the adult pancreas resulted in upregulated Ngn3 expression and a CK19+ ductal-to-beta cell conversion²⁰⁷. Recently, Ngn3 lineage tracing in an AKITA diabetic mouse model revealed a substantial increase in traced insulin+ or somatostatin+ cells located in the ducts. Single-cell transcriptomics on islets containing traced Ngn3+ cells demonstrated that Ngn3+ cells contributed to the insulin+ cell population via a somatostatin+ state²⁰⁴.

1.4.6 Rare Pancreatic Populations with Progenitor-like Characteristics

Delta cells have also been proposed as a beta cell progenitor in the pancreas (Figure 1.2), although their limited quantity renders lineage tracing of the delta cell population challenging. Nevertheless, somatostatin+ cell lineage tracing in juvenile mice has shown that delta cells can reconstitute beta cells via an Ngn3+ intermediate following

diphtheria toxin-induced injury²⁰⁸. Ngn3+ cells in the ducts have shown to contribute to beta cell regeneration via a somatostatin+ delta cell intermediate during both homeostasis and diabetes induced by the AKITA mutation²⁰⁴.

A few common markers that represent stem or progenitor cell populations in other tissues have been used in the search of a pancreatic progenitor cell. Recently, protein C receptor (Procr) positive cells were identified as a long-term resident multipotent endocrine progenitor cell in the adult mouse pancreas²⁰⁹ (Figure 1.2). Lineage tracing showed Procr+ cells were the progeny of Ngn3+ endocrine progenitors and generated all 4 endocrine cell types in adult mice under physiological conditions. Procr+ cells were also capable of generating islet organoids *in vitro* that had glucose-lowering capacity after implantation *in vivo*²⁰⁹. Cells expressing double cortin-like kinase 1 (Dclk1) have also been suggested in mouse and human to be a quiescent, long-lived progenitor necessary for pancreatic regeneration following injury²¹⁰. Lastly, Pdx1+/activin-like kinase 3+ cells isolated from human pancreatic ducts and pancreatic duct glands show multilineage differentiation *in vitro* and can be expanded and progenitor characteristics can be maintained via stimulation of bone morphogenetic protein-7 signalling²¹¹.

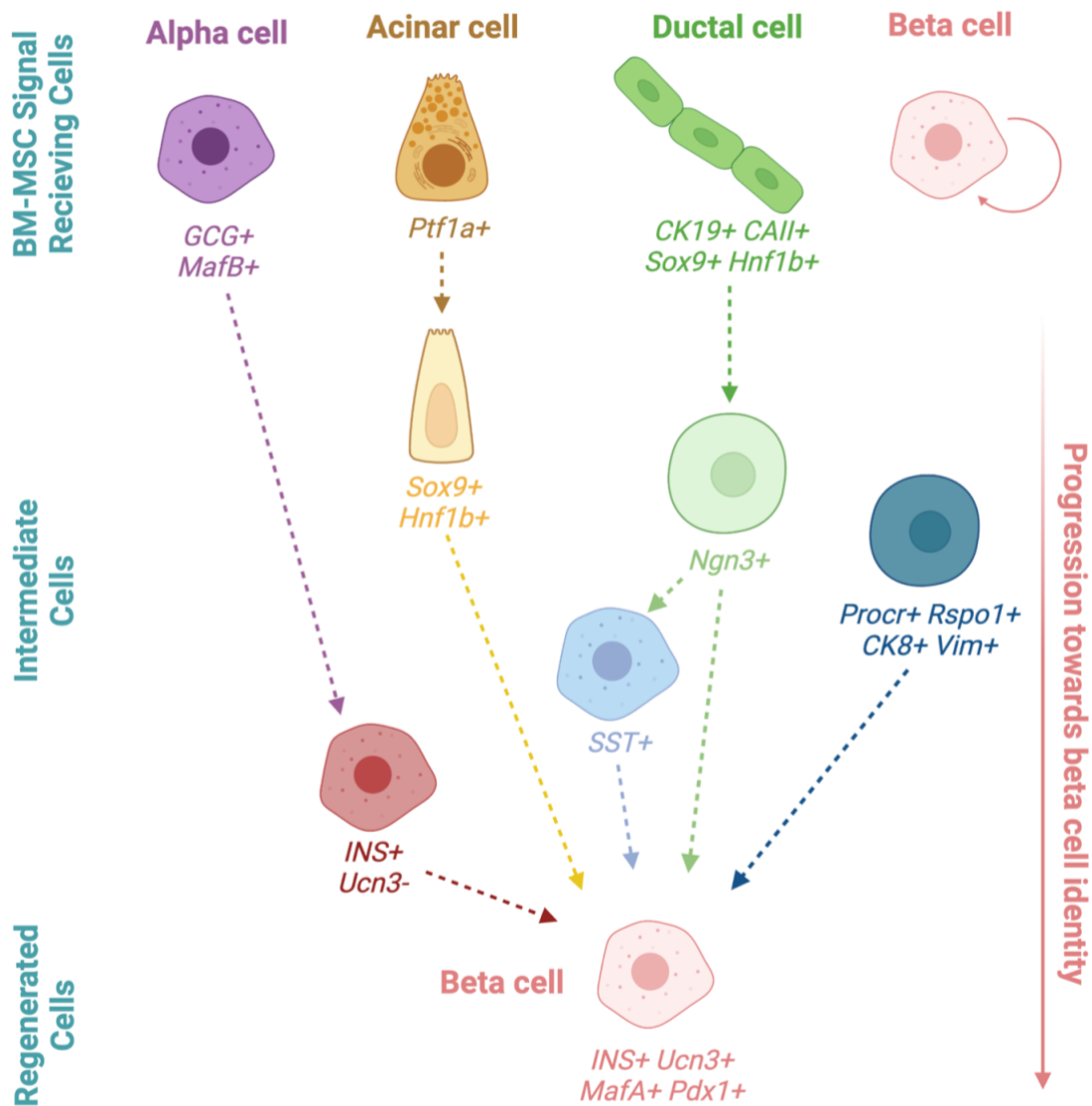


Figure 1.2. Overview of BM-MSC “signal-receiving” cells in the pancreas and their progression towards regenerating beta cells. Alpha cells may transition to beta cells via an Ucn3-negative immature beta cell intermediate. Acinar-to-beta cell conversion may transition via a Sox9+/Hnf1b+ multipotent intermediate. Ductal cells may regain expression of Ngn3+ and, possibly followed by a somatostatin+ intermediate, convert to beta cells. Procr+ cells may directly regenerate beta cells. Lastly, beta cells may self-replicate upon stimulation by BM-MSC. Created with BioRender.com.

Table 1.1. Summary of lineage tracing studies investigating various pancreatic cell types and their conversion to beta cells in the adult mouse pancreas.

Reference	Traced cell type	Lineage tracing model	Model of beta cell damage/regeneration	Conversion to beta cells?
Dor et al. (2004)	Beta cells	INS promoter-CreERT	Homeostasis	Yes
			70% Pancreatectomy (Px)	Yes
Zhao et al. (2021)	All non-beta cells	INS2-Dre; Rosa26-iCre	Homeostasis	No
			Pregnancy	No
			STZ (150 mg/kg)	No
			70% Px	No
			Pancreatic ductal ligation (PDL)	No
	Diphtheria toxin	Yes; alpha and delta cells		
Xiao et al. (2018)	Alpha cells	GCG-CreERT	Alloxan + Pdx1/MafA viral delivery	Yes
Collombat et al. (2009)	Alpha cells	GCG-Cre	STZ (200 mg/kg) + Pax4 overexpression in alpha cells	Yes
Courtney et al. (2013)	Alpha cells	GCG-Cre GCG-rtTA/TetO-Cre	STZ (100-200 mg/kg) + Arx knockout in alpha cells	Yes
Ben-Othman et al. (2017)	Alpha cells	GCG-Cre	Long-term GABA treatment	Yes
	Ductal cells	Ngn3-CreERT		Yes
Thorel et al. (2010)	Alpha cells	GCG-rtTA/TetO-Cre	Diphtheria toxin	Yes
van der Meulen et al. (2017)	Alpha cells	GCG-CreERT2	Homeostasis	Yes
Pan et al. (2013)	Acinar cells	Ptf1a-CreERT	PDL alone	Yes
			PDL + STZ (100 mg/kg/day x 2 days)	Yes

Zhou et al. (2008)	Acinar cells	Cpa1-CreERT2	Ngn3/Pdx1/MafA viral delivery	Yes
Inada et al. (2008)	Ductal cells	CAII-CreERT	PDL	Yes
Dirice et al. (2019)	Ductal cells	CAII-CreERT	Pregnancy	Yes
El-Gohary et al. (2016)	Ductal cells	Sox9-CreERT	50-60% Px + TGF-beta type II receptor upregulation	Yes
Kopp et al. (2011)	Ductal cells	Sox9-CreERT2	Homeostasis PDL	No No
Zhang et al. (2016)	Ductal cells	Sox9-CreERT2	Alloxan+ long-term gastrin and EGF treatment	Yes
Solar et al. (2009)	Ductal cells	Hnf1b-CreERT2	PDL Alloxan+ long-term gastrin and EGF treatment	No No
Gribben et al. (2021)	Ductal cells	Hnf1b-CreERT2	Homeostasis	Yes
		Ngn3-CreERT	AKITA mutant insulin 2	Yes
Al-Hasani et al. (2013)	Ductal cells	Ngn3-CreERT	STZ (100-200 mg/kg) + Pax4 overexpression in alpha cells	Yes
		Hnf1b-CreERT2		Yes
Sancho et al. (2014)	Ductal cells	CK19-CreERT	Fbw7 knockout in ductal cells	Yes
Chera et al. (2014)	Delta cells	SST-Cre	Diphtheria toxin	Yes (Juvenile mice only)
Wang et al. (2020)	Protein C receptor+ cells	Procr-CreERT2	Homeostasis	Yes

1.5 Rationale and Project Overview

Our previous studies investigating islet regeneration in STZ-treated NOD/SCID mice indicate that transplanted BM-MSC do not generate the beta cells themselves^{135,140}. Rather, systemic BM-MSC transplantation stimulated the emergence of small islet clusters associated with the ductal epithelium and increased number of islets containing CK19+ cells within the pancreas¹⁴⁰. Similarly, intrapancreatic (iPAN) injection of BM-MSC Wnt+ CdM in STZ-treated mice resulted in the appearance of islet-like clusters immediately adjacent to the ductal epithelial niche¹⁶¹. Our previous *in vitro* studies showed that co-culture of human ductal cells with regenerative BM-MSC increased ductal cell proliferation, but did not increase beta cell proliferation¹⁴⁰. Furthermore, DBA lectin+ ductal cells isolated from the pancreas of NOD/SCID mice showed significantly increased proliferation when supplemented with Untreated or Wnt+ CdM compared to basal media in culture²¹².

Altogether, BM-MSC likely induce beta cell regeneration by signalling to resident progenitor cells in the pancreas, resulting in their differentiation into new beta cells. The concept of "stem cell-stimulated islet regeneration" and the induction of an islet neogenic program recapitulating development is supported by evidence of numerous small islets associated with the ductal epithelium following both BM-MSC transplantation and Wnt+ CdM injection. Genetic lineage tracing is now required to prove beta cell neogenesis from ductal-derived progenitors *in vivo*. With the use of CdM in place of human BM-MSC transplantation, we are no longer limited to the use of immunodeficient mouse models and genetic lineage tracing mouse models can now be employed.

The CK19-CreERT Rosa26-mTomato genetic lineage tracing mouse model allows for tamoxifen-dependent permanent labelling of CK19+ cells and their progeny with fluorescent reporter tdTomato. STZ treatment in immune-competent mice results in leukocyte infiltration into the islets, posing an additional barrier to achieving beta cell regeneration. Herein, for the first time, we investigated Wnt+ CdM-stimulated beta cell regeneration in an immune-competent CK19+ lineage tracing model. This model will allow us to assess the contribution of CK19+ cells to Wnt+ CdM-induced beta cell mass expansion once achieved.

1.6 Hypothesis and Objectives

We hypothesized that CK19+ pancreatic ductal cells contain a progenitor cell population that gives rise to beta cells in the adult mouse pancreas following STZ treatment and subsequent iPAN injection of Wnt+ MSC CdM (Figure 1.3).

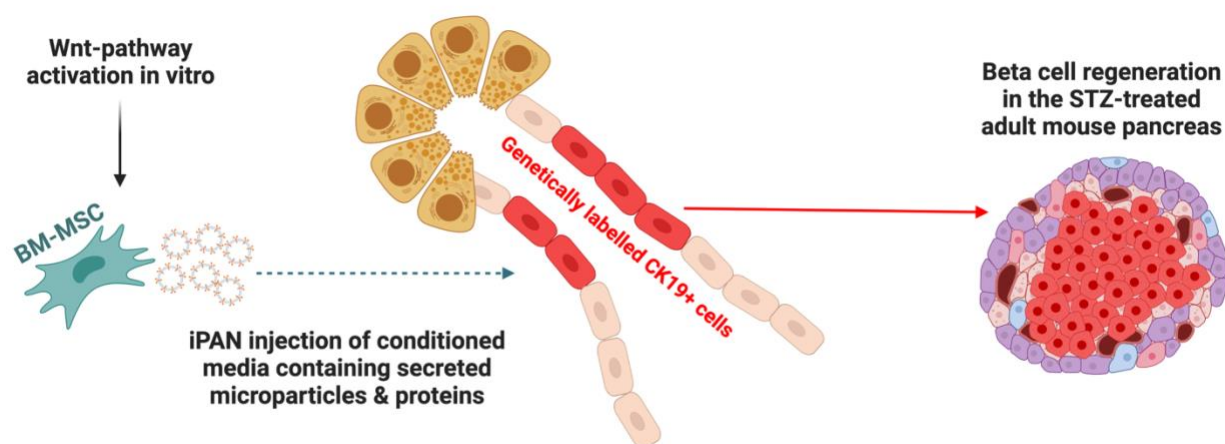


Figure 1.3. Overview of BM-MSC derived Wnt+ CdM-induced beta cell regeneration from a CK19+ ductal cell origin. Created with BioRender.com.

To address this hypothesis, we proposed the following objectives:

- (1) To induce beta cell regeneration following beta cell ablation with STZ and iPAN injection of Wnt+ CdM.
- (2) To use genetic lineage tracing to track the contribution of CK19+ ductal cell progeny during beta cell regeneration.

Delineating the cellular mechanism behind Wnt+ CdM-induced beta cell regeneration by elucidating the origin of regenerated beta cells is crucial to our understanding of Wnt+ CdM as a potential therapy for recovering beta cell loss during diabetes.

2.0 Materials and Methods

2.1 BM-MSC Culture and Conditioned Media Collection

2.1.1 Primary BM-MSC Isolation

Human bone marrow (BM) samples from healthy consenting donors were collected at the London Health Sciences Centre (University Hospital, London, ON). The Western University Human Research Ethics Board approved the use of all human BM sourced material for the induction of beta cell regeneration (REB#12934, see Appendix 2). BM aspirates underwent Hypaque-ficoll centrifugation to isolate the mononuclear cell (MNC) fraction. Followed by red blood cell lysis in ammonium chloride solution, MNCs were plated at 270 000 cells/cm² in AmnioMax™ C-100 Complete Media (ThermoFisher Scientific, Waltham, MA) containing fetal bovine serum, gentamicin, and L-glutamine to establish plastic-adherent BM-MSC colonies.

2.1.2 Preparation of BM-MSC Conditioned Media

BM-MSC were expanded until passage 4, washed twice with phosphate-buffered saline to remove residual growth factors, and re-plated in serum and growth factor-free basal AmnioMax™ media (ThermoFisher Scientific) without supplement. BM-MSC were either treated with 10 μM CHIR99021 (AbMole Biosciences, Houston Tx) or were left untreated (Figure 2.1)¹⁶¹. After 24 hours of culture, conditioned media (CdM) was collected in 3kDa centrifugal filter units with either regenerated cellulose filters (Millipore, Burlington MA) or polyethersulfone filters (ThermoFisher Scientific). BM-MSC CdM was centrifuged at 4100 x g for 90 minutes at 4 °C when using the cellulose columns or 4700 x g for 3.5 hours at 4 °C when using the polyethersulfone columns. Proteins remaining above the 3 kDa filter were quantified using the Pierce 660 nm protein assay (ThermoFisher Scientific) and diluted to approximately 0.1-0.3 μg/μl in basal media. CdM was either used immediately for *in vivo* experiments or frozen at -80 °C for later use.

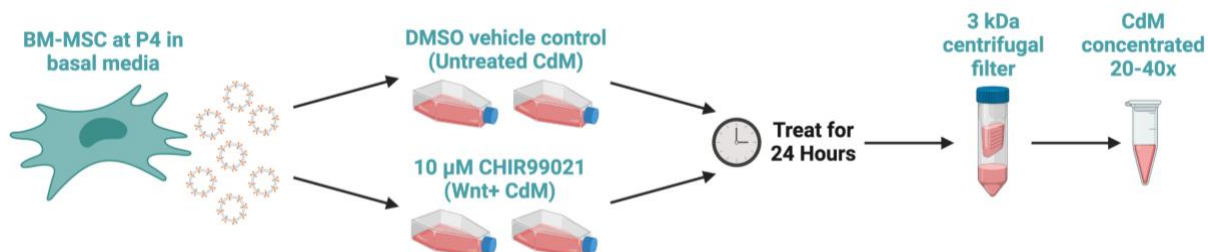


Figure 2.1. Generation of concentrated Wnt+ and Untreated CdM from BM-MSC.

BM-MSC were treated with CHIR99021 to generate Wnt+ CdM or were left Untreated to generate Untreated CdM. Following 24 hours of treatment, CdM was collected and concentrated 20-40x. Created with BioRender.com.

2.2 Flow Cytometry on BM-MSC

2.2.1 Cell Surface Marker Analysis

BM-MSC at P4 were washed twice with phosphate-buffered saline and re-plated in basal AmnioMax™ media without supplement and treated with 10 μM CHIR99021 or left untreated for 24 hours. Cells were incubated with antibodies for: A) CD73, CD90, and CD105 for 30 minutes at 4 °C; or B) CD34 and CD45 for 30 minutes at room temperature (RT). All antibodies are detailed in Table 2.1. Cells were analyzed using flow cytometry (LSRII, BD Biosciences, Mississauga, ON) at the London Regional Flow Cytometry Facility. Data was analyzed using FlowJo software (FlowJo LLC, Ashland, OR).

2.2.2 Total Intracellular Beta-Catenin Analysis

All incubations were carried out at RT. BM-MSC at P4 were washed twice with phosphate-buffered saline and re-plated in basal AmnioMax™ media without supplement and treated with 10 μM CHIR99021 or left untreated for 24 hours. Cells were fixed with 10% formalin for 5 min. and permeabilized with 0.1% Triton X-100 for 15 min. Cells were incubated with anti-human beta-catenin antibody (Table 2.1) for 30 min. and analyzed by flow cytometry.

Table 2.1. Antibody specifications for flow cytometry experiments.

Antibody	Fluorophore	Catalog #	Company	Concentration
Monoclonal mouse anti-CD73	BV421	344008	Biologend	1/75
Monoclonal mouse anti-CD90	FITC	328108	Biologend	1/75
Monoclonal mouse anti-CD105	PE/Dazzle 594	323224	Biologend	1/75
Monoclonal mouse anti-CD34	BV421	562577	BD Biosciences	1/75
Monoclonal mouse anti-CD45	PE/Cy7	304016	Biologend	1/100
Monoclonal mouse anti-beta-catenin	AF488	53-2567-42	Invitrogen	1/40
Monoclonal rabbit anti-CK19	AF488	Ab192643	Abcam	1/400
Monoclonal mouse anti-insulin	AF647	565689	BD Biosciences	1/100
Monoclonal mouse anti-glucagon	BV421	565891	BD Biosciences	1/100

2.3 BM-MSC Nuclear Beta-Catenin Quantification

BM-MSC at P4 were washed twice with phosphate-buffered saline and re-plated in basal AmnioMax™ media without supplement and treated with 10 μM CHIR99021 or left untreated for 24 hours. Cells were collected and nuclear and cytoplasmic proteins were extracted using a cytoplasmic and nuclear protein fractionation kit as per manufacturer's instructions (Boster Bio, Pleasanton, CA). Nuclear beta-catenin protein amounts were determined using the human beta-catenin SimpleStep ELISA kit as per manufacturer's instructions (Abcam, Cambridge, UK).

2.4 Mouse Treatments and Monitoring

Animal procedures were reviewed and approved by the Animal Care Committee at the University of Western Ontario (AUP 2018-184, see Appendix 3) and all colonies were maintained following guidelines published by the Canadian Council for Animal Care.

2.4.1 CK19-CreERT Rosa26-mTomato Model

Homozygous CK19-CreERT mice on a C57BL/6J background (Jackson Labs, Bar Harbor, ME #026925)²¹³ were crossed with homozygous Rosa26-mTomato reporter mice on a C57BL/6J;129S6 mixed background (Jackson Labs #007905)²¹⁴ to generate CK19-CreERT Rosa26-mTomato lineage tracing mice, which label CK19+ cells with fluorescent reporter tdTomato upon tamoxifen administration.

2.4.2 Tamoxifen Dose Optimization

Tamoxifen (MP Biomedicals, Solon, OH), dissolved in corn oil at 30 mg/mL, was administered to 8-10-week-old CK19-CreERT Rosa26-mTomato mice by oral gavage at increasing concentrations: single dose of 1, 3, or 6 mg, or 6 mg per day for 2 days (total of 12 mg). One week following tamoxifen administration, mice were euthanized, and pancreata were harvested and dissected laterally to be analyzed by immunofluorescence microscopy and flow cytometry (see below).

2.4.3 Streptozotocin (STZ) Dose Optimization

To specifically ablate beta cells and induce hyperglycemia, STZ (Sigma, St. Louis, MO), dissolved in citric acid buffer (CAB) at 7.5 mg/ml, was administered to 8-10-week-old CK19-CreERT Rosa26-mTomato mice from Days 0-4 (Figure 2.2) by intraperitoneal (i.p.) injection at increasing concentrations: 40 mg/kg/day, 50 mg/kg/day, and 60 mg/kg/day. CAB control mice were i.p. injected with CAB from Days 0-4. Mice were weighed and non-fasted blood glucose was measured between 8:00-10:00 am using a FreeStyle Lite glucometer (Abbott Diabetes Care, Mississauga, ON) on Days 0, 7, 10, 14, 17, and 21. At Days 10 and 21 glucose tolerance tests (GTT) were performed (Figure

2.2). Mice were euthanized 24 hours following GTT and pancreata were harvested to be analyzed by immunohistochemistry (IHC, see below).

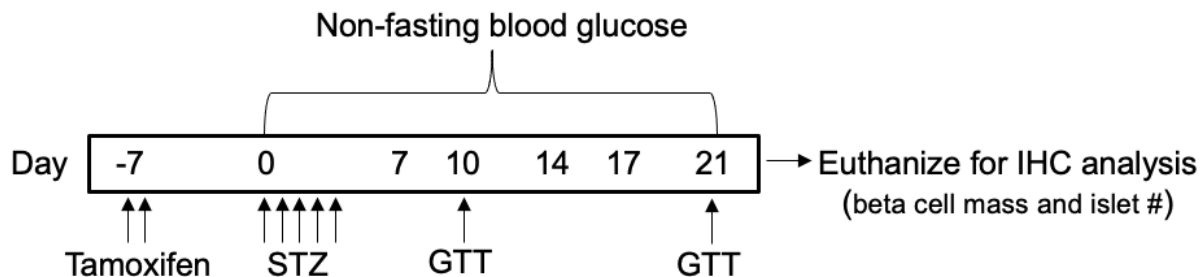


Figure 2.2. STZ dose optimization timeline. Mice were given increasing doses of STZ (40, 50, and 60 mg/kg/day) from Days 0-4. Mice were given glucose tolerance tests (GTT) on Days 10 and 21. Pancreata were collected 24 hours after Day 21 GTT for IHC analysis.

2.4.4 Intrapancreatic (iPAN) injection of CdM and Lineage Tracing Experiments

CK19-CreERT Rosa26-mTomato (8-10 weeks old) were treated with 6 mg of tamoxifen by oral gavage on Days -7 and -6 and after 5 days of rest, mice were i.p. injected with 50 mg/kg/day of STZ from Days 0-4 to ablate beta cells and induce hyperglycemia (Figure 3.6A). On Day 10 (short-term) or Day 14 (long-term), hyperglycemic mice with non-fasted blood glucose levels of 12-25 mmol/L were given a single intra-pancreatic (iPAN) injection as previously described^{157,161}. Mice were iPAN injected with 20 μ L of Wnt+ or Untreated CdM (containing approximately 2-6 μ g of secreted protein) or basal AmnioMAX mediaTM. Mice were monitored weekly for non-fasted blood glucose by tail vein puncture using the FreeStyle Lite glucometer.

2.4.5 EdU Injections

Mice were given 0.25 mg EdU for 3 consecutive days (Day 14-16) via once daily i.p. injection (Figure 3.16A). Pancreata were collected for analysis on Day 17 (24 hours following the final EdU injection).

2.4.6 Insulin Treatments

Insulin glargine Lantus (Sanofi-aventis, Laval, QC) was diluted 1/25 in phosphate buffered saline. Mice were injected subcutaneously with 10U/kg of Lantus^{215–217} at 8:00 am and 8:00 pm daily from Days 15-21 following iPAN injection on Day 14 (Figure 3.9A).

2.4.7 Glucose Tolerance Test (GTT)

GTT was performed on Days 10 and 21 (STZ Optimization experiments) or Day 42 (iPAN injection experiments). D-Glucose (Sigma) was dissolved at 0.25 g/mL in phosphate buffered saline. Mice were fasted for 4 hours prior to i.p. injection of the sterile glucose solution (2.0 mg/kg). Blood glucose levels were measured by tail vein punctures at 0, 5, 10, 15, 30, 45, 60, 90, and 120 minutes post-bolus.

2.5 Flow Cytometry on Pancreas Tissue

All incubations were carried out at RT unless specified. Pancreas samples dissected laterally (including both head and tail compartments) were digested using collagenase V (Sigma) for 20 min. at 37 °C and TrypLE (ThermoFisher Scientific) for 5 min. at 37 °C. Cell viability was assessed by incubating samples with Zombie Yellow (BioLegend) for 15 min. prior to fixation with 10% formalin for 5 min. and permeabilization with 1% Triton X-100 for 15 min. Cells were incubated with antibodies for CK19, insulin, and glucagon for 1 hour. All antibodies and concentrations are detailed in Table 2.1. Cells were analyzed using flow cytometry (LSRII, BD Biosciences).

2.6 Immunohistochemistry and Immunofluorescence Microscopy

2.6.1 Pancreas Tissue Preparation and Sectioning

Pancreas tissues were excised, weighed, and dissected laterally. Half the pancreas tissue (including both head and tail compartments) was snap-frozen in optimal cutting temperature media (Tissue Tek; Sakura-Finetek) at -30 °C. The other half was submersion-fixed in 4% paraformaldehyde for 15 min., placed in 30% sucrose until equilibrium was reached, and frozen in optimal cutting temperature media at -30 °C.

Frozen samples were cryo-sectioned at 12 μm . Three sections per mouse $>150 \mu\text{m}$ (>1 islet diameter) apart were analyzed for each measurement.

2.6.2 Immunohistochemistry (IHC) for Beta Cell Mass and Islet Number Quantification

All incubations were carried out at RT. Pancreas sections were fixed with 10% formalin for 15 min., followed by blocking with peroxidase block for 5 min. and horse serum for 1 hour. Sections were incubated with an anti-insulin primary antibody for 1 hour, followed a peroxidase anti-mouse secondary antibody (Vector Labs, Burlington, ON) for 30 minutes. Antibody details and concentrations for IHC are indicated in Table 2.2. ImmPACT™ DAB (Vector Labs) staining was performed to detect antibody binding, followed by a hematoxylin counterstain and slide mounting with Vectamount (Vector Labs). An islet was defined as a minimum of 10 clustered insulin+ cells. Beta cell mass and insulin+ islet number were quantified using light microscopy and QuPath software²¹⁸. Beta cell mass was calculated by:

$$\text{Beta cell mass} = (\text{Beta cell area} / \text{Total pancreas section area}) \times \text{Whole pancreas weight}$$

2.6.3 Immunofluorescence (IF) Staining, Imaging, and Quantification

All incubations were carried out at RT. Pancreas sections were fixed with 10% formalin for 15 min. and permeabilized with 1% Triton X-100 for 20 min. Sections were blocked for 1 hour and incubated with primary antibodies to detect CK19, Mpx1, insulin, and/or glucagon followed by staining with fluorescent secondary antibodies. Antibody details and concentrations are described in Table 2.2. Nuclei were detected using a 5 min. incubation with DAPI. Slides were imaged using the Zeiss Axio Imager Z2 fluorescent microscope and images were quantified using QuPath software²¹⁸. To quantify the frequency of tdTomato+/insulin+ cells, total numbers of insulin+ cells and tdTomato+/insulin+ cells were counted in 3 sections per mouse. To determine islet-duct association, each islet in 3 sections per mouse was designated as in direct contact with or not in direct contact with CK19+ ducts. For the quantification of EdU+ cells, sections were incubated with the EdU detection cocktail as per manufacturer's instructions (Invitrogen) and total insulin+ cells and EdU+/insulin+ cells were counted for each islet in

3 sections per mouse. 3D z-stacks depicting co-localization of insulin and tdTomato were imaged using the Nikon Ti2-E Inverted Microscope paired with the A1R HD laser-scanning confocal at the London Regional Microscopy Facility.

Table 2.2. Antibody specifications for IHC/IF staining.

Antibody	Catalog #	Company	Concentration
Rabbit anti-insulin	ab181547	Abcam, Cambridge, UK	1/500
Mouse anti-glucagon	ab10988	Abcam	1/500
Rat anti-CK19	TROMA-III	Developmental Studies Hybridoma Bank, Iowa City, IA	1/200
Rat anti-acinar (Mpx1)	MABS2144	MilliporeSigma, Burlington, MA	1/20
Fluorescein-labelled rabbit anti-rat IgG	FI-4000	Vector Labs, Burlington, ON	1/200
Texas Red [®] -labelled horse anti-mouse IgG	TI-2000	Vector Labs	1/200
Fluorescein-labelled goat anti-rabbit IgG	FI-1000	Vector Labs	1/200
Texas Red [®] -labelled goat anti-rabbit IgG	TI-1000	Vector Labs	1/200
Cy5-labelled Goat anti-rabbit IgG	ab6564	Abcam	1/200
Peroxidase-labelled goat anti-rabbit IgG	PI-1000	Vector Labs	1/200

2.7 Statistical Analysis

Data was analyzed and graphed using GraphPad Prism version 9. All data was expressed as Mean \pm standard deviation (SD). Non-fasted blood glucose curves and glucose tolerance test curves were analyzed using a repeated measures two-way analysis of variance (ANOVA). All other parameters were analyzed by one-way ANOVA unless stated otherwise. Comparisons were made using Tukey's multiple comparison test unless stated otherwise.

3.0 Results

3.1 Treatment with CHIR99021 increased nuclear beta-catenin levels and did not alter BM-MSC cell surface phenotype.

GSK3 interference by the addition of CHIR99021 to culture inhibits the function of the beta-catenin destruction complex. This allows for intracellular accumulation of beta-catenin and downstream upregulation of Wnt pathway effectors in CHIR-treated cells. To confirm whether treatment with CHIR increased beta-catenin levels, BM-MSC were assessed via flow cytometry for intracellular beta-catenin (Figure 3.1A). CHIR-treated BM-MSC showed consistently increased mean fluorescence intensity (M.F.I.) values for beta-catenin relative to untreated BM-MSC (1.40 ± 0.08 , Figure 3.1B). Nuclear and cytoplasmic protein fractionation followed by ELISA for human beta-catenin revealed that CHIR-treated cells showed increased levels of nuclear-localized beta-catenin compared to untreated cells (67.73 ± 13.21 vs 7.13 ± 3.01 ng/mL, $p < 0.01$, Figure 3.1C), suggesting that active Wnt signalling was upregulated in CHIR-treated BM-MSC.

The minimal defining criteria for MSC state that cultured cells should have over 95% expression of the stromal cell surface markers CD73, CD90, and CD105, as well as less than 2% of contamination from other cell types such as CD45+ leukocytes or CD34+ cells¹⁰⁶. Both CHIR-treated and untreated BM-MSC show >95% expression of CD73, CD90, and CD105 and <2% expression of CD45 and CD34 (Figure 3.1D,E). Collectively, BM-MSC cell surface phenotype was unaltered upon treatment with CHIR.

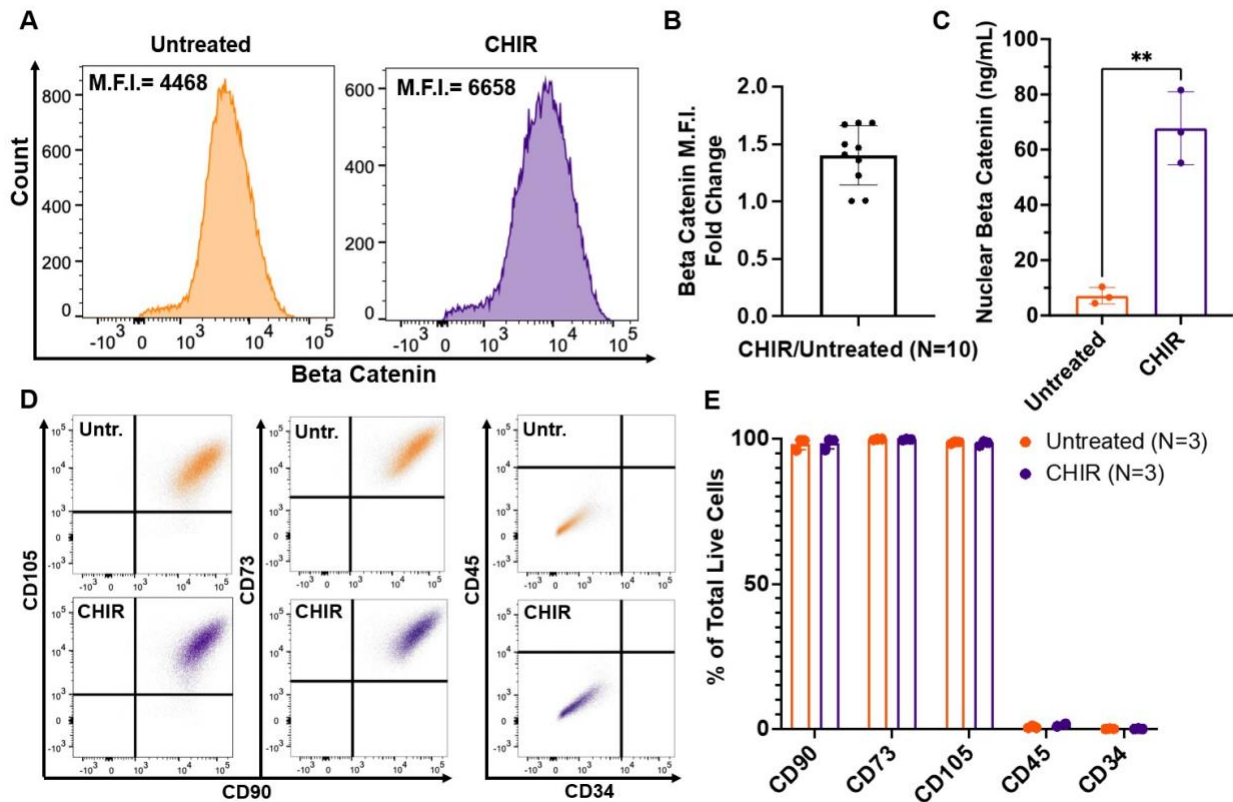


Figure 3.1. CHIR-treated MSC upregulated beta-catenin and retained expression of stromal cell markers. **(A)** Representative flow cytometry plots of beta-catenin mean fluorescence intensity (M.F.I.) in untreated BM-MSC and BM-MSC treated with 10 μ M of GSK3-inhibitor CHIR99021 (CHIR). **(B)** CHIR-treated cells showed increased expression of intracellular beta-catenin shown as fold change relative to untreated cells (N=10). **(C)** CHIR-treated cells showed increased levels of nuclear-localized beta-catenin compared to untreated cells (N=3, ** p <0.01). **(D)** Representative flow cytometry plots of BM-MSC surface marker expression. **(E)** No differences were found in CD90, CD73, CD105, CD45, and CD34 expression between CHIR-treated BM-MSC and untreated BM-MSC (N=3). Data represent Mean \pm SD. Nuclear beta-catenin was compared using an unpaired Student's t-test. Cell surface marker expression was compared using a two-way ANOVA followed by Šídák's multiple comparisons test.

3.2 Tamoxifen administration in CK19-CreERT Rosa26-mTomato mice resulted in dose-dependent labelling of CK19+ pancreatic ductal cells.

8-10-week-old mice were treated with 12 mg (6 mg per day for 2 days), 6 mg, 3 mg, or 1 mg of tamoxifen or corn oil (vehicle) and assessed for efficiency and specificity of CK19+ cell labelling with reporter tdTomato via flow cytometry 1-week post-tamoxifen. Compared to lower doses of 1 mg, 3 mg, or 6 mg, 12 mg of tamoxifen showed an increased frequency of live tdTomato+ cells (Figure 3.2A,B). 12 mg of tamoxifen resulted in an increased proportion of CK19+ ductal cells labelled with tdTomato ($21.78 \pm 9.10\%$, $p < 0.05$) compared to 1 mg of tamoxifen (5.19 ± 3.87 , Figure 3.2C,D). Less than 0.5% of CK19+ cells showed tdTomato labelling following administration of corn oil vehicle (Figure 3.2D), indicating tdTomato was not expressed without Cre activity. Dose-dependent mosaic labelling and co-localization of tdTomato in CK19+ ducts was observed in mice treated with various doses of tamoxifen (Figure 3.2E-H).

The proportion of tdTomato+ cells that co-expressed ductal cell marker CK19 remained unchanged between various doses of tamoxifen and an average of $51.14 \pm 6.58\%$ of tdTomato+ cells were CK19+ ductal cells following 12 mg of tamoxifen (Figure 3.3A,B). Co-localization of tdTomato and acinar cell surface marker Mpx1²¹⁹ expression revealed that $16.75 \pm 2.70\%$ of acinar cells were labelled with tdTomato upon administration of 12 mg of tamoxifen (Figure 3.3C,D). Insulin+ beta cells were also labelled with tdTomato at a frequency of $2.18 \pm 0.50\%$ following 12 mg of tamoxifen (Figure 3.3E,F). Direct co-localization of tdTomato in insulin+ cells was confirmed by flow cytometry (Table 3.2) and CK19 expression was not detected in tdTomato+ beta or acinar cells by fluorescence microscopy (Figure 3.3G). Thus, tdTomato expression was not limited to ductal structures and a significant proportion of acinar cells were labelled.

12 mg of tamoxifen (administered at 6 mg per day for 2 days) was chosen as the optimal dose for subsequent lineage tracing experiments due to an increased efficiency of CK19+ cell labelling with tdTomato (Figure 3.2B,D), despite co-labelling of acinar cells.

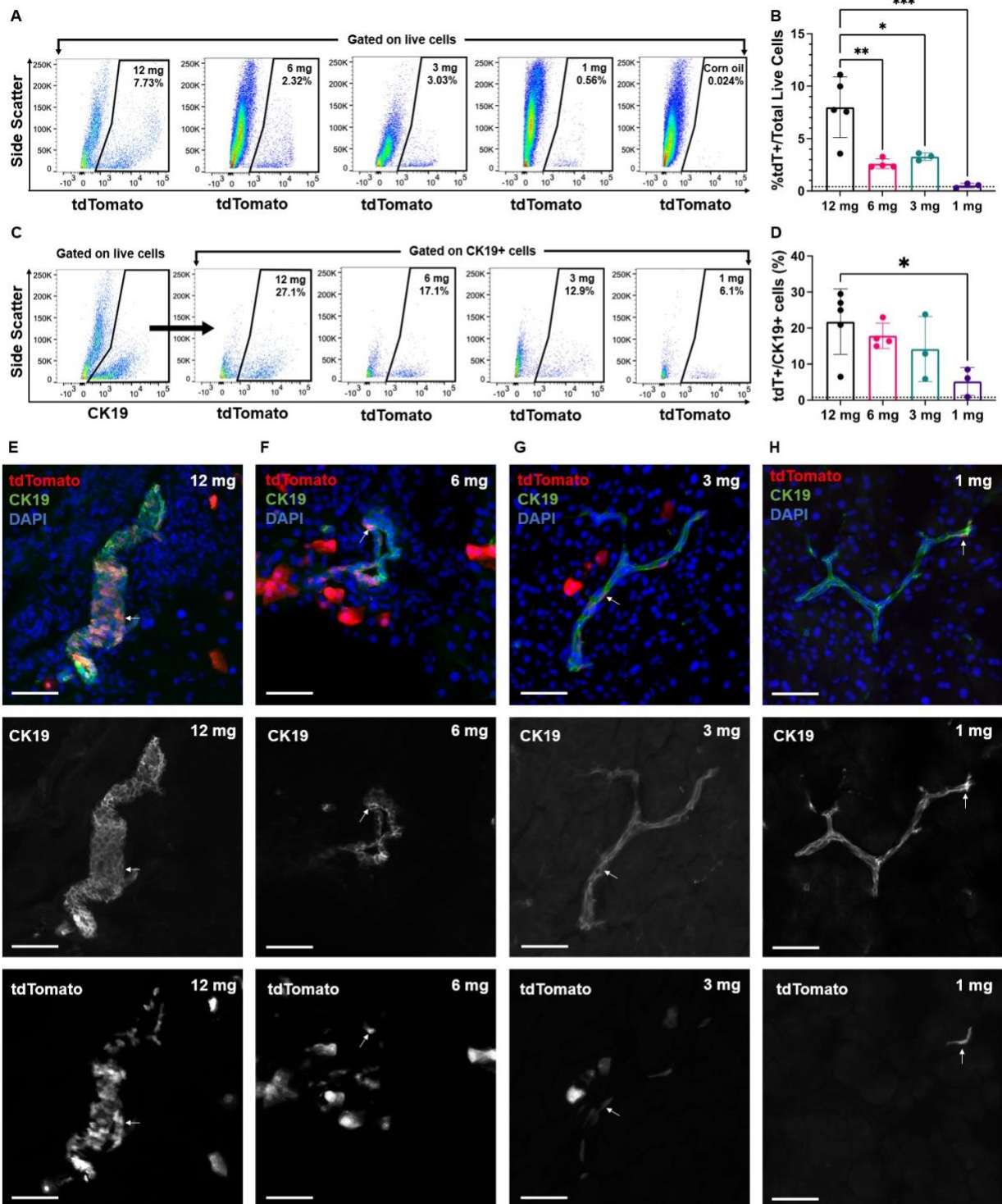


Figure 3.2. Tamoxifen treatment (12 mg) in CK19-CreERT Rosa26-mTomato mice increased the proportion of tdTomato+/CK19+ cells. (A) Representative flow cytometry plots of live tdTomato+ cells from mice treated with 12 mg (n=5), 6 mg (n=4), 3 mg (n=3), or 1 mg (n=3) of tamoxifen or corn oil vehicle control (n=3) 1-week post-administration. **(B)** 12 mg of tamoxifen resulted in an increased proportion of tdTomato+ cells amongst total live cells compared to lower doses (*p<0.05, **p<0.01, ***p<0.001). **(C)** Representative flow cytometry plots of live CK19+ ductal cells that co-expressed tdTomato from mice treated with 12 mg, 6 mg, 3 mg, or 1 mg of tamoxifen 1-week post-administration. **(D)** 12 mg of tamoxifen resulted in an increased proportion of CK19+ cells labelled with tdTomato compared to 1 mg of tamoxifen (*p<0.05). Dotted lines represent measurements observed in mice given corn oil only (n=3). Representative images of tdTomato in CK19+ ducts after **(E)** 12 mg, **(F)** 6 mg, **(G)** 3 mg, or **(H)** 1 mg of tamoxifen. Arrows indicate co-localization of tdTomato and CK19. Scale bars = 50 μ m. Data represent Mean \pm SD compared using a one-way ANOVA followed by Tukey's multiple comparison test.

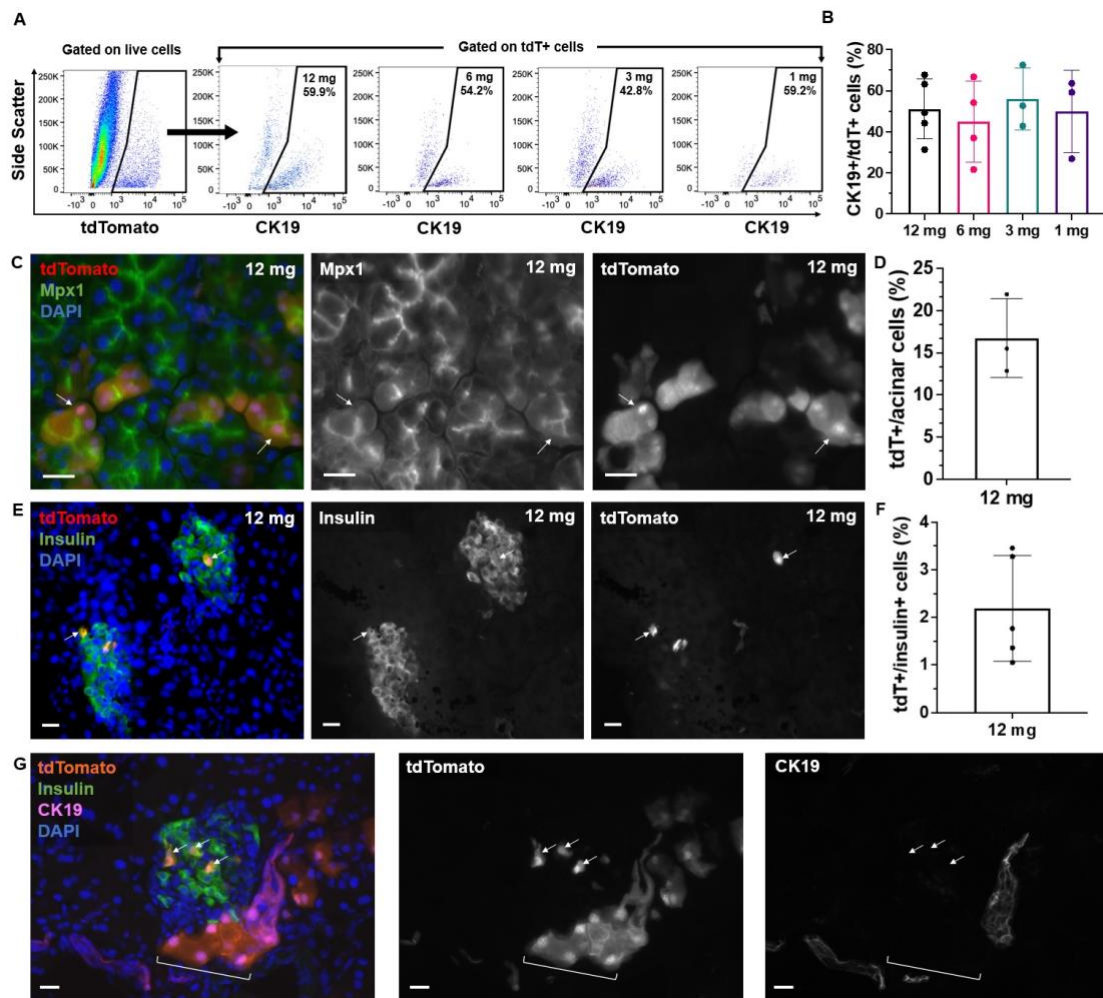


Figure 3.3. tdTomato expression was observed in pancreatic acinar and beta cells following tamoxifen treatment. (A) Representative flow cytometry plots of tdTomato+ cells that co-expressed CK19 from mice treated with 12 mg (n=5), 6 mg (n=4), 3 mg (n=3), or 1 mg (n=3) of tamoxifen 1-week post-administration. **(B)** No differences were seen in the proportion of tdTomato+ cells that co-expressed CK19 between groups. **(C)** Co-localization of tdTomato in Mpx1+ acini (indicated by arrows). **(D)** 16.75±2.70% of acinar cells were labelled with tdTomato. **(E)** Co-localization of tdTomato in insulin+ islet cells (arrows). **(F)** 2.18±0.50% of insulin+ cells were labelled with tdTomato. **(G)** Representative image of CK19 and tdTomato detection in insulin+ cells (arrows) and acinar cells (brackets). Scale bars = 20 µm. Data represent Mean ± SD compared using a one-way ANOVA followed by Tukey's multiple comparison test.

3.3 STZ treatment of 50 mg/kg/day for 5 days resulted in hyperglycemia, glucose intolerance, and decreased beta cell mass.

8-10-week-old mice were treated with 40, 50, or 60 mg/kg/day of STZ from Days 0-4 and monitored for non-fasted blood glucose (NFBG) until Day 21. Mice treated with 50 or 60 mg/kg STZ demonstrated increased NFBG levels on Days 10 and 14 (Figure 3.4A) and increased area under the curve (AUC) for NFBG (Figure 3.4B) compared to normoglycemic mice given CAB. Mice treated with 40 mg/kg STZ did not demonstrate differences in glycemia compared to CAB. At Day 10, 30% and 70% of mice treated with 50 or 60 mg/kg STZ, respectively, were hyperglycemic with NFBG ≥ 12 mmol/L. The proportion of hyperglycemic mice increased to 60% of mice treated with 50 mg/kg STZ and 100% of mice treated with 60 mg/kg STZ by Day 14 (Figure 3.4C). On both Days 10 and 14, only 10% of mice treated with 40 mg/kg STZ had NFBG levels ≥ 12 mmol/L.

On Days 10 and 21, mice were administered an intraperitoneal glucose tolerance test (GTT). Mice treated with 50 or 60 mg/kg STZ demonstrated significantly increased glucose levels from 15 to 120 minutes post-bolus and increased AUC for GTT at Day 10 compared to CAB controls (Figure 3.4D,E). No further increase compared to CAB was seen in post-prandial glucose levels of mice treated with 50 mg/kg STZ, although mice treated with 60 mg/kg STZ had further elevated glucose levels compared to CAB at Day 21 (Figure 3.4F,G), indicating that mice given 60 mg/kg STZ were severely glucose intolerant. Mice treated with 40 mg/kg STZ showed no differences in glucose levels post-bolus or AUC for GTT compared to CAB at Days 10 and 21 (Figure 3.4D-G). The body weight of mice treated with 50 or 60 mg/kg of STZ was decreased $<10\%$ at Day 21 compared to mice given CAB (Figure 3.4H), likely due to polyuria after STZ treatment.

IHC detection of insulin in pancreas sections at Day 14 showed all doses of STZ resulted in $>70\%$ decrease in beta cell mass (Figure 3.5A) and insulin+ islet number (Figure 3.5B) compared to CAB. Low magnification photomicrographs of pancreas sections from STZ-treated mice demonstrated little to no insulin+ beta cells compared to mice given CAB which demonstrated large insulin+ islets (Figure 3.5C-F).

The STZ treatment regimen of 50 mg/kg/day for 5 days was chosen as the optimal dose for future experiments as this was the lowest dose at which mice showed elevated glycemia at Days 10 and 14 (Figure 3.4A-C), glucose intolerance by Day 10 (Figure 3.4D), and reduced beta cell mass and islet number/kg by Day 14 (Figure 3.5A,B).

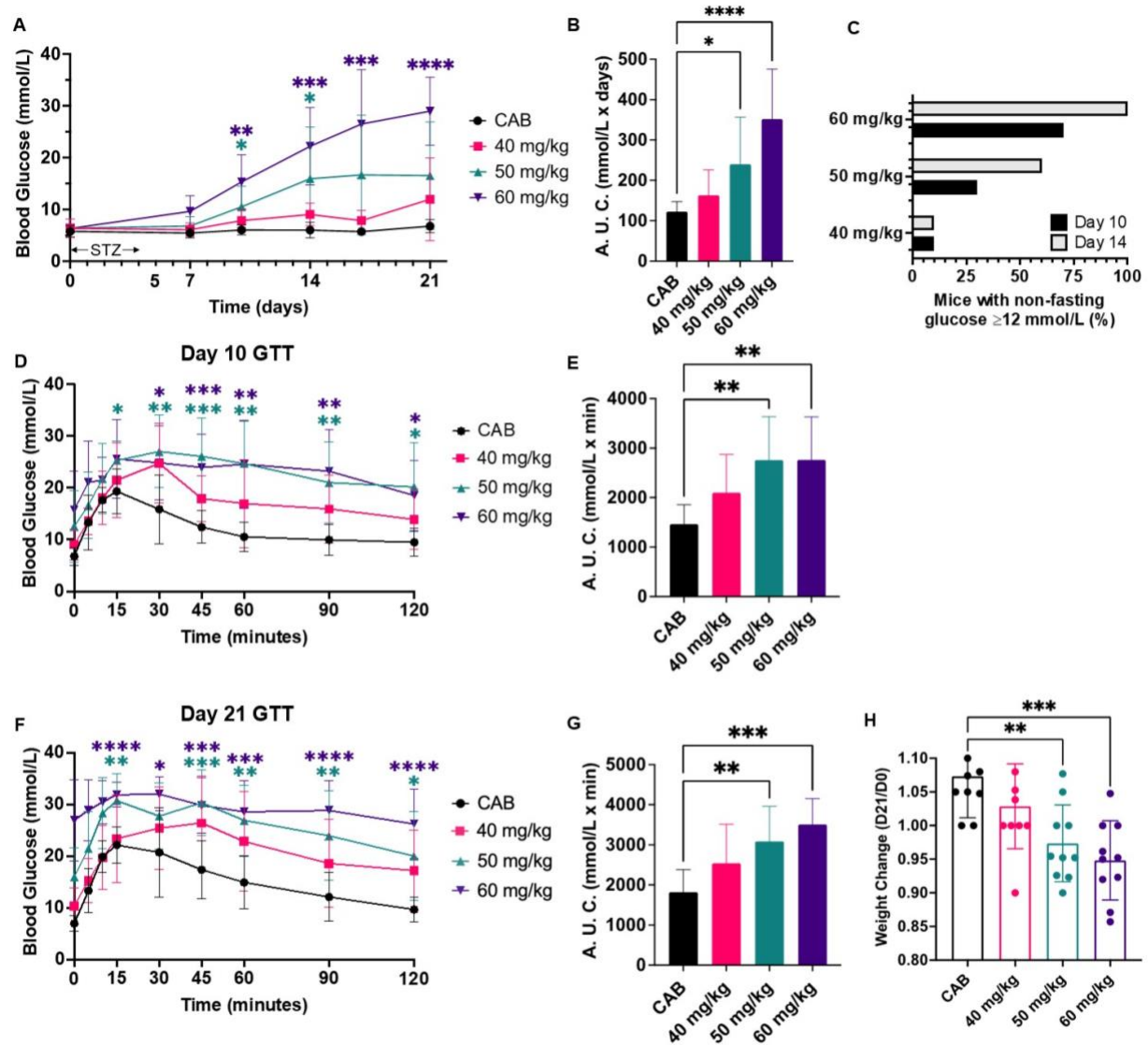


Figure 3.4. STZ treatment (50 and 60 mg/kg/day for 5 days) in CK19-CreERT Rosa26-mTomato mice resulted in hyperglycemia (≥ 12 mmol/L) by Day 14.

(A) Compared to citric acid buffer (CAB)-treated mice (n=10), non-fasted blood glucose (NFBG) levels were significantly increased in mice treated with 50 (n=10, *p<0.05) or 60 (n=10, **p<0.01, ***p<0.001) mg/kg/day STZ on Days 10 and 14. Mice treated with 40 mg/kg/day STZ (n=10) did not demonstrate differences in NFBG compared to CAB. **(B)** Mice treated with 50 (*p<0.05) or 60 (****p<0.0001) mg/kg of STZ had a significantly higher area under the curve (AUC) for NFBG compared to mice given CAB. **(C)** By Day 14, treatment with 50 or 60 mg/kg of STZ resulted in 60% and 100%, respectively, of mice with NFBG ≥ 12 mmol/L. On Day 10, mice were administered an intraperitoneal glucose tolerance test (GTT). Mice treated with 50 (n=10) or 60 (n=10) mg/kg STZ had **(D)** increased glucose levels and **(E)** increased AUC compared to mice given CAB (*p<0.05, **p<0.01, ***p<0.001). **(F-G)** On Day 21, mice treated with 60 mg/kg STZ showed minimal response to the glucose bolus. **(H)** Body weight was decreased in mice treated with 50 (**p<0.01) or 60 (**p<0.001) mg/kg of STZ compared to mice given CAB. Data represent Mean \pm SD. NFBG curves were compared using a repeated measures two-way ANOVA followed by Tukey's multiple comparison test. AUC and weight change were compared using a one-way ANOVA followed by Tukey's multiple comparison test.

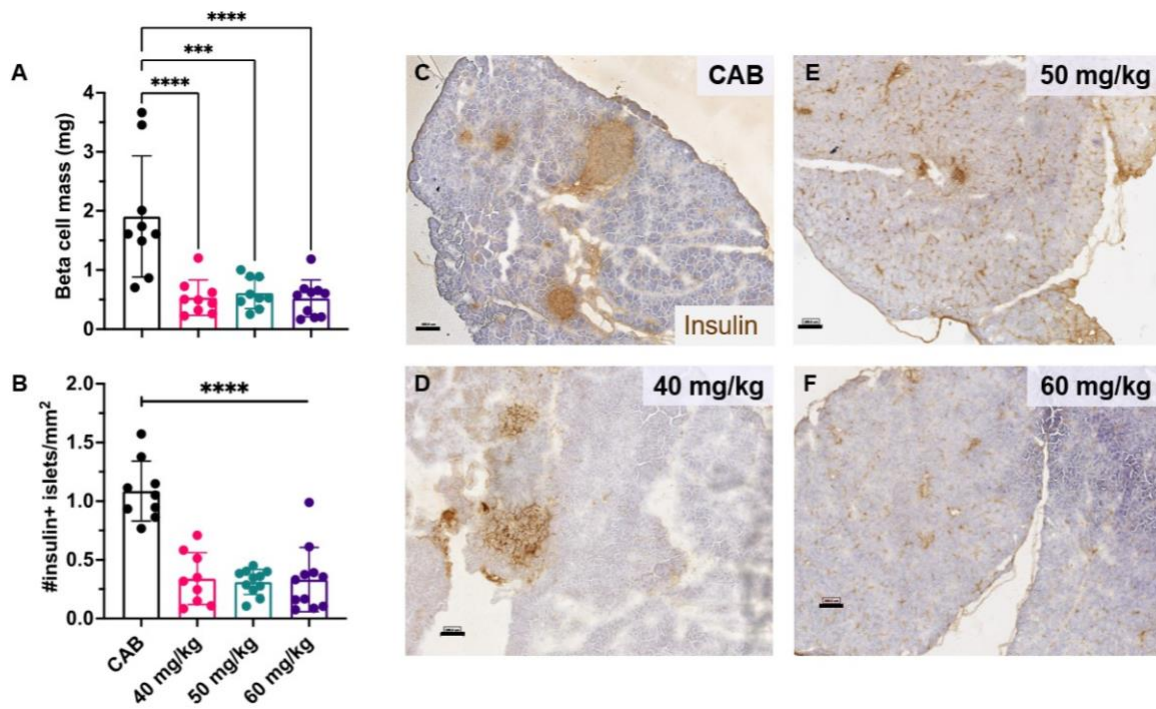


Figure 3.5. Beta cell mass and islet number were reduced in CK19-CreERT Rosa26-mTomato mice treated with STZ at Day 14. Compared to CAB treated mice (n=9), mice treated with 40 (n=9), 50 (n=10), or 60 (n=10) mg/kg/day STZ had significantly decreased **(A)** beta cell mass ($p < 0.001$, $p < 0.0001$) **(B)** and insulin+ islet number ($****p < 0.0001$). Representative images of insulin staining in pancreas sections from mice treated with **(C)** CAB, or **(D)** 40, **(E)** 50, or **(F)** 60 mg/kg/day of STZ. Scale bars = 100 μ m. Data represent Mean \pm SD compared using a one-way ANOVA followed by Tukey's multiple comparison test.

3.4 iPAN injection of Wnt+ CdM preserved beta cell mass and islet number, but did not significantly reduce hyperglycemia 11 days following injection.

CK19-CreERT Rosa26-mTomato mice (8-10 weeks old) were treated with 6 mg of tamoxifen on Days -7 and -6 followed by 50 mg/kg/day of STZ on Days 0-4 to induce hyperglycemia (Figure 3.6A). On Day 10, hyperglycemic mice (NFBG of 12-25 mmol/L) were iPAN injected with either Wnt+ CdM, Untreated CdM, or supplement-free basal AmnioMax™ media. NFBG levels of mice in all groups continued to rise from Days 10 to 21 (Figure 3.6B). No differences were seen in AUC for NFBG from Days 0 to 21 between mice treated with Wnt+ or Untreated CdM compared to basal media (Figure 3.6C).

At Day 21 pancreata were harvested for analyses of beta cell mass and insulin+ islet number. Mice treated with Wnt+ CdM demonstrated an increased beta cell mass (Figure 3.6D) and increased insulin+ islet number (Figure 3.6E) compared to mice given basal media. Average values for beta cell mass (0.46 mg) and islet number (0.56 islets/mm²) in mice given Wnt+ CdM at Day 21 were similar to that of mice given STZ only at Day 14 (0.61 mg and 0.31 islets/mm²), indicating that Wnt+ CdM may have had an islet-protective effect and prevented further STZ-induced beta cell damage.

Low magnification photomicrographs of pancreas sections from mice treated with Wnt+ CdM showed abundant insulin+ beta cells compared to mice treated with basal media (Figure 3.6F-H), although islets were still reduced in mice given Wnt+ CdM compared to the numerous large islets seen in mice given CAB (Figure 3.6I).

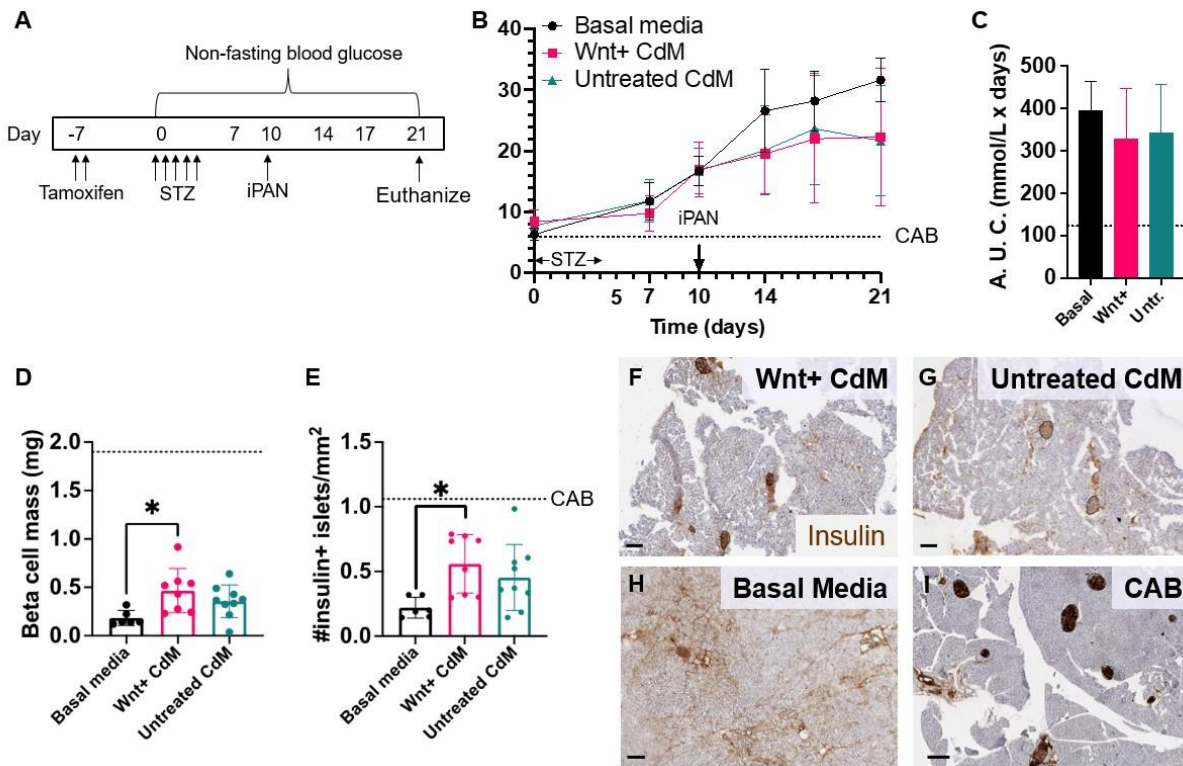


Figure 3.6. Beta cell mass and islet number were preserved following iPAN injection of Wnt+ CdM. (A) CK19-CreERT Rosa26-mTomato mice were treated with 6 mg/day tamoxifen for 2 days and 50 mg/kg/day STZ for 5 days then were iPAN-injected on Day 10 with Wnt+ CdM (n=8), Untreated CdM (n=9), or basal media (n=6). Mice were euthanized on Day 21. No significant differences were found for (B) non-fasted blood glucose (NFBG) levels and (C) area under the curve (AUC) for NFBG between mice treated with Wnt+ CdM, Untreated CdM, or basal media. Compared to mice injected with basal media that displayed a further reduction of beta cell mass, mice injected with Wnt+ CdM maintained an increased (D) beta cell mass and (E) insulin+ islet number (* $p < 0.05$). Representative images of insulin staining in pancreas sections from mice treated with (F) Wnt+ CdM, (G) Untreated CdM, (H) basal media, or (I) citric acid buffer (CAB). Scale bars = 150 μm . Dotted lines represent measurements observed in CAB control mice. Data represent Mean \pm SD. NFBG data was compared using a repeated measures two-way ANOVA and all other data was compared using a one-way ANOVA followed by Tukey's multiple comparison test. N=5 BM-MSK samples.

3.5 iPAN injection of Wnt+ CdM increased tdTomato and insulin co-expression at Day 21.

CK19-CreERT Rosa26-mTomato mice iPAN-injected on Day 10 with either Wnt+ CdM, Untreated CdM, or basal media were euthanized on Day 21 (11 days post-iPAN injection, Figure 3.6A) and pancreata were harvested and digested into a single-cell suspension for lineage tracing analyses by flow cytometry. To determine the frequency of tdTomato+ cells that expressed insulin, live events were gated on tdTomato+ events and subsequently gated on insulin+ events (Figure 3.7A). iPAN injection of Wnt+ CdM resulted in an increased frequency of insulin+/tdTomato+ cells compared to injection of basal media (Figure 3.7B, Table 3.1). To determine the frequency of tdTomato+ cells that expressed glucagon, live events were gated on tdTomato and subsequently gated on glucagon (Figure 3.7C). No differences were found in the frequency of glucagon+/tdTomato+ cells between groups (Figure 3.7D). To determine the frequency of insulin+ cells that expressed tdTomato, live events were gated on insulin and subsequently gated on tdTomato (Figure 3.7E). Mice given Wnt+ CdM demonstrated an increased frequency of tdTomato+/insulin+ cells compared to mice given basal media (Figure 3.7F, Table 3.1). To determine the frequency of insulin+ cells that co-expressed glucagon, cells that may be an intermediate of alpha-to-beta cell transition, live events were gated on insulin and subsequently gated on glucagon (Figure 3.7G). No differences were found in the frequency of glucagon+/insulin+ cells between groups (Figure 3.7D).

We conducted pulse-chase experiments to quantify labelled cells at successive timepoints following STZ treatment (50 mg/kg/day from Days 0-4). iPAN injection of Wnt+ CdM resulted in an increased frequency of tdTomato+/insulin+ cells compared to STZ-treated mice at Day 10 (Table 3.1). We decided to assess tdTomato labelling during homeostasis (no STZ) at 3, 21, and 28 days following 12 mg of tamoxifen. The frequencies of insulin+/tdTomato+, glucagon+/tdTomato+, tdTomato+/insulin+, and glucagon+/insulin+ co-expressing cells were unchanged between timepoints (Table 3.2).

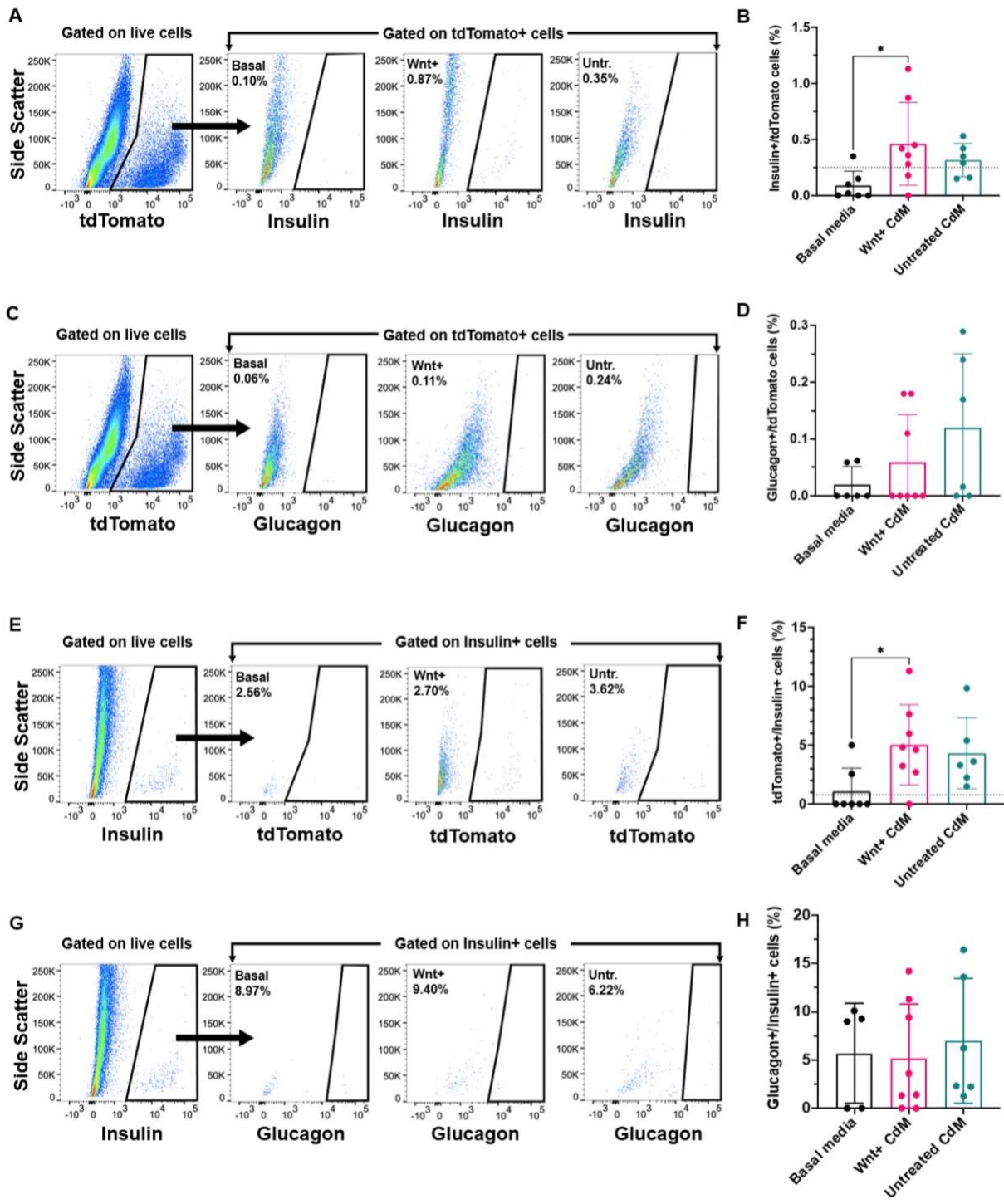


Figure 3.7. tdTomato co-expression with insulin was increased following iPAN injection of Wnt+ CdM. (A) Representative flow cytometry plots showing tdTomato+ cells that co-expressed insulin. **(B)** iPAN injection of Wnt+ CdM (n=8) resulted in an increased frequency of tdTomato+ cells that co-expressed insulin compared to injection of basal media (n=7, *p<0.05). **(C)** Representative flow cytometry plots showing tdTomato+ cells that co-expressed glucagon. **(D)** The frequency of tdTomato+ cells that co-expressed glucagon was not changed between mice treated with Wnt+ CdM or Untreated CdM, or basal media. **(E)** Representative flow cytometry plots showing insulin+ cells that co-expressed tdTomato. **(F)** iPAN injection of Wnt+ CdM resulted in an increased frequency of insulin+ cells that co-expressed tdTomato compared to basal media (*p<0.05). **(G)** Representative flow cytometry plots showing insulin+ cells that co-expressed glucagon. **(H)** The frequency of insulin+ cells that co-expressed glucagon was not changed between mice given Wnt+ or Untreated CdM, or basal media. Data represent Mean \pm SD compared by one-way ANOVA followed by Tukey's multiple comparison test.

Table 3.1. The frequency of cells that co-expressed tdTomato and insulin was increased in mice injected with Wnt+ CdM compared to basal media.

Phenotype	% of Parent Population			
	Day 10	Day 21		
	Tamoxifen + STZ (n=8)	Basal media (n=7)	Wnt+ CdM (n=8)	Untreated CdM (n=6)
tdT+/Total live cells	2.23 ± 0.29	7.34 ± 0.72	8.22 ± 1.02	6.66 ± 1.81
Insulin+/tdT+	0.26 ± 0.08	0.09 ± 0.05	0.46 ± 0.13*	0.32 ± 0.06
Glucagon+/tdT+	0.13 ± 0.07	0.09 ± 0.08	0.06 ± 0.03	0.12 ± 0.05
Ins+/Total live cells	0.73 ± 0.2	0.21 ± 0.08	0.65 ± 0.19	0.47 ± 0.06
tdT+/Insulin+	0.77 ± 0.24	1.97 ± 0.82	5.04 ± 1.20*	4.32 ± 1.23
Glucagon+/Insulin+	0.83 ± 0.33	5.67 ± 2.32	5.15 ± 1.99	7.01 ± 2.64

Data expressed as Mean ± SD compared within rows using a one-way ANOVA followed by Tukey's multiple comparison test (*p<0.05).

Table 3.2. Frequencies of cells that co-expressed tdTomato, insulin, and glucagon remained consistent following treatment with 12 mg of tamoxifen in healthy citric acid buffer (CAB) control mice.

Phenotype	% of Parent Population		
	72 hours	Day 10	Day 21
	n=6	n=3	n=6
tdT+/Total live cells	7.53 ± 1.48	1.52 ± 0.72	5.52 ± 1.33
Insulin+/tdT+	1.34 ± 0.58	1.65 ± 1.43	2.06 ± 0.32
Glucagon+/tdT+	0.03 ± 0.02	0.11 ± 0.11	0.12 ± 0.06
Insulin+/Total live cells	2.54 ± 0.56	1.01 ± 0.1	2.81 ± 0.4
tdT+/Insulin+	4.35 ± 0.46	2.42 ± 1.87	4.36 ± 0.95
Glucagon+/Insulin+	2.74 ± 0.89	3.18 ± 0.91	0.61 ± 0.22

Data expressed as Mean ± SD compared within rows using a one-way ANOVA followed by Tukey's multiple comparison test.

3.6 Regenerated insulin+ cells of STZ-treated mice iPAN-injected with CdM were devoid of a high side-scatter population.

The granularity of cells on the flow cytometer can be measured by their light side scatter properties. Healthy mice that were injected with citric acid buffer (STZ vehicle control; CAB), had two populations of live insulin+ cells, a high side scatter population and a low side scatter population (Figure 3.8A), corresponding to beta cells that contained high amounts of insulin granules versus a lower amount of insulin granules respectively. STZ-treated mice given Wnt+ CdM, Untreated CdM, or basal media were devoid of insulin+ cells with high side scatter properties compared to CAB control mice at Day 21 (Figure 3.8B). In contrast, no differences were seen in the proportion of low side scatter/insulin+ cells between mice given Wnt+ or Untreated CdM and CAB control mice (Figure 3.8B). Mice given basal media had a decreased proportion of low side scatter/insulin+ cells compared to CAB control mice (Figure 3.8B). These data suggest that regenerated beta cells after STZ treatment contained a qualitatively lower amount of insulin granules compared to healthy beta cells in CAB treated mice.

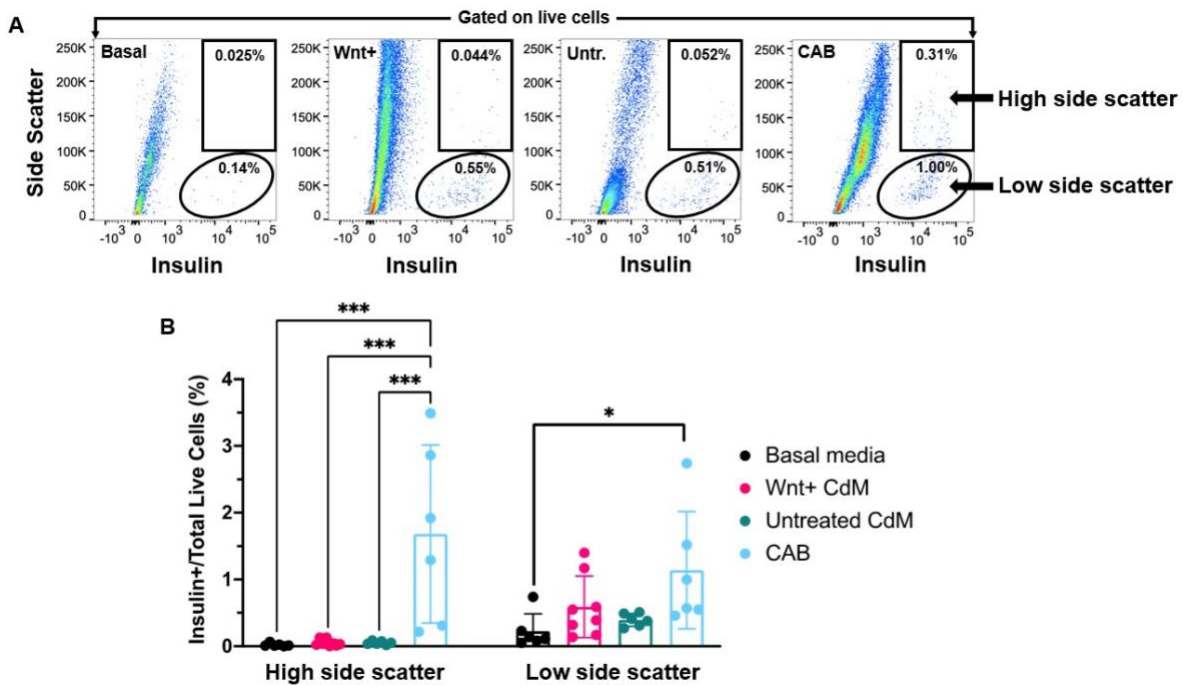


Figure 3.8. High side scatter insulin+ cells were depleted in STZ- and CdM-treated mice compared to healthy CAB control mice. (A) Representative flow cytometry plots showing high side scatter and low side scatter properties of insulin+ cells from STZ-treated mice given basal media (n=7), Wnt+ CdM (n=8), or Untreated CdM (n=6), or mice with healthy islets given citric acid buffer (CAB, n=6). **(B)** Healthy CAB mice demonstrated an increased proportion of high side scatter insulin+ cells measured by flow cytometry compared to all STZ-treated groups (** $p < 0.001$). CAB mice demonstrated an increased proportion of low side scatter insulin+ cells compared to STZ-treated mice given basal media (* $p < 0.05$). Data represent Mean \pm SD compared using a one-way ANOVA followed by Tukey's multiple comparison test. N=5 BM-MSC samples.

3.7 iPAN injection of Wnt+ CdM followed by a 7-day insulin treatment regimen did not improve hyperglycemia, glucose tolerance, or beta cell mass.

Based on previous reports that constant hyperglycemia following STZ treatment can diminish subsequent beta cell regeneration due to glucotoxicity⁶⁸, we hypothesized that treatment with insulin for 7 days following iPAN injection of CdM may normalize blood glucose levels and allow for more stable beta cell regeneration. Hyperglycemic CK19-CreERT Rosa26-mTomato mice (8-10 weeks old) were iPAN-injected on Day 14 with either Wnt+ CdM, Untreated CdM, or basal media and subsequently treated twice daily with insulin glargine from Days 15-21 (Figure 3.9A).

Contrary to what we expected, NFBG levels rebounded following the discontinuation of insulin treatments in mice treated with Wnt+ or Untreated CdM (Figure 3.9B). AUC for NFBG was unchanged between insulin-treated and non-insulin-treated mice given Wnt+ or Untreated CdM, or basal media (Figure 3.9C). At Day 42, no differences were seen between mice given Wnt+ or Untreated CdM, or basal media treated with insulin and mice not treated with insulin in the ability to regulate glycemia following administration of a glucose bolus (Figure 3.9D,E). Beta cell mass and islet number were also unaltered between insulin-treated and non-insulin-treated mice given Wnt+ or Untreated CdM, or basal media (Figure 3.9F,G).

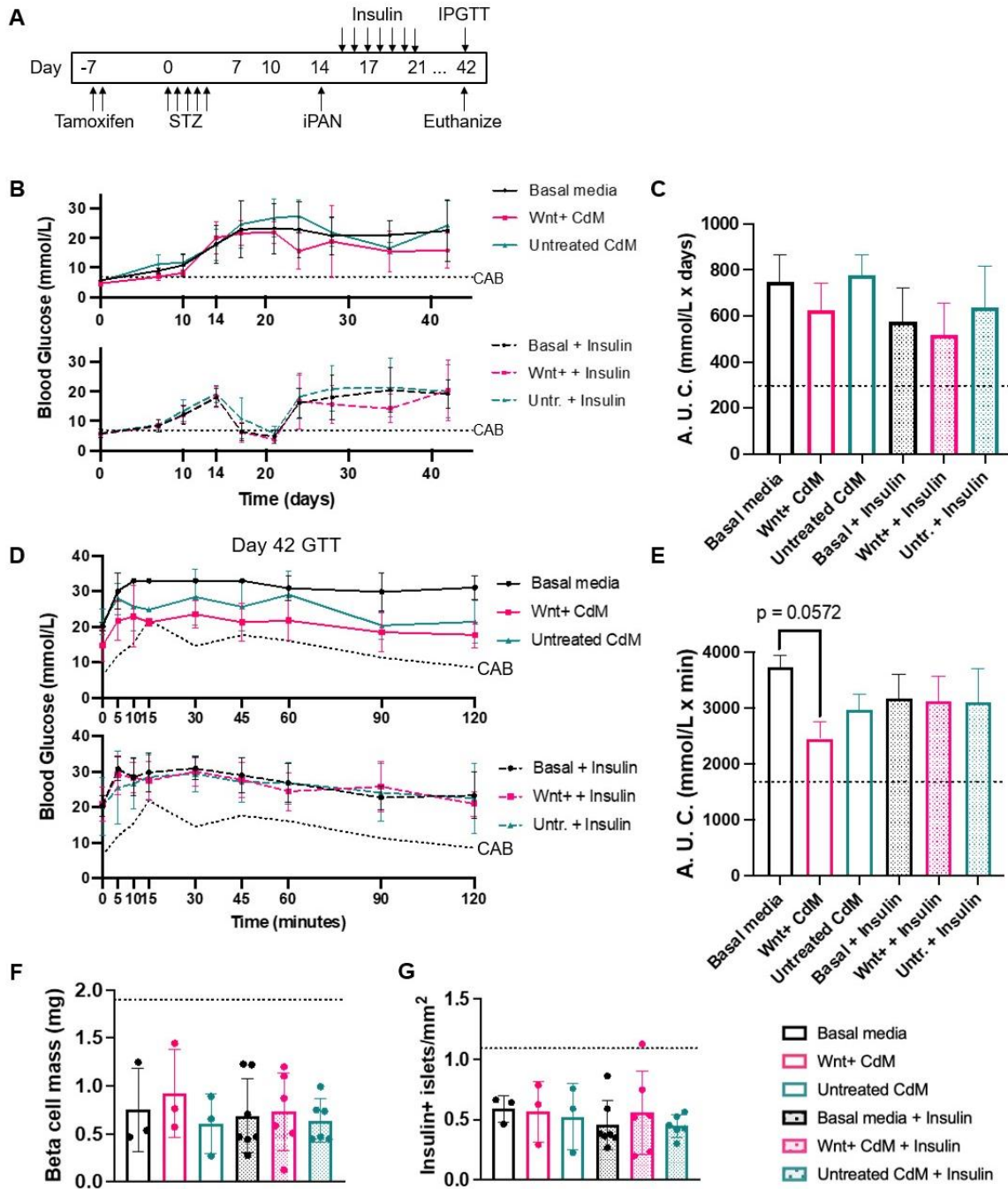


Figure 3.9. Glucose levels and beta cell mass were unchanged following iPAN injection of CdM and 7-day treatment with insulin. (A) CK19-CreERT Rosa26-mTomato mice were treated with 6 mg/day tamoxifen for 2 days and 50 mg/kg/day STZ for 5 days then were iPAN-injected on Day 14 with Wnt+ or Untreated CdM, or basal media. Mice were treated with insulin glargine (10U/kg) from Days 15-21 and euthanized on Day 42. No differences were found for **(B)** non-fasted blood glucose (NFBG) levels or **(C)** area under the curve (AUC) for NFBG between mice treated with basal media (n=3), Wnt+ CdM (n=3), Untreated CdM (n=3), basal media + insulin (n=7), Wnt+ CdM + insulin (n=6), or Untreated CdM + insulin (n=6). On Day 42, mice were given an intraperitoneal glucose tolerance test (GTT). No differences were found for **(D)** glucose levels post-bolus, **(E)** AUC for GTT, **(F)** beta cell mass, or **(G)** insulin+ islet number between groups. Dotted lines represent measurements observed in CAB control mice (n=5). Data represent Mean \pm SD. Glucose curves were compared using a repeated measures two-way ANOVA followed by Tukey's multiple comparison test. AUC, beta cell mass, and insulin+ islet number were compared using a one-way ANOVA followed by Tukey's multiple comparison test. N=3 BM-MSK samples.

3.8 iPAN injection of Wnt+ CdM reduced hyperglycemia and improved glucose tolerance over a 28-day period.

In our pilot experiments of insulin treatment following CdM injection, mice treated with Wnt+ CdM that were not given insulin showed the lowest AUC for glucose tolerance, trending towards significance when compared to basal media (Figure 3.9E). Thus, we decided to explore the effects of Wnt+ CdM on hyperglycemia and glucose tolerance recovery over a pro-longed 42-day period.

Hyperglycemic CK19-CreERT Rosa26-mTomato mice (8-10 weeks old) were iPAN-injected on Day 14 with either Wnt+ CdM, Untreated CdM, or basal media. Remarkably, mice treated with Wnt+ CdM had lower NFBG levels at Days 17, 21, and 35 compared to mice given basal media. In addition, mice treated with Untreated CdM had lower NFBG levels at Day 35 compared to basal media (Figure 3.10A). AUC for pooled NFBG data was reduced in mice treated with Wnt+ CdM compared to basal media (Figure 3.10B). Simple linear regression revealed that intracellular beta-catenin levels of the CHIR-treated BM-MSC used to generate Wnt+ CdM were correlated with AUC of the mice given Wnt+ CdM (Figure 3.10C), suggesting that as the level of Wnt pathway upregulation increased, the regenerative capacity of Wnt+ CdM increased, and blood glucose levels of mice given Wnt+ CdM were decreased.

Male and female mice were also analyzed separately to observe any sex-specific effects of Wnt+ CdM on NFBG. No differences in NFBG levels were seen between male mice treated with Wnt+ or Untreated CdM, or basal media (Figure 3.10D). In contrast, female mice treated with Wnt+ CdM demonstrated reduced NFBG levels at Days 35 and 42 compared to female mice given basal media (Figure 3.10E). AUC was decreased in female mice treated with Wnt+ CdM compared to basal media (Figure 3.10F), suggesting improved glycemic control may be more evident in female vs male mice given Wnt+ CdM.

On Day 42, mice administered Wnt+ and Untreated CdM showed correction of glycemia in response to a glucose bolus, whereas mice given basal media did not (Figure 3.10G,H). Normalization of glucose levels to baseline revealed that, compared to healthy CAB control mice, mice iPAN-injected with Wnt+ CdM, Untreated CdM, or basal media

demonstrated an attenuated response to the glucose bolus (Figure 3.10I). At Day 42, beta cell mass and insulin+ islet number were unchanged in mice given Wnt+ or Untreated CdM compared to basal media (Figure 3.11A-F).

Overall, two functional metrics of glycemic control suggest improved beta cell glucose regulatory function in mice treated with Wnt+ CdM compared to basal media.

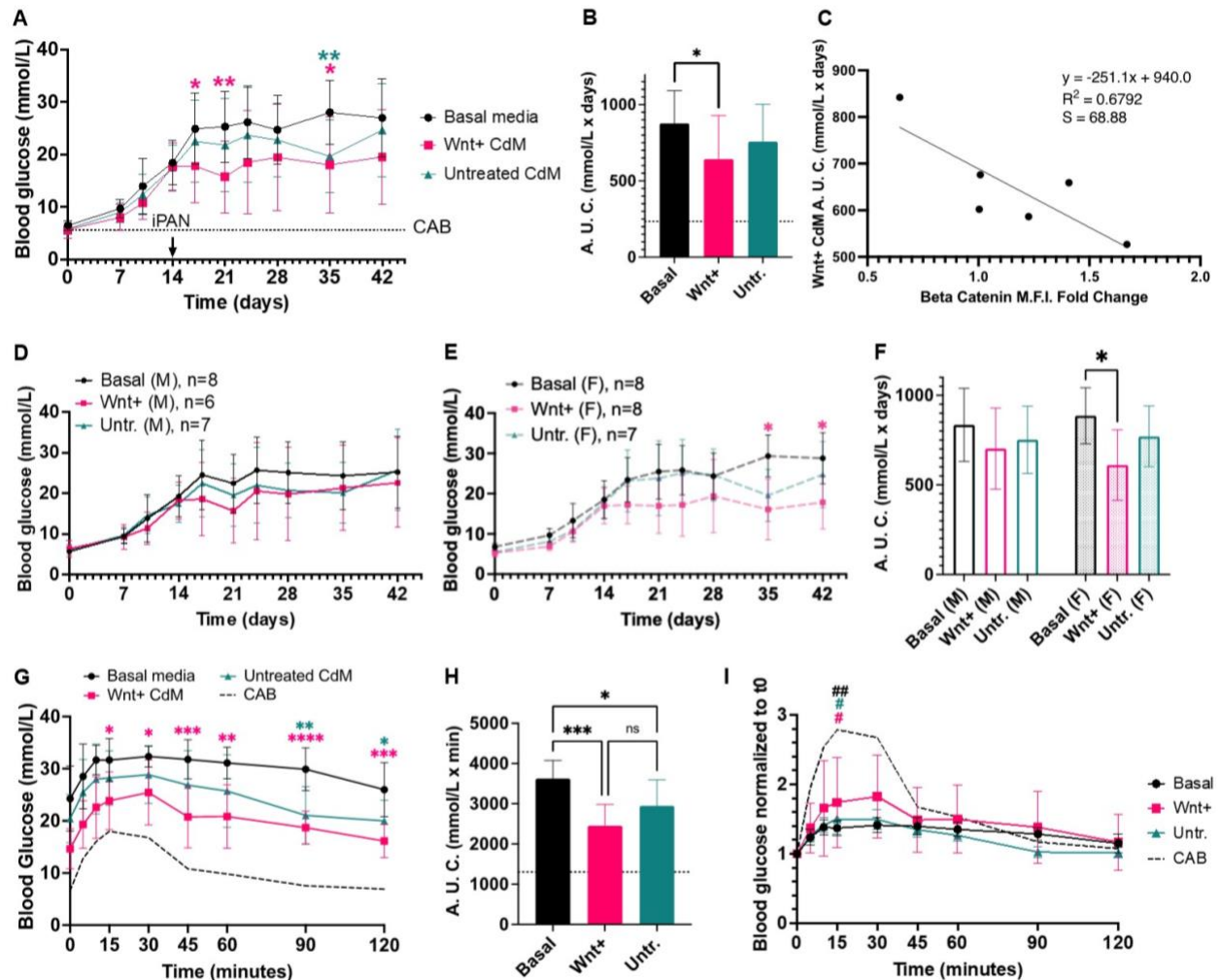


Figure 3.10. iPAN injection of Wnt+ CdM decreased non-fasted blood glucose levels and improved glucose tolerance at Day 42. (A) NFBG levels were consistently reduced in mice iPAN-injected with Wnt+ CdM (n=14) compared to basal media (n=16, *p<0.05, **p<0.01). **(B)** Area under the curve (AUC) for NFBG was lower in mice treated with Wnt+ CdM compared to basal media (*p<0.05). **(C)** Simple lineage regression correlating relative beta-catenin mean fluorescence intensity (M.F.I.) in CHIR-treated BM-MSCs to AUC of mice treated with Wnt+ CdM. **(D)** No differences in NFBG levels were seen between male mice treated with Wnt+ or Untreated CdM, or basal media. Female mice treated with Wnt+ CdM (n=8) had **(E)** reduced NFBG levels at Days 35 and 42 and **(F)** reduced AUC for NFBG compared to basal media (n=8, *p<0.05). On Day 42, mice were given an intraperitoneal glucose tolerance test (GTT). **(G)** Glucose levels and **(H)** AUC for GTT were significantly reduced in mice treated with Wnt+ CdM (n=10, ***p<0.001) and Untreated CdM (n=10, *p<0.05) compared to basal media (n=10). **(I)** Mice iPAN-injected with Wnt+ CdM (#p<0.05), Untreated CdM (#p<0.05), and basal media (##p<0.01) demonstrated an attenuated response to the glucose bolus compared to healthy mice given citric acid buffer (CAB, n=5). Dotted lines represent measurements observed in CAB control mice. Data represent Mean \pm SD. Glucose curves were compared using a repeated measures two-way ANOVA followed by Tukey's multiple comparison test. AUC data were compared using a one-way ANOVA followed by Tukey's multiple comparison test. N=7 BM-MSCs samples.

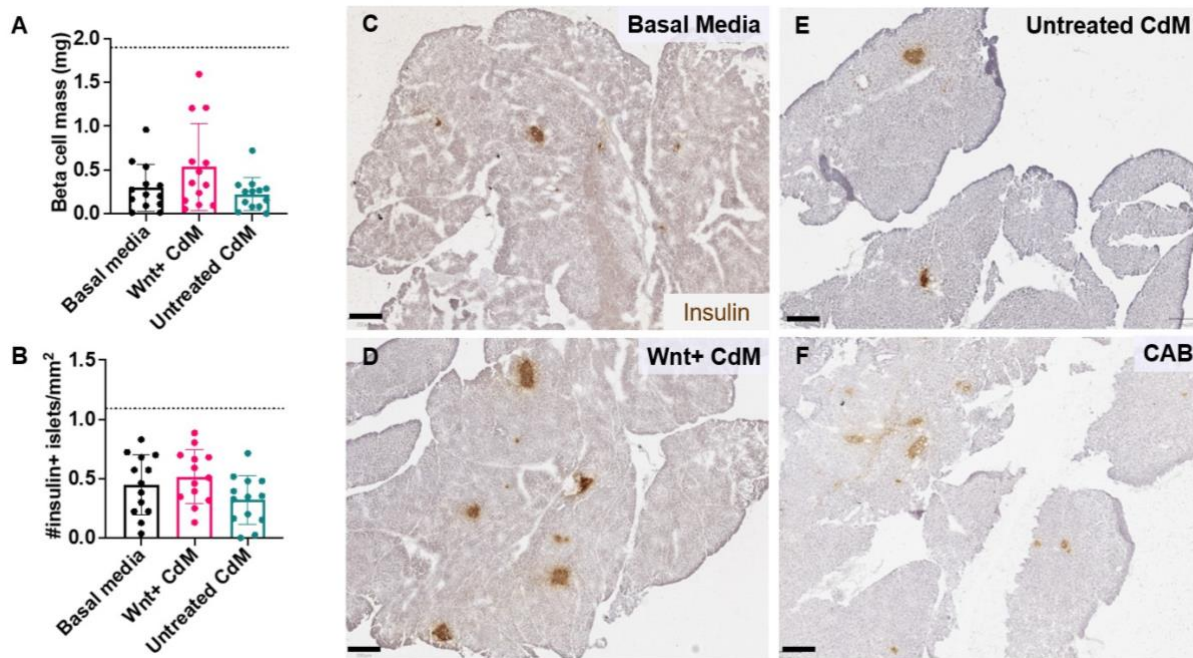


Figure 3.11. iPAN injection of Wnt+ CdM did not change beta cell mass or insulin+ islet number at Day 42. No differences were observed between mice iPAN-injected with Wnt+ CdM (n=13), Untreated CdM (n=13), or basal media (n=13) for **(A)** beta cell mass and **(B)** insulin+ islet number. Representative images of insulin staining in pancreas sections from mice treated with **(C)** basal media, **(D)** Wnt+ CdM, **(E)** Untreated CdM, or **(F)** CAB at Day 42. Scale bars = 250 μ m. Dotted lines represent measurements observed in CAB control mice (n=5). Data represent Mean \pm SD compared using a one-way ANOVA followed by Tukey's multiple comparison test. N=7 BM-MSC samples.

3.9 Increased insulin+ cell labelling with tdTomato observed at Day 21 following iPAN injection of Wnt+ and Untreated CdM is decreased by Day 42.

Histological quantification of total tdTomato+/insulin+ co-stained cells at 3-, 21-, 28-, and 50-days following treatment with 12 mg of tamoxifen revealed that the frequency of beta cells labelled with tdTomato did not change over time in the absence of STZ-mediated beta cell damage and CdM injection (Figure 3.12A).

We performed detailed time course experiments euthanizing cohorts of CdM-treated mice at Days 17, 21, or 42 for analysis of traced beta cells. Mice euthanized at Day 17 (3-days post-injection) showed low levels (<1%) of tdTomato+/insulin+ cells, with no differences observed between groups (Figure 3.12B). However, the frequencies of tdTomato+/insulin+ cells were increased in mice treated with Wnt+ or Untreated CdM from Days 17 to 21 (Figure 3.12B). At Day 21, mice given Untreated CdM showed an increased frequency of tdTomato+/insulin+ cells compared to basal media. Interestingly, by Day 42, the frequencies of tdTomato+/insulin+ cells in mice given Wnt+ or Untreated CdM were decreased compared to Day 21 (Figure 3.12B,E-M), suggesting that ductal or acinar cell conversion to beta cells was heightened at Day 21, but diminished by Day 42.

Previous studies on beta cell neogenesis have regarded small or extra-islet beta cell clusters as evidence that neogenesis had occurred⁶¹. Accordingly, we defined islets as >20 insulin+ cells and small clusters as <10 insulin+ cells and analyzed tdTomato+ beta cells in islets and small clusters independently at the Day 21 timepoint (where CK19+ cell contribution to beta cells was most evident). The frequency of tdTomato+/insulin+ cells in islets was increased in mice treated with Wnt+ CdM or Untreated CdM compared to mice given basal media (Figure 3.12C). For analyses of small clusters only, mice treated with Untreated CdM showed an increased frequency of tdTomato+/insulin+ cells compared to mice treated with Wnt+ CdM (Figure 3.12D). Thus, regenerated beta cells from a CK19+ cell origin were observed within small insulin+ clusters in mice given Untreated CdM. Conversely, mice given Wnt+ CdM showed an increased incorporation of neogenic beta cells from a CK19+ origin in larger islets.

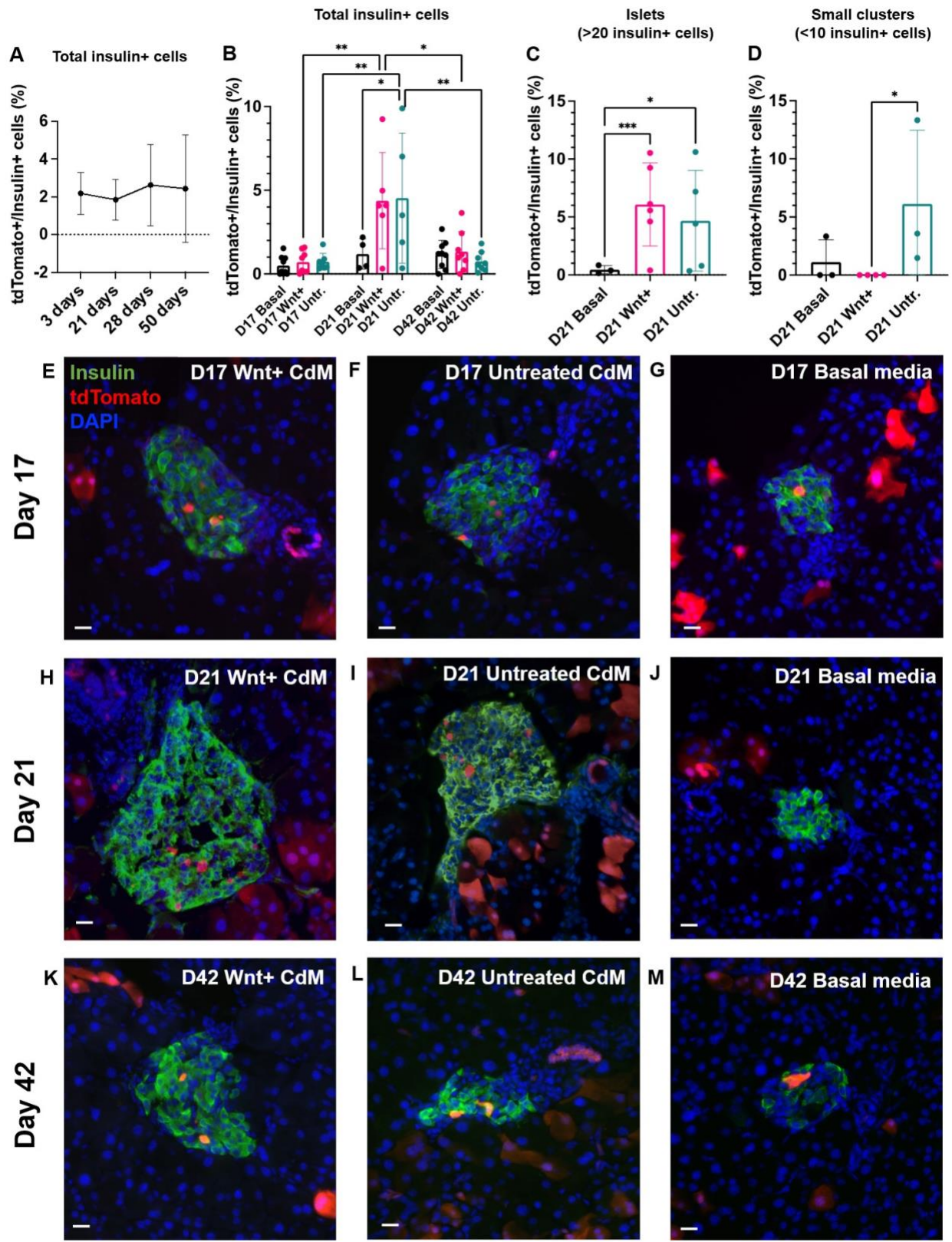
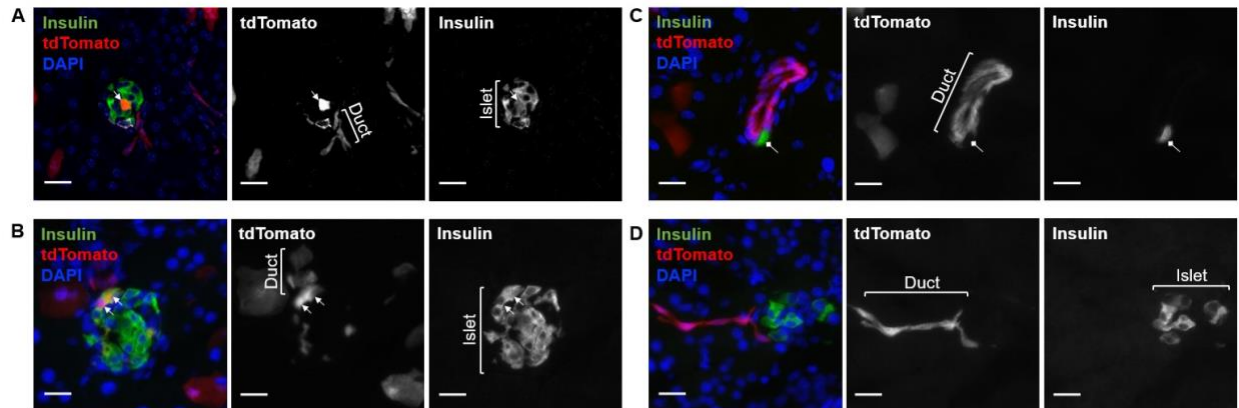


Figure 3.12. iPAN injection of Wnt+ and Untreated CdM increased the frequency of tdTomato+/insulin+ co-expressing cells at Day 21. (A) No differences were seen in the frequency of tdTomato+/insulin+ cells from 3-50 days post-tamoxifen treatment without STZ and CdM injection. **(B)** Mice given Wnt+ CdM (n=6, **p<0.01) or Untreated CdM (n=5, **p<0.01) showed increased frequencies of tdTomato+/insulin+ cells at Day 21 compared to Day 17. At Day 21, mice given Untreated CdM demonstrated a higher frequency of total tdTomato+/insulin+ cells compared to basal media (n=4, *p<0.05). At Day 42, mice given Wnt+ or Untreated CdM showed decreased frequencies of tdTomato+/insulin+ cells compared to Day 21 (*p<0.05, **p<0.01). **(C)** Compared to islets (>20 insulin+ cells) from mice given basal media, islets from mice given Wnt+ CdM (**p<0.001) or Untreated CdM (*p<0.05) showed a higher frequency of tdTomato+/insulin+ cells. **(D)** At Day 21, small clusters (<10 insulin+ cells) from mice given Untreated CdM showed a higher frequency of tdTomato+/insulin+ cells compared to Wnt+ CdM (*p<0.05). Representative images of tdTomato+/insulin+ cells from mice given **(E)** Wnt+ CdM, **(F)** Untreated CdM, or **(G)** basal media at Day 17, **(H)** Wnt+ CdM, **(I)** Untreated CdM, or **(J)** basal media at Day 21, and **(K)** Wnt+ CdM, **(L)** Untreated CdM, or **(M)** basal media at Day 42. Scale bars = 20 μ m. Data represent Mean \pm SD compared using a one-way ANOVA followed by Tukey's multiple comparison test.

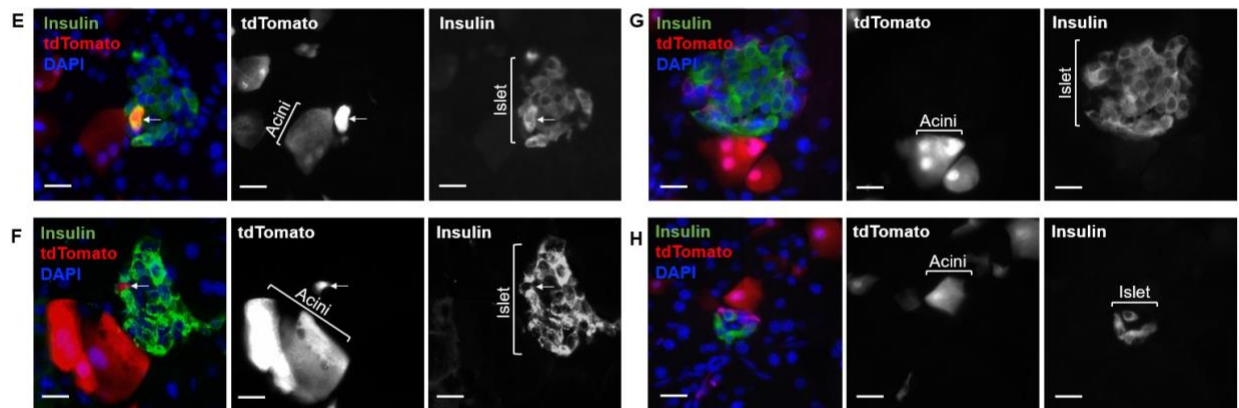
3.10 Regenerated tdTomato+/insulin+ cells may have originated from tdTomato+ ductal, acinar, or beta cells.

The tdTomato+/insulin+ co-expressing cells observed in islets following Wnt+ or Untreated CdM injection could be beta cells that have regenerated via 3 possible mechanisms observed in this model. The most likely mechanism that contributed to the traced beta cell population was ductal or acinar cell differentiation into beta cells, due to the higher labelling efficiency of these cell types. Rare occurrences of tdTomato+ ducts adjacent to tdTomato+/insulin+ cells have been qualitatively observed (Figure 3.13A,B). However, insulin+ cell clusters with no tdTomato labelling were more commonly observed adjacent to tdTomato+ ducts (Figure 3.13C,D). We observed a few instances where tdTomato+/insulin+ cells were located near tdTomato+ acinar cells (Figure 3.13E,F), although we routinely observed labelled acinar cells directly in contact with insulin+ cells with no tdTomato labelling (Figure 3.13G,H). Non-labelled beta cells adjacent to tdTomato+ ducts and acini may have been more common due to incomplete labelling of only 22% of ductal cells with tdTomato. Nevertheless, our qualitative observations suggest that the increase in traced beta cells seen at Day 21 following treatment with Wnt+ or Untreated CdM were likely beta cells originating from previously labelled ductal or acinar cells that differentiated and migrated from exocrine structures into the islets. We also frequently observed tdTomato+/insulin+ cells directly adjacent to one another in islets (Figure 3.13I-L), suggesting some labelled beta cells arose from self-replication of previously labelled beta cells.

Ductal-to-beta mechanism



Acinar-to-beta mechanism



Beta cell duplication

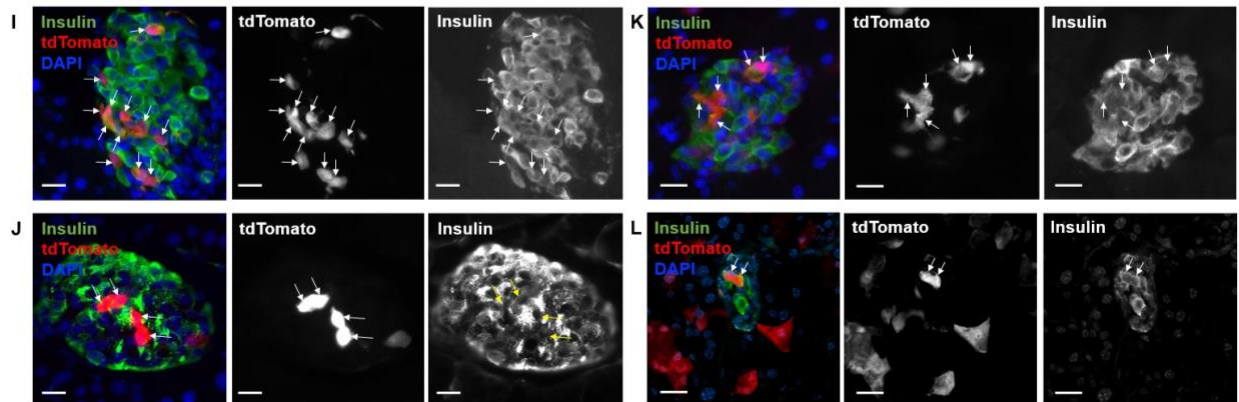


Figure 3.13. Three mechanisms were traced in CK19-CreERT Rosa26-mTomato mice. (A-B) Beta cells that may have originated from adjacent tdTomato⁺ ductal cells. **(C-D)** Beta cells that did not originate from adjacent tdTomato⁺ ductal cells were more commonly observed. **(E-F)** Beta cells that may have originated from adjacent tdTomato⁺ acinar cells. **(G-H)** Beta cells that did not originate from adjacent tdTomato⁺ acinar cells were more commonly observed. **(I-L)** tdTomato⁺ beta cells that may have duplicated were commonly observed. Arrows indicate co-localization of tdTomato and insulin within cells. Scale bars = 20 μ m.

3.11 iPAN injection of CdM did not alter islet-duct association or the frequency of islets with CK19⁺ cells.

We have previously observed that after Wnt⁺ CdM injection, regenerating islets were associated with ductal structures and contained CK19⁺ cells^{140,161}. Islets were designated as associated with ducts if an insulin⁺ islet was in direct contact with or one cell width apart from a CK19⁺ duct. No differences were seen in islet-duct association at Days 21 and 42 between mice given Wnt⁺ or Untreated CdM compared to basal media (Figure 3.14A). However, islets that were associated with ducts were seen at Day 21 (Figure 3.14B-D) and Day 42 (Figure 3.14E-G) in mice given Wnt⁺ CdM, Untreated CdM, or basal media. Furthermore, the frequency of islets that contained CK19⁺ cells at Days 21 was unchanged between mice given Wnt⁺ or Untreated CdM compared to basal media (Figure 3.14H-K). At Day 42, mice treated with Untreated CdM demonstrated an increased frequency of islets with CK19⁺ cells compared to basal media (Figure 3.14H, L-N). Thus, an increased association of regenerated islets with the ductal epithelium was not observed, although CK19⁺ cells may appear within regenerated islets following iPAN injection of CdM.

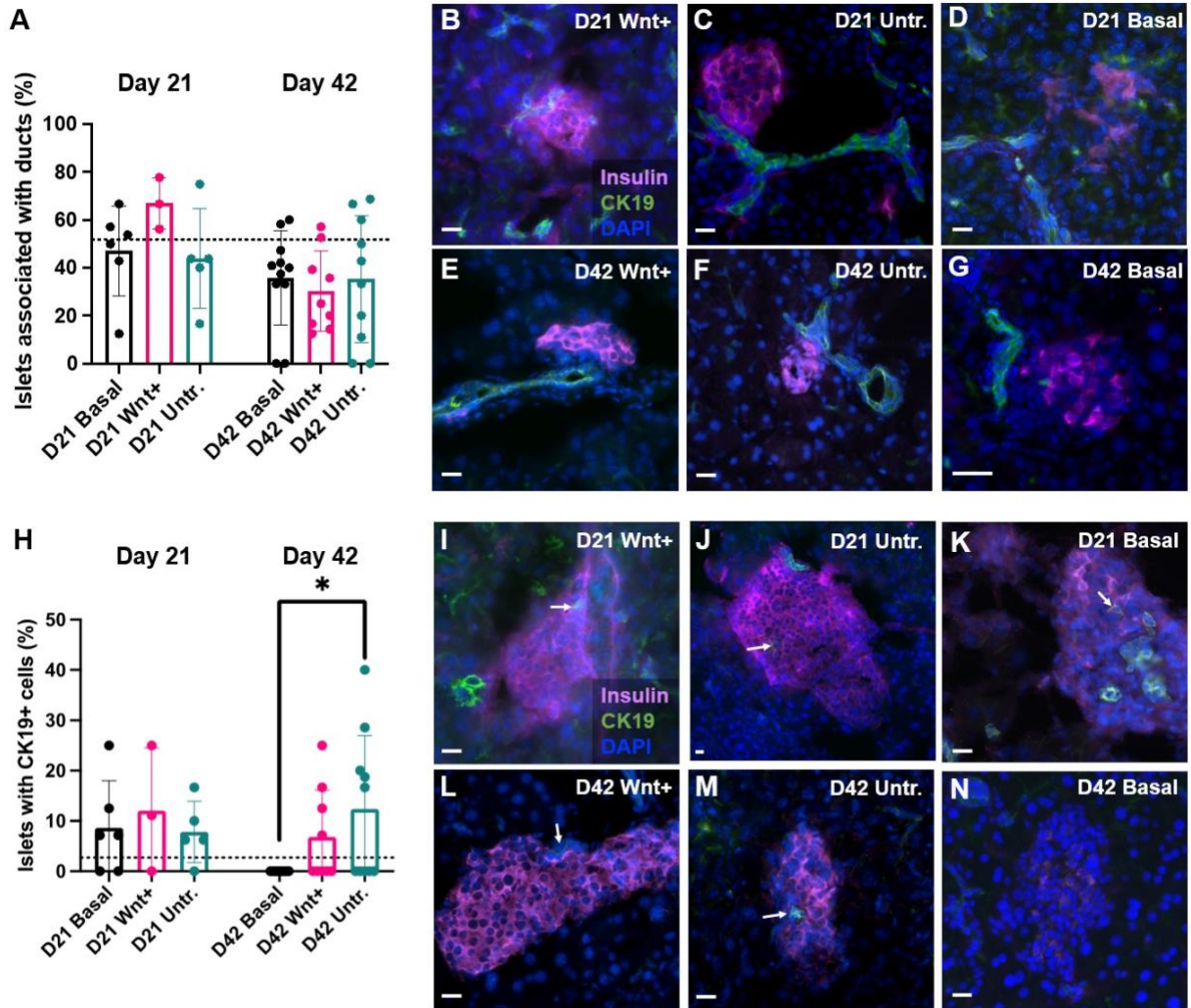


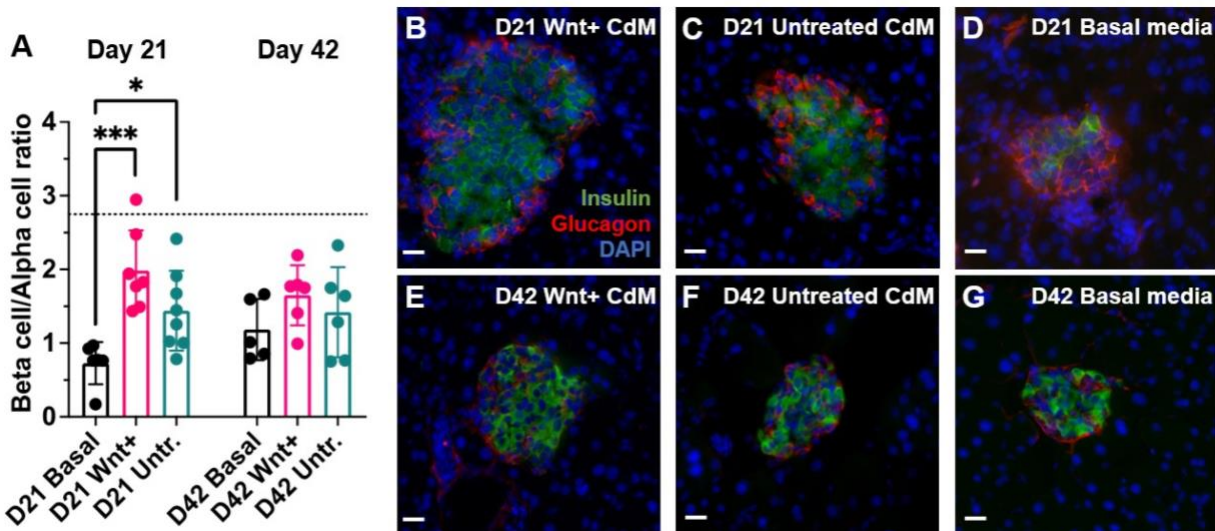
Figure 3.14. Islet-duct association and islets with CK19+ cells were not changed following iPAN injection of Wnt+ CdM. (A) No differences were seen in the frequency of islets associated with CK19+ ducts in mice given Wnt+ CdM, Untreated CdM, or basal media at Days 21 and 42. Representative images of insulin+ islets and CK19+ ducts in mice given (B) Wnt+ CdM, (C) Untreated CdM, or (D) basal media at Day 21, and (E) Wnt+ CdM, (F) Untreated CdM, or (G) basal media at Day 42. (H) At Day 42, mice treated with Untreated CdM showed a higher frequency of islets with CK19+ cells compared to basal media (* $p < 0.05$). Representative images of CK19+ cells in insulin+ islets (indicated by arrows) from mice given (I) Wnt+ CdM, (J) Untreated CdM, or (K) basal media at Day 21, and (L) Wnt+ CdM, (M) Untreated CdM, or (N) basal media at Day 42. Dotted lines represent measurements observed in CAB control mice (n=5). Scale bars = 20 μm . Data represent Mean \pm SD compared using a one-way ANOVA followed by Tukey's multiple comparison test.

3.12 Islets from mice treated with Wnt+ CdM and Untreated CdM demonstrated improved beta cell/alpha cell ratio.

Wildtype mouse islets typically contain a greater percentage of beta cells (85%)²²⁰ compared to alpha cells (7.5%), with beta cells located at the core of the islet and alpha cells located at the islet periphery²²¹. The ratio of insulin+/glucagon+ cells, as a proxy of beta cell/alpha cell ratio, per islet was quantified at Day 21. Mice iPAN-injected with Wnt+ CdM (1.99 ± 0.21 , $p < 0.001$) and Untreated CdM (1.44 ± 0.19 , $p < 0.05$) showed a higher beta cell/alpha cell ratio compared to mice given basal media (0.73 ± 0.12) at Day 21 (Figure 3.15A-D). No differences were seen in beta cell/alpha cell ratio at Day 42 between mice given Wnt+ CdM, Untreated CdM, or basal media (Figure 3.15A,D-G).

3.13 Treatment with STZ followed by Wnt+ CdM delivery increased levels of beta cell proliferation compared to healthy mice.

Our previous study of Wnt+ CdM reported an increase in beta cell proliferation within 1 week of iPAN injection¹⁶¹. Thus, to capture all beta cell proliferation following iPAN injection on Day 14, we injected mice with EdU once daily from Days 14-16 (Figure 3.16A). Mice were euthanized on Day 17 to analyze islets for EdU and insulin co-expression to identify proliferating beta cells. Interestingly, STZ-treated mice given Wnt+ CdM showed a higher frequency of EdU+ beta cells compared to healthy CAB control mice ($1.04 \pm 0.27\%$ vs $0.36 \pm 0.07\%$, $p < 0.05$, Figure 3.16B). No differences were seen in the frequency of EdU+ beta cells at Day 17 between mice treated with Wnt+ CdM, Untreated CdM, or basal media (Figure 3.16B-D), indicating that treatment with STZ can stimulate beta cell proliferation, although no further increase is provided by treatment with Wnt+ CdM.



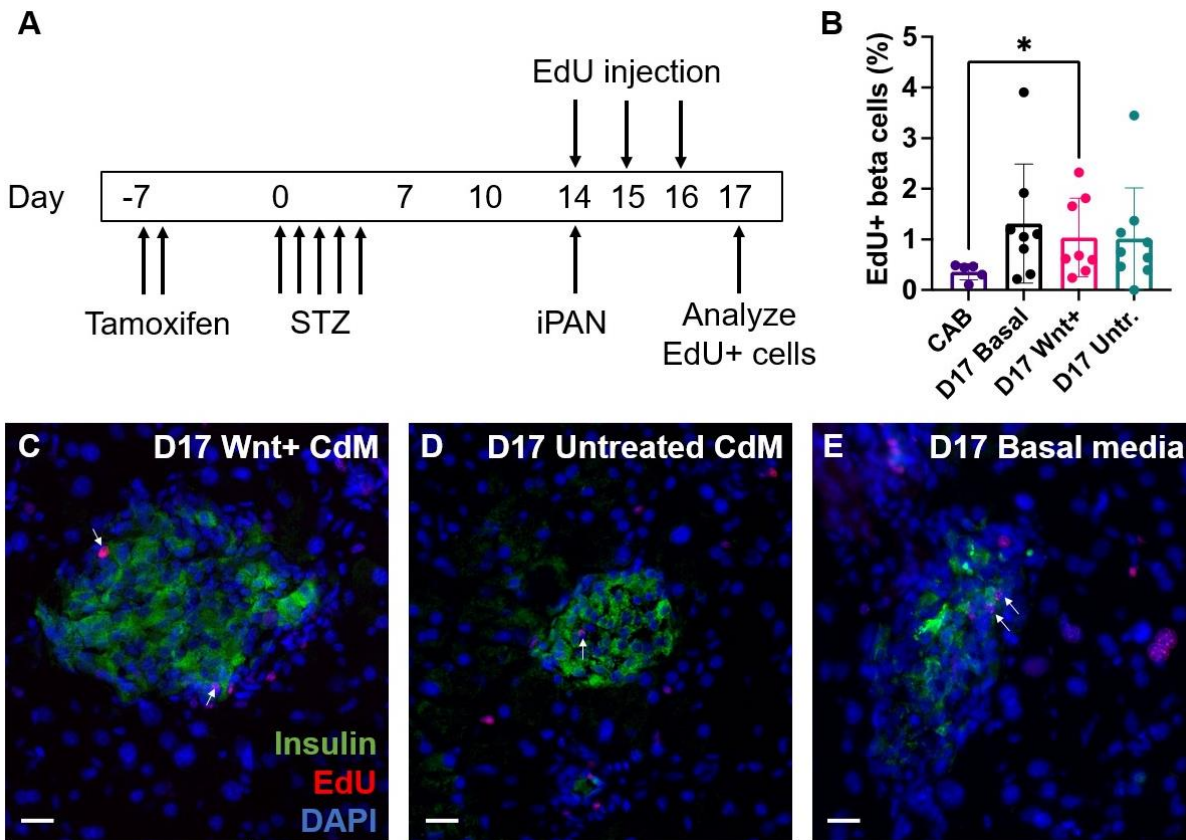


Figure 3.16. The frequency of proliferating beta cells at Day 17 was not changed following iPAN injection of Wnt+ CdM. (A) Mice were iPAN injected with CdM on Day 14 with Wnt+ CdM (n=8), Untreated CdM (n=9), or basal media (n=8) and i.p. injected with 0.25 mg of EdU on Days 14-16. Pancreata were collected for analyses 24 hours following the final EdU injection. **(B)** Compared to healthy CAB controls (n=5), mice treated with Wnt+ CdM demonstrated an increased frequency of EdU+ beta cells (* $p < 0.05$). No differences in the frequency of EdU+ beta cells were found between mice given Wnt+ or Untreated CdM, or basal media at Day 17. Representative images of EdU+/insulin+ beta cells (indicated by arrows) in mice treated with **(C)** Wnt+ CdM, **(D)** Untreated CdM, or **(E)** basal media. Scale bars = 20 μm . Data represent Mean \pm SD compared using a one-way ANOVA followed by Tukey's multiple comparison test.

4.0 Discussion

4.1 Summary of Findings

The following findings contributed to our knowledge of beta cell-regenerative mechanisms induced by iPAN injection of Wnt+ CdM:

- (1) Treatment with CHIR99021 in BM-MSC culture consistently upregulated nuclear beta-catenin levels, indicating canonical Wnt/beta-catenin signalling was activated in CHIR-treated cells.
- (2) Tamoxifen treatment (12 mg) in CK19-CreERT Rosa26-mTomato mice resulted in the mosaic labelling of 22% of pancreatic ductal cells and 17% of acinar cells, and infrequent labelling of 2% of beta cells with tdTomato.
- (3) An STZ dosing regimen of 50 mg/kg/day for 5 days was determined to be optimal to induce hyperglycemia and glucose intolerance in the CK19-CreERT Rosa26-mTomato model.
- (4) iPAN injection of Wnt+ CdM maintained beta cell mass and the number of islets per mm² but did not result in recovery from hyperglycemia within 11 days.
- (5) Mice treated with Wnt+ CdM significantly lowered non-fasted blood glucose levels and increased the ability to regulate a glucose load over a 28-day period compared to controls given basal media.
- (6) At 11 days following iPAN injection of Wnt+ and Untreated CdM, tdTomato+/insulin+ co-expressing cells were increased to ~5% (quantified by flow cytometry and IHC), 4-fold higher than that of controls given basal media.

4.2 Wnt+ CdM delivery in hyperglycemic mice preserved beta cell mass at Day 21, although did not lower hyperglycemia.

The first aim of this project was to assess the capability of Wnt+ CdM to stimulate beta cell regeneration in an immune-competent, lineage tracing mouse model for the first time. At Day 21, Wnt+ CdM delivery maintained beta cell mass and islet number although mice remained unable to regulate NFBG (Figure 3.6). These data indicate that further STZ-induced beta cell damage may be prevented following Wnt+ CdM injection but continued hyperglycemia suggested that the remaining beta cells were insufficient to control glycemia. In healthy mice, islets are comprised of 85% beta cells²²⁰ and 7.5% alpha cells²²¹. Following STZ-mediated beta cell ablation, islets lose beta cells while the alpha cells remain, leading to a decreased beta cell/alpha cell ratio²²². When analyzing islets by IF microscopy, mice iPAN-injected with Wnt+ or Untreated CdM showed an improved beta cell/alpha cell ratio compared to mice given basal media (Figure 3.15), indicating that beta cells may be regenerated by Day 21.

The side scatter profile of cells measured by flow cytometry can provide a unique insight into the granularity of the cell type analyzed. Beta cells release insulin in secretory granules, thus the side scatter profile of cells actively generating insulin granules should be higher than cells that produce less insulin granules. Beta cells from mice given Wnt+ CdM were devoid of high side scatter properties at Day 21 compared to healthy CAB control mice (Figure 3.8), indicating regenerated beta cells qualitatively contained lower insulin granules compared to beta cells from healthy mice. Studies of MSC infusion in STZ-treated rats previously showed that newly regenerated beta cells were not able to fully mature and had improper insulin secretory function¹⁴⁵. It is possible that beta cells observed at Day 21 may require additional stimuli to allow them to mature and properly package and secrete insulin. For example, compared to MSC alone, MSC delivery in combination with Exendin-4, a GLP-1 agonist, further improved glucose-stimulated insulin secretion of beta cells *in vitro* and *in vivo* and increased beta cell expression of maturation markers Pdx1, FoxO1, and MafA¹³⁸. Additionally, the neogenic beta cells may be a 'band-aid' to reduce hyperglycemia and may never become equivalent to wild type beta cells.

Further investigation into the effects of Wnt+ CdM on glucose-stimulated insulin secretion and expression of functional beta cell markers such as GLUT2 in isolated mouse or human pancreatic islets is warranted.

4.3 Insulin treatment following iPAN injection of Wnt+ CdM did not permit enhanced beta cell regeneration.

Prolonged exposure to high systemic glucose levels can cause glucotoxicity-induced apoptosis in beta cells²²³. Cheng et al. (2015) investigated beta cell regeneration following a single high dose of STZ in rats. They observed rapid regeneration 16-24 hours post-STZ treatment, although the putative neogenic beta cell population rapidly diminished over the following days, likely due to glucotoxicity⁶⁸. To combat prolonged glucotoxicity and to allow for stable beta cell regeneration, the investigators treated the rats with a long-acting human insulin analogue for 7 days. They found that, compared to non-insulin treated rats, those treated with insulin demonstrated an increased surviving beta cell number following 7 days of treatment⁶⁸. The effect on beta cell regeneration after discontinuation of insulin treatment was not explored. Thus, we decided to treat mice with insulin for 7 days post-iPAN injection to permit Wnt+ CdM-induced beta cell expansion without glucotoxicity-induced deletion of regenerated beta cells.

Unexpectedly, mice given Wnt+ CdM and subsequently treated with insulin glargine (Lantus) did not maintain reduced glycemia following discontinuation of insulin treatments and were unable to regulate a glucose bolus on Day 42 (Figure 3.9). Further, no differences were seen in NFBG levels between mice treated with insulin and those not treated with insulin over the 28-day period following CdM injection. A study investigating beta cell regeneration following single high-dose STZ treatment in mice found that 120 days, but not 60 days, of insulin treatment was sufficient to restore euglycemia and increase beta cell mass⁷⁵. Islet transplantation resulted in better glycemic control and enhanced restoration of beta cell mass compared to subcutaneous insulin implants⁷⁵. Islets provide additional signals and cues to beta cells, such as somatostatin, pancreatic polypeptide and even small amounts of GLP-1, that improve stable glycemic control often not achieved by insulin treatment alone. Further, it has been found that insulin signalling

and strict glucose regulation were necessary for beta cell maturation and development²¹⁷. Short-term treatment with insulin glargine only partially recovered beta cell maturity following insulin gene deletion in mice, whereas islet transplantation that provided long-term stable glycemic control resulted in mature beta cell formation²¹⁷. Thus, it is possible that a longer period of insulin treatment or islet transplantation is required to allow for consistent recovery from hyperglycemia in our model system.

4.4 Wnt pathway stimulation of BM-MSC may be involved in improved glucose homeostasis.

Mice treated with Wnt+ CdM demonstrated a significant decrease in NFBG levels over a 28-day period post-Wnt+ CdM injection and an improved ability to regulate a glucose bolus at Day 42 compared to mice given basal media (Figure 3.10). Lower NFBG levels at Day 35 and improved glucose tolerance was also observed in mice given Untreated CdM compared to basal media. Additionally, no significant differences in NFBG levels and glucose tolerance were observed between Wnt+ and Untreated CdM.

Canonical Wnt/Beta-catenin signalling is central to stem cell function and has been highly implicated in the regenerative processes of many tissues^{224,225}. BM-MSC communicate with the bone marrow microenvironment via Wnt ligands and Wnt pathway activation plays a fundamental role in MSC fate decisions, proliferation, and clonogenicity¹⁵⁹. Wnt pathway stimulation in BM-MSC has previously generated CdM with improved regenerative potential in STZ-treated mice compared to non-Wnt-stimulated CdM^{149,161}. In these studies, the CHIR-treated and untreated BM-MSC that were used to generate Wnt+ CdM and Untreated CdM were evaluated for beta-catenin expression by flow cytometry. Beta-catenin mean fluorescence intensity (M.F.I.) was consistently upregulated in CHIR-treated BM-MSC relative to Untreated BM-MSC (Figure 3.1). Simple linear regression rendered a slight correlation ($R=0.82$) between increased beta-catenin M.F.I. of 6 CHIR-treated BM-MSC samples and decreased AUC for NFBG levels for mice treated with Wnt+ CdM generated from those samples (Figure 3.10). This is not direct evidence that Wnt-pathway stimulation is crucial to the beta cell regenerative function of

BM-MSc and a thorough comparison of the regenerative factors contained in Wnt+ CdM and Untreated CdM using proteomics or miRNA-sequencing is necessary.

Following PDL in adult mice, Wnt signalling was upregulated in the ductal epithelium and the addition of R-spondin, a potent Wnt-pathway agonist, to pancreatic ductal cell cultures promoted long-term expansion and multipotency²²⁶. Moreover, pancreatic pericyte expression of TCF7L2, a transcription factor downstream of the Wnt-signalling pathway, has been implicated beta cell function. Downregulation of TCF7L2 in pancreatic pericytes resulted in the decreased glucose-stimulated insulin secretion and lower expression of MafA and Pdx1 in beta cells²²⁷. Although differences in glucose regulation were not found between mice given Untreated CdM and Wnt+ CdM, mice given Wnt+ CdM showed larger differences compared to mice given basal media. Thus, Wnt+ CdM containing increased Wnt pathway effectors may provide an extra signal to enhance beta cell regeneration in the pancreas of hyperglycemic mice. Other active signalling pathways and their cross-talk with the Wnt-pathway may also be involved and further exploration into the pathways that affect BM-MSc regenerative function is needed.

4.5 Differences in glycemia reduction were discerned in female mice, but not male mice, treated with Wnt+ CdM once analyzed separately.

Historically, female mice have been excluded from diabetes research, particularly when using STZ models, due to increased variability in glucose levels and increased resistance to STZ-induced hyperglycemia²²⁸. We included both female and male mice in our studies of Wnt+ CdM-induced beta cell regeneration. When stratifying the glucose data based on sex, we found no differences in non-fasted glucose levels amongst male mice given Wnt+ CdM or basal media. Compared to female mice given basal media, female mice given Wnt+ CdM had significantly lower glucose levels at Days 35 and 42 and a reduced AUC (Figure 3.10). Although improved glucose control was more evident in female mice, no differences were seen when directly comparing female and male mice treated with Wnt+ CdM that display similar glucose curves. Furthermore, no differences were seen in beta cell mass and islet number when stratified by sex (data not shown).

Significant differences seen amongst female, but not male, mice may be due to increased hyperglycemia in female vs male mice given basal media.

4.6 Increased beta cell mass following Wnt+ CdM delivery may be confounded by regeneration occurring as a result of STZ-mediated beta cell ablation.

At Day 21, beta cell mass and islet number were increased in mice given Wnt+ CdM. However, at Day 42, this increase was no longer significant and no difference in beta cell mass was observed between mice given Wnt+ CdM or basal media (Figure 3.11). This discrepancy may be explained, in part, by the slight but non-significant increase in beta cell mass and islet number from Days 21 to 42 observed in mice given basal media. There are conflicting reports as to whether beta cells in the adult mouse can regenerate following STZ ablation without additional stimuli. One report suggested regenerative capacity declines in aged mice and found that, following 5 daily injections of low-dose (30 mg/kg) STZ, 2-month-old mice had a modest increase of 0.36% per day in beta cell proliferation whereas 14-month-old mice had a small increase of only 0.04% per day⁶⁹. Another study found, following a single high dose (90 mg/kg) of STZ, beta cell proliferation was diminished in 8-month-old mice compared to 6-week-old mice⁷⁰, although these studies did not consider the contribution of neogenesis. On the other hand, multiple reports have found adaptive beta cell proliferation and re-establishment of beta cell mass via epigenetic changes following STZ-mediated beta cell destruction^{71,72}. One study observed a spontaneous increase (16-fold) in beta cell number 48 hours after a single high dose (65 mg/kg) of STZ in 8-week-old rats⁶⁸. When looking at the pancreas at Days 10 or 14 following STZ treatment (50 mg/kg, Days 0-4), we observed a 70% reduction in beta cell mass compared to healthy CAB control mice (Figure 3.5). Thus, it is possible that 5 daily injections of moderate STZ treatment (50 mg/kg) alone may simulate endogenous beta cell regeneration, contributing to modestly increased beta cell mass that may be augmented by Wnt+ CdM injection. Importantly, we used 8-10 week-old mice in all our studies. Because regenerative capacity of the adult mouse pancreas has shown to decrease over time^{69,70}, future studies of Wnt+ CdM delivery should

investigate the effects of age on beta cell regeneration by comparing the responses of older (>6-month-old) and younger (8-10-week-old) adult mice.

Collectively, we observed improved glucose homeostasis and regulation of glucose load at Day 42 in mice treated with Wnt+ CdM (Figure 3.10), indicating increased beta cell functionality in the pancreas of mice treated with Wnt+ CdM compared to basal media. Spontaneous regeneration following STZ treatment may occur, but it is clear that Wnt+ CdM provides an additional stimulus needed for regenerated beta cell maturation and function. Further investigation into: (1) beta cell maturation over time following iPAN injection of Wnt+ CdM compared to basal media by staining for markers such as MafA and Nkx6.1, and (2) identification of biochemical targets of the regenerative factors contained in Wnt+ CdM using bioinformatics approaches will allow us to further uncover the mechanisms behind glycemic control induced by Wnt+ CdM.

4.7 Wnt+ CdM-stimulated beta cell regeneration in CK19-CreERT Rosa26-mTomato mice was not as strong as in the NOD/SCID model.

Beta cell regeneration induced by Wnt+ CdM injection in CK19-CreERT Rosa26-mTomato mice was not as robust as previously observed in the NOD/SCID model. Following iPAN injection of Wnt+ CdM in NOD/SCID mice, we previously saw a dramatic reduction in glucose levels to the ~10 mmol/L range and normalized glucose tolerance over a 28-day period¹⁶¹. In CK19-CreERT Rosa26-mTomato mice, we observed a stabilization of glucose levels in the 15-20 mmol/L range over the 28-day period following injection of Wnt+ CdM while mice given basal media showed rising glucose levels >25 mmol/L (Figure 3.10). Thus, the marked reduction in hyperglycemia seen in NOD/SCID mice after iPAN injection of Wnt+ CdM was not as vigorously detected in CK19-CreERT Rosa26-mTomato mice.

First, this discrepancy in hyperglycemia reduction ability may be due to the strain-specific differences in the injured state of the pancreas following STZ treatment. The CK19 model used herein, which has a C57BL/6 background, is a fully immune-competent mouse model, unlike the immunodeficient NOD/SCID model. NOD/SCID mice have a mutation in DNA dependent protein kinase that leads to decreased innate immunity and

a complete depletion of mature T and B cells, rendering the NOD/SCID mouse an ideal model to study human cell transplantation²²⁹. Previous characterization of CK19-CreERT Rosa26-mTomato mice, showed that treatment with 60 mg/kg/day STZ for 5 days resulted in an infiltration of CD45+ leukocytes in the pancreas. This immune response to STZ-induced damage was absent in the pancreas of NOD/SCID mice treated with only 35 mg/kg/day STZ for 5 days²¹². Leukocyte infiltration into the islets and surrounding areas and subsequent insulinitis creates a pro-inflammatory microenvironment in the pancreas of CK19 mice, posing an additional barrier to achieving regeneration.

Secondly, in Kuljanin et al. (2019), NOD/SCID mice were treated with a lower dose (35 mg/kg/day) of STZ for 5 days. In contrast, CK19-CreERT Rosa26-mTomato mice required treatment with 50 mg/kg/day of STZ to achieve equivalent hyperglycemia by Day 14 (Figure 3.4). Therefore, a higher dose of STZ may have a more sustained effect on beta cell ablation seen over the 28-day period examined, resulting in altered hyperglycemia recovery kinetics. C57BL/6 mice are typically more sensitive to STZ treatment compared to Balb/cJ mice due to increased STZ metabolite accumulation in C57BL/6 beta cells^{228,230}, possibly hindering regeneration via Wnt+ CdM injection.

Finally, there is variability in glucose homeostasis between different strains of mice. For example, C57BL/6 mice have mutated nicotinamide nucleotide transhydrogenase, an enzyme involved in NADPH synthesis²²⁸. This mutation has been linked to impaired function and reduced glucose stimulated insulin secretion in beta cells²³¹. Thus, STZ accumulation and defective energy metabolism in CK19-CreERT Rosa26-mTomato mice may have a synergistic effect on beta cells and their ability to regenerate.

Interestingly, repeated, high dose tamoxifen administration (0.2 mg/g per day for 5 days) in C57BL/6 mice reduced fasted and random blood glucose levels within 2 weeks following treatment²³². Improved glucose regulation following tamoxifen may occur due to agonistic binding of the estrogen receptor, which can increase beta cell function⁷⁷. Clearly, there are a myriad of variables that could impact the beta cell functional outputs analyzed in these studies.

4.8 Tamoxifen administration in CK19-CreERT Rosa26-mTomato lineage tracing mice resulted the labelling of pancreatic ductal, acinar, and beta cells.

The optimal dose of tamoxifen was determined to be 12 mg (administered at 6 mg per day for 2 days), at which an average of 22% of CK19+ ductal cells were labelled with tdTomato at one-week post-administration (Figure 3.2). In CreERT models, tamoxifen treatment typically results in random recombination of a subset of cells expressing Cre recombinase²⁰³. Accordingly, it was expected that only a portion of CK19+ ductal cells would be labelled with tdTomato. Increasing the dose of tamoxifen further to 18 mg (administered at 6 mg per day for 3 days) resulted in body weight decline in the mice (data not shown), in line with findings that tamoxifen can be toxic to the gastrointestinal tract. Tamoxifen has shown to induce gastric injury involving parietal cell loss, although tissue repair processes recovered this loss by 4 weeks post-tamoxifen²³³. Although the labelling efficiency at 12 mg of tamoxifen was low, labelling 1 in 5 ductal cells was enough to assess whether or not they contributed to Wnt+ CdM-stimulated beta cell regeneration.

To evaluate the specificity of our reporter, we looked at the proportion of tdTomato+ cells that expressed CK19+, the marker chosen for ductal cell tracing. At 12 mg of tamoxifen, an average of 50% of tdTomato+ cells co-stained for ductal marker CK19, quantified by flow cytometry (Figure 3.3). IHC detection of acinar marker Mpx1 and beta cell marker insulin in pancreas sections revealed that 17% of acinar cells and 2% of beta cells were also labelled with tdTomato one-week post-tamoxifen, calling to question the specificity of this CK19-CreERT lineage tracing model. Lowering the dose of tamoxifen to a single dose of 1, 3, or 6 mg did not reduce the labelling frequencies of these off-target cell types. This conflicts with previous reports on the CK19-CreERT Rosa26-YFP mouse that stated <1% of acinar cells were labelled with YFP following 12 mg of tamoxifen²¹³, likely due to our Rosa26-mTomato mice having increased sensitivity to Cre compared to Rosa26-YFP mice previously used²¹⁴. In 2019, Kanayama et al., characterized a CK19-iCre lineage tracing mouse that was crossed to the same Rosa26-mTomato reporter²¹⁴ and found iCre mRNA and tdTomato expression in both pancreatic ductal and acinar cells, although the percentages of labelled acinar and ductal cells were not quantified²³⁴.

To generate CK19-CreERT transgenic mice, CreERT and a polyadenylation signal were inserted upstream of the CK19 start codon, reducing the production of CK19 protein while minimally affecting transcriptional regulatory elements²¹³. We previously considered CK19 to be a ductal-specific marker in the pancreas²³⁵ as staining for CK19 by IHC resulted in a positive signal restricted to the ductal epithelium. Mouse pancreatic acinar cells have reported to express low levels of apical CK19²³⁶ and CK19 expression in acinar cells has shown to be upregulated following caerulein-induced injury²³⁷. Furthermore, acinar cells have shown to contribute to beta cell regeneration following genetic manipulation^{104,186,187} and pancreatic ductal ligation¹⁷¹. Thus, low activity at the CK19 promoter may be enough to induce Cre-recombination without producing a detectable level of CK19 protein.

On the other hand, beta cells were not known to express CK19^{203,238} and we did not detect expression of CK19 in tdTomato+ beta cells of control mice via IHC. This brings about the question of whether Cre recombinase was expressed in beta cells or if the Rosa26-mTomato reporter was leaky and tdTomato was expressed in cells without Cre recombination. CK19-CreERT Rosa26-mTomato mice given corn oil only did not display tdTomato expression (Figure 3.2A,B), indicating that Cre entry into the nucleus was required for tdTomato expression. Cre recombinase mRNA or protein levels in beta cells should be evaluated to confirm the reason behind tdTomato expression in these beta cells. For the purposes of this thesis, ductal, acinar, and beta cells were regarded as having equal potential to contribute to beta cell regeneration following Wnt+ CdM, although newly formed tdTomato+ beta cells were more likely to originate from ductal or acinar cells that showed increased labelling with tdTomato (22% and 17%) compared to beta cells that showed minimal labelling with tdTomato (2.2%). Other pancreatic cell types may also be labelled with tdTomato following tamoxifen administration. The relative activity of Cre recombinase in different pancreatic cell types can be investigated using a Cre reporter mouse (Jackson Labs #013587) that labels cells with either GFP or tdTomato depending on their level of Cre recombinase expression.

4.9 Pancreatic ductal cells as the origin of regenerated beta cells?

The primary objective of this project was to trace CK19+ ductal cells in the pancreas following Wnt+ CdM-induced islet regeneration. We investigated co-expression of tdTomato, our lineage tracing marker, with insulin and glucagon by flow cytometry and IF microscopy. Most previous ductal lineage tracing studies have found ductal-to-beta cell conversion after PDL-induced injury, indicating that ductal cells may act as facultative beta cell progenitors^{62,64,199,206,226,239}. Indeed, autoimmune diabetes and inflammatory cytokine-induced damage to the mouse pancreas *in vivo* and human ductal cells *in vitro* has resulted in ductal-to-endocrine cell conversion indicated by the acquisition of Ngn3 and pro-insulin in ductal cells²³⁹. Evidence for a dedicated ductal cell progenitor that contributes to regular beta cell turnover in the adult pancreas has not been found until recently^{170,203,204}. Gribben et al. (2021) used adult Hnf1b lineage tracing mice to observe that ductal cells contributed to 0.66% of the insulin+ cell population per week during islet homeostasis²⁰⁴. We analyzed the population of insulin+ cells labelled with tdTomato at 3, 21, and 28 days following tamoxifen treatment alone (without STZ or CdM injection) and did not see any differences in the frequency of labelled insulin+ cells over time when analyzed via flow cytometry (Table 3.1) or IHC (Figure 3.12), although it is possible that a longer study period is required for slight changes in the labelled beta cell population to become apparent.

At Day 21, mice injected Wnt+ CdM demonstrated an increased frequency of tdTomato+ and insulin+ co-expressing cells compared to mice injected with basal media by flow cytometry (Figure 3.7B,F). 3D z-stack imaging confirmed that insulin and tdTomato were directly co-localized within islet cells (Supplementary Figure 1). Intriguingly, the percentage of insulin+ cells labelled with tdTomato was higher in mice given Wnt+ CdM compared to STZ-treated mice euthanized on Day 10, the day of iPAN injection ($5.04 \pm 3.41\%$ vs $0.77 \pm 0.68\%$, $p < 0.05$, Table 3.2), indicating >4% of regenerated insulin+ cells originated from tdTomato+ progenitors, likely previously labelled ductal or acinar cells. When analyzing tdTomato labelling in total insulin+ cells by IHC at Day 21, mice given Untreated CdM showed an increased frequency of tdTomato+/insulin+ cells compared to basal media, whereas mice given Wnt+ CdM did not (Figure 3.12). When

looking at small insulin+ clusters (<10 insulin+ cells) and larger islets (>20 insulin+ cells) separately at Day 21, islets from mice given Wnt+ CdM showed an increased frequency of tdTomato+/insulin+ cells compared to basal media, whereas small insulin+ clusters from mice Wnt+ CdM did not show any tdTomato+ labelling (Figure 3.12).

At Day 17, 3-days post-iPAN injection, the labelled insulin+ cell population was low as beta cell regeneration was not yet evident. There was a substantial increase in the proportion of insulin+ cells labelled with tdTomato from Day 17 to Day 21 in mice given Wnt+ CdM ($0.71 \pm 0.23\%$ vs $4.37 \pm 1.18\%$, $p < 0.01$) or Untreated CdM ($0.73 \pm 0.19\%$ vs $4.53 \pm 1.74\%$, $p < 0.01$), indicating that a boost of beta cell regeneration, likely from a CK19+ ductal or acinar origin, may occur during a critical period of 3-10 days after iPAN CdM injection. From Day 21 to Day 42, the frequency of labelled insulin+ cells also decreased in mice given Wnt+ CdM ($4.37 \pm 1.18\%$ vs $1.34 \pm 0.42\%$, $p < 0.05$) or Untreated CdM ($4.53 \pm 1.74\%$ vs $0.74 \pm 0.21\%$, $p < 0.05$), suggesting that CK19-traced tdTomato+ islet cells were diluted as additional sources of regenerated cells contributed to the islet population. Overall, our data provides evidence that CK19+ ductal and/or acinar cells showed a partial contribution to beta cell regeneration stimulated by Wnt+ CdM within 10-days following iPAN injection. Of note, the contribution of ductal-derived progenitor cells to islet regeneration may be underestimated as only 22% of ductal cells were labelled with tdTomato following 12 mg of tamoxifen. If the labelling efficiency was increased and all ductal cells were traced, we would expect the contribution of ductal cells to the regenerated beta cell population to be more evident, with a further increase in the frequency of tdTomato+/insulin+ cells after Wnt+ CdM injection.

If regenerated beta cells were derived from ductal progenitor cells, we may have observed insulin+ cells labelled with tdTomato nearby or directly adjacent to tdTomato+ ducts. Although the frequency of this occurrence was not directly quantified, we did observe rare instances of tdTomato+/insulin+ cells in the proximity of tdTomato+ ducts following the delivery of Wnt+ or Untreated CdM (Figure 3.13 A,B). More commonly, we detected insulin+ cells not labelled with tdTomato directly adjacent to ducts that were fully labelled with tdTomato (Figure 3.13). Although it is possible that these cells arose from a non-labelled ductal cell, we can be certain that these islets did not come from fully labelled

ducts. Lastly, regenerated islets containing substantial frequency of tdTomato+ cells were not observed following iPAN injection of Wnt+ CdM, thus CK19+ ductal-derived progenitor cells were highly unlikely to repopulate entire islets via clonal expansion.

The same principle holds true for acinar-to-beta cell conversion. Occasionally, tdTomato+/insulin+ cells were seen in direct contact with or in the proximity of tdTomato+ acini, suggesting these labelled beta cells may have been derived from labelled acinar cells. However, we quite frequently detected labelled acinar cells in proximity with non-labelled beta cells. Thus, acinar-to-beta cell transition remains plausible in this model.

Since we did not commonly observe tdTomato+/insulin+ cells next to tdTomato+ ducts nor did we observe an increase in islet-duct association following treatment with Wnt+ CdM, it is possible that the regenerated labelled beta cells budded from labelled ducts and migrated into pre-existing islets. Recently, Ngn3+ cell lineage tracing found that ductal cells contained a progenitor cell population that displayed multipotent endocrine differentiation²⁰⁴. The contribution of these ductal cells to islet regeneration may have required cell migration as Ngn3-traced small insulin+/somatostatin+ clusters were observed between ducts and islets during both homeostasis and during AKITA mutation-induced diabetes²⁰⁴. Further investigation into the downregulation of cell adhesion molecules and expression of epithelial-to-mesenchymal markers in traced ductal and insulin+ cells is needed to further decipher this mechanism.

Finally, it is possible that there is a subset of ductal cells with unique ability to dedifferentiate and contribute to beta cell regeneration via a developmental mechanism. Single-cell RNA sequencing of mouse pancreatic ductal cells has shown that distinct ductal subpopulations such as OPN+/TFF1+ ductal cells²⁴⁰ and ALK3+/PDX1+/CAII-ductal cells²⁴¹ retain progenitor cell-like characteristics. A proposed mechanism of beta cell neogenesis involves a de-differentiation of a subset of ductal cells that acquire Ngn3 expression prior to differentiating into insulin-producing cells^{62,63,204,206,242,243}. Ductal cells primed to acquire Ngn3 expression and serve as endocrine lineage progenitor cells may represent a potential “signal-receiving” cell for Wnt+ CdM-stimulated beta cell regeneration. Future lineage tracing studies following STZ treatment and subsequent iPAN injection of Wnt+ CdM should investigate ductal-focused mechanisms using an

Ngn3 genetic lineage tracing model to assess whether Ngn3+ cells uniquely contribute to the regenerated beta cell population .

4.10 Other mechanisms of Wnt+ CdM-induced beta cell regeneration may be at play.

Another possible mechanism of beta cell regeneration that may have occurred is alpha-to-beta cell transition. Glucagon and insulin co-localization in islets was previously seen at early timepoints iPAN injection of Wnt+ CdM¹⁶¹. The expression of MafA, a master regulator of insulin transcription, and Nkx6.1, a transcription factor critical to beta cell function, was also observed in glucagon+ cells following Wnt+ CdM delivery¹⁶¹. In our study, we used flow cytometry to more accurately quantify insulin and glucagon co-expressing cells. At Day 21, no differences were seen in the frequency of insulin+ cells that co-expressed glucagon in mice treated with CdM (Figure 3.7). Further, the frequency of tdTomato+ cells that co-expressed glucagon was low and remained unchanged between groups, suggesting that the beta cell regeneration observed did not transition significantly via an alpha cell intermediate.

Beta cell replication may contribute to regeneration of beta cell mass in this model. Kuljanin et al. (2019) found that beta cell proliferation, detected by *in vivo* EdU incorporation, was increased in the pancreas of mice treated with Wnt+ CdM compared to basal media at early time points (1 and 3 days following iPAN injection)¹⁶¹. Other groups have also concluded that beta cell proliferation is the prevailing mechanism of beta cell expansion in the adult mouse^{78,179,180}. Thus, the decline in frequencies of tdTomato+/insulin+ cells seen from Day 21 to Day 42 may be a result of increased beta cell replication. Since only 2.2% of beta cells were labelled following tamoxifen and this fell to 0.8% after STZ alone, proliferation of non-labelled cells would have diluted the labelled population over time. Although the prevalence of multiple adjacent tdTomato+ beta cells was not quantified, we commonly observed numerous tdTomato+ beta cells adjacent to one another (Figure 3.13).

Surely, analysis of EdU+/insulin+ cells at Day 17 revealed that beta cell replication was increased in Wnt+ CdM-treated mice compared to healthy mice given CAB (1.04±0.27% vs 0.36±0.07%, p<0.05). No differences were seen between mice given

Wnt+ CdM and mice given Untreated CdM or basal media (Figure 3.16). This indicates that beta cell proliferation was increased following STZ treatment and no further increase was seen following delivery of Wnt+ CdM. Tamoxifen has shown to have cytostatic effects on beta cells in C57BL/6 mice, reducing beta cell proliferation by 59% at high doses of up to 40 mg administered over 5 days²³². Studies investigating beta cell proliferation using lineage tracing models should be aware of this limitation imposed by tamoxifen-inducible Cre systems and may consider other mechanisms of temporal gene expression such as the reverse tetracycline trans-activator (rtTA) doxycycline-inducible system.

4.11 Limitations

Herein, we present a thorough characterization of Wnt+ CdM-induced beta cell regeneration in CK19 lineage tracing mice at early (Day 21) and late (Day 42) timepoints. However, there are a few confounding variables that may have influenced the results of this study. The product used to collect and concentrate MSC CdM differed between the Day 21 and majority of the Day 42 experiments. For the Day 21 experiments and some of the Day 42 experiments, CdM was concentrated 40x in spin columns with a regenerated cellulose membrane and diluted in AmnioMAX™ basal media to a protein concentration of approximately 0.1-0.3 µg/µl. These columns became unavailable for purchase, thus we switched to a polyethersulfone (PES)-based column for subsequent Day 42 experiments. These PES columns allowed for a maximum 20x concentration of CdM, allowing for a protein concentration of 0.1-0.2 µg/µl. This may have contributed to the variability seen within groups at Day 42 and differences when comparing Day 21 and Day 42 data. Aside from protein there are miRNAs, exosomes, and other biological factors that can effect beta cell regeneration once injected into the pancreas. Future studies should focus on developing reliable methods to concentrate and standardize the biological molecules contained in BM-MSC CdM to ensure consistency and reproducibility of results.

During iPAN injection, a microneedle is used to inject 20 µL of CdM into the splenic portion of the pancreas¹³⁶. The precise location where the needle dispenses CdM into the pancreas may vary from injection to injection. Thus, CdM may be retained in the pancreas

at different rates and the failure to consistently reduce hyperglycemia close to normoglycemic levels following iPAN injection of Wnt+ CdM may be due to differences in the availability of MSC-secreted stimuli to signal receiving cells within the pancreas. Furthermore, injection of CdM into the tail portion of the pancreas may not reach the head portion of the pancreas and future studies should compare evidence for beta cell regeneration in the head vs tail of the pancreas following CdM injection. Finally, the stability and longevity of BM-MSC-secreted factors once injected into the pancreas is unknown and it is possible that multiple injections of Wnt+ CdM are needed to achieve a more consistent and sustained reduction of non-fasted glucose levels.

There were some limitations when using the CK19-CreERT Rosa26-mTomato model to assess whether pancreatic ductal cells generate new beta cells following iPAN injection of Wnt+ CdM. Firstly, upon administration of 12 mg of tamoxifen only 22% of CK19+ cells were labelled with tdTomato. Consequently, only a portion of ductal cells could be traced and observed as contributing to beta cell neogenesis. Whether or not CK19+ ductal cells contributed to Wnt+ CdM-stimulated beta cell regeneration could still be assessed, although the absolute contribution couldn't be accurately quantified as only 1 in 5 CK19+ cells were labelled.

The labelling of 16.8% of pancreatic acinar cells and 2.2% of beta cells with tdTomato upon tamoxifen administration was unexpected as CK19 was considered a ductal cell-specific marker in the pancreas. For the purposes of this study it was presumed beta and acinar cells may also contribute to beta cell regeneration. Thus, all 3 cell types were traced and interrogated as potential sources of newly regenerated beta cells. It is possible that other cell types in the pancreas were labelled with tdTomato following tamoxifen administration, although we did not investigate tdTomato expression in every pancreatic cell type. An alternate high efficiency, ductal-specific lineage tracing model, such as the Hnf1b-CreERT mouse^{203,204}, could be used in future experiments to exclude the contribution of acinar cells and confirm the contribution of ductal cells to Wnt+ CdM-induced beta cell regeneration.

4.12 Significance

A curative therapy for diabetes would be transformative for patients living with this all-consuming disease. Stimulating endogenous regeneration using conditioned media derived from BM-MSC grown under Wnt pathway stimulation (Wnt+ CdM) remains a promising approach to replenish lost beta cells in individuals with diabetes. Given the controversy surrounding the occurrence of beta cell neogenesis from a resident precursor in the adult pancreas, an investigation into the cellular mechanisms by which Wnt+ CdM stimulated beta cell regeneration was highly warranted. Overall, results of the studies outlined in this thesis suggest that iPAN injection of Wnt+ CdM can stimulate beta cell regeneration in the presence of an active immune system following STZ-mediated beta cell ablation. Lineage tracing of CK19+ cells revealed ductal and/or acinar cells show a minor contribution to beta cell regeneration induced by Wnt+ CdM. In conclusion, these studies are not only critical to our understanding of Wnt+ CdM as a protein-based regenerative therapy for diabetes, but also attempt to lend support for the existence of a ductal-derived beta cell progenitor in the adult pancreas. This body of work contributes to our growing knowledge base on the turnover and plasticity of pancreatic cell types for the advancement of regenerative medicine therapies for pancreatic disorders.

References

1. Diabetes. World Health Organization. <https://www.who.int/news-room/fact-sheets/detail/diabetes>. Published 2020. Accessed February 22, 2021.
2. Chen C, Cohrs CM, Stertmann J, Bozsak R, Speier S. Human beta cell mass and function in diabetes: Recent advances in knowledge and technologies to understand disease pathogenesis. *Mol Metab.* 2017;6(9):943-957. doi:10.1016/j.molmet.2017.06.019
3. American Diabetes Association. Classification and diagnosis of diabetes: Standards of medical care in diabetes. *Diabetes Care.* 2019;42:S13-S28. doi:10.2337/dc19-S002
4. Diabetes rates continue to climb in Canada. Diabetes Canada.
5. New Data Shows Diabetes Rates And Economic Burden On Families Continue To Rise In Ontario. Diabetes Canada. <https://www.diabetes.ca/media-room/press-releases/new-data-shows-diabetes-rates-and-economic-burden-on-families-continue-to-rise-in-ontario-->. Published 2019. Accessed February 22, 2021.
6. Rawshani A, Sattar N, Franzén S, et al. Excess mortality and cardiovascular disease in young adults with type 1 diabetes in relation to age at onset: a nationwide, register-based cohort study. *Lancet.* 2018;392(10146):477-486. doi:10.1016/S0140-6736(18)31506-X
7. Mayer-Davis EJ, Lawrence JM, Dabelea D, et al. Incidence Trends of Type 1 and Type 2 Diabetes among Youths, 2002–2012. *N Engl J Med.* 2017;376(15):1419-1429. doi:10.1056/nejmoa1610187
8. Patterson CC, Harjutsalo V, Rosenbauer J, et al. Trends and cyclical variation in the incidence of childhood type 1 diabetes in 26 European centres in the 25 year period 1989–2013: a multicentre prospective registration study. *Diabetologia.* 2019;62(3):408-417. doi:10.1007/s00125-018-4763-3
9. Kondrashova A, Reunanen A, Romanov A, et al. A six-fold gradient in the incidence of type 1 diabetes at the eastern border of Finland. *Ann Med.* 2005;37(1):67-72. doi:10.1080/07853890410018952
10. Patterson CC, Karuranga S, Salpea P, et al. Worldwide estimates of incidence, prevalence and mortality of type 1 diabetes in children and adolescents: Results from the International Diabetes Federation Diabetes Atlas, 9th edition. *Diabetes Res Clin Pract.* 2019;157:107842. doi:10.1016/j.diabres.2019.107842
11. Lawrence JM, Divers J, Isom S, et al. Trends in Prevalence of Type 1 and Type 2 Diabetes in Children and Adolescents in the US, 2001-2017. *JAMA - J Am Med Assoc.* 2021;326(8):717-727. doi:10.1001/jama.2021.11165
12. MacDonald MJ, Gottschall J, Hunter JB, Winter KL. HLA-DR4 in insulin-dependent diabetic parents and their diabetic offspring: A clue to dominant

- inheritance. *Proc Natl Acad Sci U S A*. 1986;83(18):7049-7053.
doi:10.1073/pnas.83.18.7049
13. Stankov K, Benc D, Draskovic D. Genetic and epigenetic factors in etiology of diabetes mellitus type 1. *Pediatrics*. 2013;132(6):1112-1122.
doi:10.1542/peds.2013-1652
 14. Virtanen S. Dietary factors in the development of type 1 diabetes. *Pediatr Diabetes*. 2016;17(S22):49-55.
 15. Diaz-Horta O, Baj A, Maccari G, Salvatoni A, Toniolo A. Enteroviruses and causality of type 1 diabetes: how close are we? *Pediatr Diabetes*. 2012;13(1):92-99.
 16. Kolb H, Martin S. Environmental/lifestyle factors in the pathogenesis and prevention of type 2 diabetes. *BMC Med*. 2017;15(131). doi:10.1186/s12916-017-0901-x
 17. Langenberg C, Lotta LA. Genomic insights into the causes of type 2 diabetes. *Lancet*. 2018;391(10138):2463–2474.
 18. Arner P, Arner E, Hammarstedt A, Smith U. Genetic Predisposition for Type 2 Diabetes, but Not for Overweight/Obesity, Is Associated with a Restricted Adipogenesis. *PLoS One*. 2011;6(4):e18284.
doi:10.1371/journal.pone.0018284.t001
 19. Thorens B. GLUT2, glucose sensing and glucose homeostasis. *Diabetologia*. 2015;58(2):221-232. doi:10.1007/s00125-014-3451-1
 20. Culina S, Brezar V, Mallone R. Insulin and type 1 diabetes: immune connections. *Eur J Endocrinol*. 2012;168(2):R19–R31.
 21. Thomas H, Kay T. Intracellular pathways of pancreatic β -cell apoptosis in type 1 diabetes. *Diabetes Metab Res Rev*. 2011;27:790–796. doi:10.1002/dmrr
 22. Yuan T, Annamalai K, Naik S, et al. The Hippo kinase LATS2 impairs pancreatic β -cell survival in diabetes through the mTORC1-autophagy axis. *Nat Commun*. 2021;12(1):1-18. doi:10.1038/s41467-021-25145-x
 23. Zhang Z, Gao Y, Meng ZX. Transcriptional control of pancreatic β -cell identity and plasticity during the pathogenesis of type 2 diabetes. *J Genet Genomics*. 2022;49(4):316-328. doi:10.1016/j.jgg.2022.03.002
 24. Porte D, Schwartz MW. Diabetes Complications: Why Is Glucose Potentially Toxic? *Science (80-)*. 1996;272(5262):699.
 25. Inoguchi T, Sonta T, Tsubouchi H, et al. Protein Kinase C–Dependent Increase in Reactive Oxygen Species (ROS) Production in Vascular Tissues of Diabetes: Role of Vascular NAD(P)H Oxidase. *J Am Soc Nephrol*. 2003;(3):S227-S23.
 26. Papatheodorou K, Banach M, Bekiari E, Rizzo M, Edmonds M. Complications of Diabetes 2017. *J Diabetes Res*. 2018;2018, Arti:4.

27. Zheng F, Yan L, Yang Z, Zhong B, Xie W. HbA1c, diabetes and cognitive decline: the English Longitudinal Study of Ageing. *Diabetologia*. 2018;61(4):839-848. doi:10.1007/s00125-017-4541-7
28. Harding JL, Pavkov ME, Magliano DJ, Shaw JE, Gregg EW. Global trends in diabetes complications: a review of current evidence. *Diabetologia*. 2019;62(1):3-16. doi:10.1007/s00125-018-4711-2
29. Rosenfeld L. Insulin: discovery and controversy. *Clin Chem*. 2002;48(12):2270-2288. doi:10.1093/clinchem/48.12.2270
30. Marín-Peñalver JJ, Martín-Timón I, Sevillano-Collantes C, Cañizo-Gómez FJ del. Update on the treatment of type 2 diabetes mellitus. *World J Diabetes*. 2016;7(17):354–395.
31. Hess DA, Verma S, Bhatt D, et al. Vascular repair and regeneration in cardiometabolic diseases. *Eur Heart J*. 2022;43(6):450-459b. doi:10.1093/eurheartj/ehab758
32. Cernea S, Raz I. Insulin Therapy: Future Perspectives. *Am J Ther*. 2020;27(1):E121-E132. doi:10.1097/MJT.0000000000001076
33. Rawshani A, Rawshani A, Franzén S, et al. Mortality and Cardiovascular Disease in Type 1 and Type 2 Diabetes. *N Engl J Med*. 2017;376(15):1407-1418. doi:10.1056/nejmoa1608664
34. Foster NC, Beck RW, Miller KM, et al. State of Type 1 Diabetes Management and Outcomes from the T1D Exchange in 2016-2018. *Diabetes Technol Ther*. 2019;21(2):66-72. doi:10.1089/dia.2018.0384
35. Shapiro AMJ, Lakey JRT, Ryan EA, et al. Islet Transplantation in Seven Patients with Type 1 Diabetes Mellitus Using a Glucocorticoid-Free Immunosuppressive Regimen. *N Engl J Med*. 2000;343(4):230-238. doi:10.1056/nejm200007273430401
36. Ryan EA, Paty BW, Senior PA, et al. Five-year follow-up after clinical islet transplantation. *Diabetes*. 2005;54(7):2060-2069. doi:10.2337/diabetes.54.7.2060
37. Shapiro AMJ, Ricordi C, Hering BJ, et al. International Trial of the Edmonton Protocol for Islet Transplantation. *N Engl J Med*. 2006;355(13):1318-1330. doi:10.1056/nejmoa061267
38. *Collaborative Islet Transplant Registry Eleventh Allograft Report*. Rockville, MD; 2022. [https://citregistry.org/system/files/11th Allograft report May 31 2022.pdf](https://citregistry.org/system/files/11th%20Allograft%20report%20May%2031%202022.pdf).
39. Thomson JA. Embryonic stem cell lines derived from human blastocysts. *Science* (80-). 1998;282(5391):1145-1147. doi:10.1126/science.282.5391.1145
40. Takahashi K, Yamanaka S. Induction of Pluripotent Stem Cells from Mouse Embryonic and Adult Fibroblast Cultures by Defined Factors. *Cell*. 2006;126(4):663-676. doi:10.1016/j.cell.2006.07.024

41. D'Amour KA, Bang AG, Eliazar S, et al. Production of pancreatic hormone-expressing endocrine cells from human embryonic stem cells. *Nat Biotechnol.* 2006;24(11):1392-1401. doi:10.1038/nbt1259
42. Nostro M, Sarangi F, Ogawa S, et al. Stage-specific signaling through TGF β family members and WNT regulates patterning and pancreatic specification of human pluripotent stem cells. *Dev.* 2011;138(5):861-871.
43. Rezania A, Bruin JE, Arora P, et al. Reversal of diabetes with insulin-producing cells derived in vitro from human pluripotent stem cells. *Nat Biotechnol.* 2014;32(11):1121-1133. doi:10.1038/nbt.3033
44. Pagliuca FW, Millman JR, Gürtler M, et al. Generation of functional human pancreatic β cells in vitro. *Cell.* 2014;159(2):428-439. doi:10.1016/j.cell.2014.09.040
45. Veres A, Faust AL, Bushnell HL, et al. Charting cellular identity during human in vitro β -cell differentiation. *Nature.* 2019;569(7756):368-373. doi:10.1038/s41586-019-1168-5
46. Alvarez-Dominguez JR, Donaghey J, Rasouli N, et al. Circadian Entrainment Triggers Maturation of Human In Vitro Islets. *Cell Stem Cell.* 2020;26(1):108-122.e10. doi:10.1016/j.stem.2019.11.011
47. Balboa D, Barsby T, Lithovius V, et al. Functional, metabolic and transcriptional maturation of human pancreatic islets derived from stem cells. *Nat Biotechnol.* 2022. doi:10.1038/s41587-022-01219-z
48. ViaCyte. A Safety, Tolerability, and Efficacy Study of VC-01™ Combination Product in Subjects With Type I Diabetes Mellitus. ClinicalTrials.gov identifier: NCT02239354. 2022. <https://www.clinicaltrials.gov/ct2/show/study/NCT02239354>.
49. ViaCyte. A Safety, Tolerability, and Efficacy Study of VC-02™ Combination Product in Subjects With Type 1 Diabetes Mellitus and Hypoglycemia Unawareness. ClinicalTrials.gov Identifier: NCT03163511. 2022. <https://www.clinicaltrials.gov/ct2/show/NCT03163511>.
50. Shapiro AMJ, Thompson D, Donner TW, et al. Insulin expression and C-peptide in type 1 diabetes subjects implanted with stem cell-derived pancreatic endoderm cells in an encapsulation device Insulin expression and C-peptide in type 1 diabetes subjects implanted with stem cell-derived pancreatic end. *Cell Reports Med.* 2021;100466. doi:10.1016/j.xcrm.2021.100466
51. Ramzy A, Thompson DM, Ward-hartstonge KA, et al. Clinical and Translational Report Implanted pluripotent stem-cell-derived pancreatic endoderm cells secrete glucose-responsive C-peptide in patients with type 1 diabetes II Clinical and Translational Report Implanted pluripotent stem-cell-derived pancrea. *Stem Cell.* 2021;28(12):2047-2061.e5. doi:10.1016/j.stem.2021.10.003
52. Markmann JF, Naji A, RICKELS MR, et al. Stem Cell–Derived, Fully Differentiated

- Islet Cells for Type 1 Diabetes. In: *American Diabetes Association 82nd Scientific Sessions*. New Orleans; 2022.
<https://epro02.ativ.me/src/EventPilot/php/express/web/page.php?page=IntHtml&project=ADA22&id=540>. Accessed June 6, 2022.
53. Keenan HA, Sun JK, Levine J, et al. Residual insulin production and pancreatic β -cell turnover after 50 years of diabetes: Joslin medalist study. *Diabetes*. 2010;59(11):2846-2853. doi:10.2337/db10-0676
 54. Lam CJ, Jacobson DR, Rankin MM, Cox AR, Kushner JA. β Cells persist in T1D pancreata without evidence of ongoing β -Cell turnover or neogenesis. *J Clin Endocrinol Metab*. 2017;102(8):2647-2659. doi:10.1210/jc.2016-3806
 55. Brockenbrough JS, Weir GC, Bonner-Weir S. Discordance of Exocrine and Endocrine Growth After 90% Pancreatectomy in Rats. *Diabetes*. 1988;37(2):232–236.
 56. Bonner-Weir S, Trent DF, Weir GC. Partial pancreatectomy in the rat and subsequent defect in glucose-induced insulin release. *J Clin Invest*. 1983;71(6):1544–1553.
 57. Mozar A, Lin H, Williams K, et al. Parathyroid Hormone-Related Peptide (1-36) Enhances Beta Cell Regeneration and Increases Beta Cell Mass in a Mouse Model of Partial Pancreatectomy. *PLoS One*. 2016.
 58. Xu G, Stoffers DA, Habener JF, Bonner-Weir S. Exendin-4 Stimulates Both Beta-Cell Replication and Neogenesis, Resulting in Increased Beta-Cell Mass and Improved Glucose Tolerance in Diabetic Rats. *Diabetes*. 1999;48:2270-2276. doi:10.1063/1.3022720
 59. Téllez N, Joanny G, Escoriza J, Vilaseca M, Montanya E. Gastrin treatment stimulates β -cell regeneration and improves glucose tolerance in 95% pancreatectomized rats. *Endocrinology*. 2011;152(7):2580-2588.
 60. Téllez N, Vilaseca M, Martí Y, Pla A, Montanya E. B-Cell Dedifferentiation, Reduced Duct Cell Plasticity, and Impaired B-Cell Mass Regeneration in Middle-Aged Rats. *Am J Physiol - Endocrinol Metab*. 2016;311(3):E554-E563. doi:10.1152/ajpendo.00502.2015
 61. Wang RN, Kliippel G, Bouwens L. Duct- to islet-cell differentiation and islet growth in the pancreas of duct-ligated adult rats. *Diabetologia*. 1995;38:1405-1411.
 62. Xu X, D'Hoker J, Stangé G, et al. β Cells Can Be Generated from Endogenous Progenitors in Injured Adult Mouse Pancreas. *Cell*. 2008;132(2):197-207. doi:10.1016/j.cell.2007.12.015
 63. Van De Casteele M, Leuckx G, Baeyens L, et al. Neurogenin 3+ cells contribute to b-cell neogenesis and proliferation in injured adult mouse pancreas. *Cell Death Dis*. 2013;4(3):1-11. doi:10.1038/cddis.2013.52
 64. Inada A, Nienaber C, Katsuta H, et al. Carbonic anhydrase II-positive pancreatic

- cells are progenitors for both endocrine and exocrine pancreas after birth. *Proc Natl Acad Sci U S A*. 2008;105(50):19915-19919. doi:10.1073/pnas.0805803105
65. Hao E, Lee S-H, Levine F. Efficient beta-cell regeneration by a combination of neogenesis and replication following beta-cell ablation and reversal of pancreatic duct ligation. *Stem Cells*. 2013;31:2388–2395.
 66. Cavelti-Weder C, Shtessel M, Reuss JE, et al. Pancreatic Duct Ligation After Almost Complete β -Cell Loss: Exocrine Regeneration but No Evidence of β -Cell Regeneration. *Endocrinology*. 2013;154(12):4493-4502.
 67. Lenzen S. The mechanisms of alloxan- and streptozotocin-induced diabetes. *Diabetologia*. 2008;51(2):216-226. doi:10.1007/s00125-007-0886-7
 68. Cheng Y, Kang H, Shen J, et al. Beta-cell regeneration from vimentin + /MafB + cells after STZ-induced extreme beta-cell ablation. *Sci Rep*. 2015;5:1-12. doi:10.1038/srep11703
 69. Rankin MM, Kushner JA. Adaptive β -cell proliferation is severely restricted with advanced age. *Diabetes*. 2009;58(6):1365-1372. doi:10.2337/db08-1198
 70. Tschen SI, Dhawan S, Gurlo T, Bhushan A. Age-dependent decline in β -cell proliferation restricts the capacity of β -cell regeneration in mice. *Diabetes*. 2009;58(6):1312-1320. doi:10.2337/db08-1651
 71. Chen H, Gu X, Su IH, et al. Polycomb protein Ezh2 regulates pancreatic β -cell Ink4a/Arf expression and regeneration in diabetes mellitus. *Genes Dev*. 2009;23(8):975-985. doi:10.1101/gad.1742509
 72. Dhawan S, Tschen SI, Bhushan A. Bmi-1 regulates the Ink4a/Arf locus to control pancreatic β -cell proliferation. *Genes Dev*. 2009;23(8):906-911. doi:10.1101/gad.1742609
 73. Haro-Hernandez R De, Cabrera-Munoz L, Mendez JD. Regeneration of β -Cells and Neogenesis From Small Ducts or Acinar Cells Promote Recovery of Endocrine Pancreatic Function in Alloxan-Treated Rats. *Arch Med Res*. 2004;35:114–120.
 74. Jacob S. Regeneration of the islets of Langerhans in the Guinea pig. *Cell Tissue Res*. 1977;181(2):277–286.
 75. Grossman EJ, Lee DD, Tao J, et al. Glycemic control promotes pancreatic beta-cell regeneration in streptozotocin-induced diabetic mice. *PLoS One*. 2010;5(1):1-6. doi:10.1371/journal.pone.0008749
 76. Dirice E, De Jesus DF, Kahraman S, et al. Human duct cells contribute to β cell compensation in insulin resistance. *JCI Insight*. 2019;4(8):1-14. doi:10.1172/jci.insight.99576
 77. Millette K, Rodriguez K, Sheng X, Finley SD, Georgia S. Exogenous Lactogenic Signaling Stimulates Beta Cell Replication In Vivo and In Vitro. *Biomolecules*.

- 2022;12(2):1-10. doi:10.3390/biom12020215
78. Zhao H, Huang X, Liu Z, et al. Pre-existing beta cells but not progenitors contribute to new beta cells in the adult pancreas. *Nat Metab.* 2021;3(3):352-365. doi:10.1038/s42255-021-00364-0
 79. Fanjul M, Gmyr V, Sengenès C, et al. Evidence for epithelial-mesenchymal transition in adult human pancreatic exocrine cells. *J Histochem Cytochem.* 2010;58(9):807-823. doi:10.1369/jhc.2010.955807
 80. Butler AE, Janson J, Bonner-weir S, Ritzel R, Rizza R a, Butler PC. Humans With Type 2 Diabetes. *Diabetes.* 2003;52(January):102-110. <http://www.ncbi.nlm.nih.gov/pubmed/12502499>.
 81. Gregg BE, Moore PC, Demozay D, et al. Formation of a Human β -Cell Population within Pancreatic Islets Is Set Early in Life. *J Clin Endocrinol Metab.* 2012;97(9):3197–3206.
 82. Fiaschi-Taesch NM, Kleinberger JW, Salim FG, et al. Human Pancreatic β -Cell G1/S Molecule Cell Cycle Atlas. *Diabetes.* 2013;62(7):2450–2459.
 83. Tyrberg B, Ustinov J, Otonkoski T, Andersson A. Stimulated endocrine cell proliferation and differentiation in transplanted human pancreatic islets: effects of the ob gene and compensatory growth of the implantation organ. *Diabetes.* 2001;50(2):301-307.
 84. Willcox A, Richardson SJ, Bone AJ, Foulis AK, Morgan NG. Evidence of increased islet cell proliferation in patients with recent-onset type 1 diabetes. *Diabetologia.* 2010;53:2020–2028.
 85. Berrocal T, Luque AA, Pinilla I, Lassaletta L. Pancreatic regeneration after near-total pancreatectomy in children with nesidioblastosis. *Pediatr Radiol.* 2005;35(11):1066-1070.
 86. Menge BA, Tannapfel A, Belyaev O, et al. Partial pancreatectomy in adult humans does not provoke β -cell regeneration. *Diabetes.* 2008;57(1):142-149. doi:10.2337/db07-1294
 87. Bwititi P, Musabayane CT, Nhachi CFB. Effects of *Opuntia megacantha* on blood glucose and kidney function in streptozotocin diabetic rats. *J Ethno-Pharmacology.* 2000;69:247-252.
 88. Jouad H, Eddouks M, Lacaille-Dubois MA, Lyoussi B. Hypoglycaemic effect of *Spergularia purpurea* in normal and streptozotocin-induced diabetic rats. *J Ethno-Pharmacology.* 2000;71:169-177.
 89. Wang Y, Liu Y, Wang H, Li C, Qi P, Bao J. *Agaricus bisporus* lectins mediates islet β -cell proliferation through regulation of cell cycle proteins. *Soc Exp Biol Med.* 2012;237(3):287-296.
 90. Attanayake AP, Jayatilaka KAPW, Mudduwa LKB, Pathirana C. β -cell

- Regenerative Potential of Selected Herbal Extracts in Alloxan Induced Diabetic Rats. *Curr Drug Discov Technol.* 2019;16(3):278-284.
91. Singh N, Gupta M. Regeneration of beta cells in islets of Langerhans of pancreas of alloxan diabetic rats by acetone extract of *Momordica charantia* (Linn.) (bitter gourd) fruits. *Indian J Exp Biol.* 2007;45(12):1055–1062.
 92. Wang HL, Li CY, Zhang B, et al. Mangiferin Facilitates Islet Regeneration and β -Cell Proliferation through Upregulation of Cell Cycle and β -Cell Regeneration Regulators. *Int J Mol Sci.* 2014;15(5):9016-9035. doi:10.3390/ijms15059016
 93. Muruganandan S, Srinivasan K, Gupta S, Gupta PK, Lal J. Effect of mangiferin on hyperglycemia and atherogenicity in streptozotocin diabetic rats. *J Ethno-Pharmacology.* 2005;97:497-501.
 94. Wang P, Alvarez-Perez JC, Felsenfeld DP, et al. A high-throughput chemical screen reveals that harmine-mediated inhibition of DYRK1A increases human pancreatic beta cell replication. *Nat Med.* 2015;21(4):383-388. doi:10.1038/nm.3820
 95. Barzowska A, Pucelik B, Pustelny K, et al. DYRK1A Kinase Inhibitors Promote β -Cell Survival and Insulin Homeostasis. *Cells.* 2021;10(9):2263.
 96. Kumar K, Wang P, Swartz EA, et al. Structure-Activity Relationships and Biological Evaluation of 7-Substituted Harmine Analogs for Human β -Cell Proliferation. *Molecules.* 2020;25(8):1983.
 97. Brown ML, Schneyer AL. Emerging roles for the TGF β family in pancreatic beta-cell homeostasis. *Trends Endocrinol Metab.* 2010;21(7):441-448.
 98. Dhawan S, Dirice E, Kulkarni RN, Bhushan A. Inhibition of TGF- β Signaling Promotes Human Pancreatic β -Cell Replication. *Diabetes.* 2016;65(5):1208-1218.
 99. Dirice E, Walpita D, Vetere A, et al. Inhibition of DYRK1A Stimulates Human β -Cell Proliferation. *Diabetes.* 2016;65(6):1660-1671.
 100. Shen W, Taylor B, Jin Q, et al. Inhibition of DYRK1A and GSK3B induces human β -cell proliferation. *Nat Commun.* 2015;6:8372.
 101. Acekifi C, Wang P, Karakose E, et al. GLP-1 receptor agonists synergize with DYRK1A inhibitors to potentiate functional human β cell regeneration. *Sci Transl Med.* 2020;12(530). doi:10.1126/scitranslmed.aaw9996
 102. Ben-Othman N, Vieira A, Courtney M, et al. Long-Term GABA Administration Induces Alpha Cell-Mediated Beta-like Cell Neogenesis. *Cell.* 2017;168(1-2):73-85.e11. doi:10.1016/j.cell.2016.11.002
 103. Rooman I, Bouwens L. Combined gastrin and epidermal growth factor treatment induces islet regeneration and restores normoglycaemia in C57Bl6/J mice treated with alloxan. *Diabetologia.* 2004;47:259–265.
 104. Zhou Q, Brown J, Kanarek A, Rajagopal J, Melton DA. In vivo reprogramming of

- adult pancreatic exocrine cells to β -cells. *Nature*. 2008;455(7213):627-632. doi:10.1038/nature07314
105. Crisan M, Yap S, Casteilla L, et al. A Perivascular Origin for Mesenchymal Stem Cells in Multiple Human Organs. *Cell Stem Cell*. 2008;3(3):301-313. doi:10.1016/j.stem.2008.07.003
 106. Dominici M, Le Blanc K, Mueller I, et al. Minimal criteria for defining multipotent mesenchymal stromal cells. The International Society for Cellular Therapy position statement. *Cytotherapy*. 2006;8(4):315-317. doi:10.1080/14653240600855905
 107. Soliman H, Theret M, Scott W, et al. Multipotent stromal cells: One name, multiple identities. *Cell Stem Cell*. 2021;28(10):1690-1707. doi:10.1016/j.stem.2021.09.001
 108. Capoccia BJ, Robson DL, Levac KD, et al. Revascularization of ischemic limbs after transplantation of human bone marrow cells with high aldehyde dehydrogenase activity. *Blood*. 2009;113(21):5340-5351. doi:10.1182/blood-2008-04-154567
 109. Pereira RF, Halford KW, O'Hara MD, et al. Cultured adherent cells from marrow can serve as long-lasting precursor cells for bone, cartilage, and lung in irradiated mice. *Proc Natl Acad Sci U S A*. 1995;92(11):4857-4861.
 110. Caplan AI, Correa D. The MSC: An injury drugstore. *Cell Stem Cell*. 2011;9(1):11-15. doi:10.1016/j.stem.2011.06.008
 111. Nicola M Di, Carlo-Stella C, Magni M, et al. Human bone marrow stromal cells suppress T-lymphocyte proliferation induced by cellular or nonspecific mitogenic stimuli. *Blood*. 2002;99(10):3838-3843.
 112. Fiori A, Uhlig S, Klüter H, Bieback K. Human Adipose Tissue-Derived Mesenchymal Stromal Cells Inhibit CD4+ T Cell Proliferation and Induce Regulatory T Cells as Well as CD127 Expression on CD4+CD25+ T Cells. *Cells*. 2021;10(1):58.
 113. Aggarwal S, Pittenger MF. Human mesenchymal stem cells modulate allogeneic immune cell responses. *Blood*. 2005;105(4):1815–1822.
 114. Xue Q, Luan X-Y, Gu Y-Z, et al. The negative co-signaling molecule b7-h4 is expressed by human bone marrow-derived mesenchymal stem cells and mediates its T-cell modulatory activity. *Stem Cells Dev*. 2010;19(1):27-38.
 115. Glennie S, Soeiro I, Dyson PJ, Lam EW-F, Dazzi F. Bone marrow mesenchymal stem cells induce division arrest anergy of activated T cells. *Blood*. 2005;105(7):2821-2827.
 116. Augello A, Tasso R, Negrini SM, et al. Bone marrow mesenchymal progenitor cells inhibit lymphocyte proliferation by activation of the programmed death 1 pathway. *Eur J Immunol*. 2005;35(5):1482-1490.

117. Krampera M, Cosmi L, Angeli R, et al. Role for interferon-gamma in the immunomodulatory activity of human bone marrow mesenchymal stem cells. *Stem Cells*. 2006;24(2):386-398.
118. Jiang X-X, Zhang Y, Liu B, et al. Human mesenchymal stem cells inhibit differentiation and function of monocyte-derived dendritic cells. *Blood*. 2005;105(10):4120-4126.
119. Ramasamy R, Fazekasova H, Lam EW-F, Soeiro I, Lombardi G, Dazzi F. Mesenchymal stem cells inhibit dendritic cell differentiation and function by preventing entry into the cell cycle. *Transplantation*. 2007;83(1):71-76.
120. Spaggiari GM, Capobianco A, Abdelrazik H, Becchetti F, Mingari MC, Moretta L. Mesenchymal stem cells inhibit natural killer-cell proliferation, cytotoxicity, and cytokine production: role of indoleamine 2, 3-dioxygenase and prostaglandin E2. *Blood*. 2008;111(3):1327-1333.
121. Ben-Ami E, Berrih-Aknin S, Miller A. Mesenchymal stem cells as an immunomodulatory therapeutic strategy for autoimmune diseases. *Autoimmun Rev*. 2011;10(7):410-415. doi:10.1016/j.autrev.2011.01.005
122. Galderisi U, Peluso G, Bernardo G Di. Clinical Trials Based on Mesenchymal Stromal Cells are Exponentially Increasing: Where are We in Recent Years? *Stem Cell Rev Reports*. 2022;18(1):23-36.
123. Ferreira JR, Teixeira GQ, Santos SG, Barbosa MA, Almeida-Porada G, Gonçalves RM. Mesenchymal stromal cell secretome: Influencing therapeutic potential by cellular pre-conditioning. *Front Immunol*. 2018;9(December):1-17. doi:10.3389/fimmu.2018.02837
124. Cho J, D'Antuono M, Glicksman M, Wang J, Jonklaas J. A review of clinical trials: mesenchymal stem cell transplant therapy in type 1 and type 2 diabetes mellitus. *Am J Stem Cells*. 2018;7(4):82-93. <http://www.ncbi.nlm.nih.gov/pubmed/30510843>.
125. Kim JW, Luo JZQ, Luo L. *Bone Marrow Mesenchymal Stem Cells as a New Therapeutic Approach for Diabetes Mellitus*. Elsevier Inc.; 2018. doi:10.1016/B978-0-12-811920-4.00010-0
126. Gabr MM, Zakaria MM, Refaie AF, et al. Insulin-Producing Cells From Adult Human Bone Marrow Mesenchymal Stem Cells Control Streptozotocin-Induced Diabetes In Nude Mice. *Cell Transpl*. 2013;22(1):133-145.
127. Tang D-Q, Cao L-Z, Burkhardt BR, et al. In Vivo and In Vitro Characterization of Insulin-Producing Cells Obtained From Murine Bone Marrow. *Diabetes*. 2004;53(7):1721-1732.
128. Lanus A, Holz G, Theise N, Hussain M. In vivo derivation of glucose-competent pancreatic endocrine cells from bone marrow without evidence of cell fusion. *J Clin Invest*. 2003;111:843–850.

129. Liu C, Zhang W, Peradze N, et al. Mesenchymal stem cell (MSC)-mediated survival of insulin producing pancreatic β -cells during cellular stress involves signalling via Akt and ERK1/2. *Mol Cell Endocrinol*. 2018;473:235-244. doi:10.1016/j.mce.2018.01.024
130. Bao Y, Zhao Z, Gao H. Effect of hTIMP-1 overexpression in human umbilical cord mesenchymal stem cells on the repair of pancreatic islets in type-1 diabetic mice. *Cell Biol Int*. 2021;45(5):1038-1049. doi:10.1002/cbin.11548
131. Gamble A, Pawlick R, Pepper AR, et al. Improved islet recovery and efficacy through co-culture and co-transplantation of islets with human adipose-derived mesenchymal stem cells. *PLoS One*. 2018;13(11):e0206449.
132. Yeung TY, Seeberger KL, Kin T, et al. Human mesenchymal stem cells protect human islets from pro-inflammatory cytokines. *PLoS One*. 2012;7(5):1-9. doi:10.1371/journal.pone.0038189
133. de Souza BM, Bouças AP, de Oliveira FDS, et al. Effect of co-culture of mesenchymal stem/stromal cells with pancreatic islets on viability and function outcomes: a systematic review and meta-analysis. *Islets*. 2017;9(2):30-42.
134. Hess D, Li L, Martin M, et al. Bone marrow-derived stem cells initiate pancreatic regeneration. *Nat Biotechnol*. 2003;21(7):763-770. doi:10.1038/nbt841
135. Bell GI, Broughton HC, Levac KD, Allan DA, Xenocostas A, Hess DA. Transplanted human bone marrow progenitor subtypes stimulate endogenous islet regeneration and revascularization. *Stem Cells Dev*. 2012;21(1):97-109. doi:10.1089/scd.2010.0583
136. Bell GI, Putman DM, Hughes-Large JM, Hess DA. Intrapancreatic delivery of human umbilical cord blood aldehyde dehydrogenase-producing cells promotes islet regeneration. *Diabetologia*. 2012;55(6):1755-1760. doi:10.1007/s00125-012-2520-6
137. Lee RH, Seo MJ, Reger RL, et al. Multipotent stromal cells from human marrow home to and promote repair of pancreatic islets and renal glomeruli in diabetic NOD/scid mice. *Proc Natl Acad Sci U S A*. 2006;103(46):17438-17443. doi:10.1073/pnas.0608249103
138. Song X, Sun X, Hao H, Han Q, Han W, Mu Y. Combined Treatment with Bone Marrow-Derived Mesenchymal Stem Cells and Exendin-4 Promotes Islet Regeneration in Streptozotocin-Induced Diabetic Rats. *Stem Cells Dev*. 2021;30(9):502-514. doi:10.1089/scd.2020.0137
139. Kawada-Horitani E, Kita S, Okita T, et al. Human adipose-derived mesenchymal stem cells prevent type 1 diabetes induced by immune checkpoint blockade. *Diabetologia*. 2022;65(7):1185-1197. doi:10.1007/s00125-022-05708-3
140. Bell GI, Meschino MT, Hughes-Large JM, Broughton HC, Xenocostas A, Hess DA. Combinatorial human progenitor cell transplantation optimizes islet

- regeneration through secretion of paracrine factors. *Stem Cells Dev.* 2012;21(11):1863-1876. doi:10.1089/scd.2011.0634
141. Khatri R, Petry SF, Linn T. Intrapancreatic MSC transplantation facilitates pancreatic islet regeneration. *Stem Cell Res Ther.* 2021;12(1):1-14. doi:10.1186/s13287-021-02173-4
 142. Montanucci P, Pescara T, Greco A, et al. Co-microencapsulation of human umbilical cord-derived mesenchymal stem and pancreatic islet-derived insulin producing cells in experimental type 1 diabetes. *Diabetes Metab Res Rev.* 2021;37(2):1-13. doi:10.1002/dmrr.3372
 143. Jurewicz M, Yang S, Augello A, et al. Congenic mesenchymal stem cell therapy reverses hyperglycemia in experimental type 1 diabetes. *Diabetes.* 2010;59(12):3139-3147. doi:10.2337/db10-0542
 144. Kenyon NS, Willman MA, Han D, et al. Extended survival versus accelerated rejection of nonhuman primate islet allografts: Effect of mesenchymal stem cell source and timing. *Am J Transplant.* 2021;21(11):3524-3537. doi:10.1111/ajt.16693
 145. Si Y, Zhao Y, Hao J, et al. Infusion of mesenchymal stem cells ameliorates hyperglycemia in type 2 diabetic rats: Identification of a novel role in improving insulin sensitivity. *Diabetes.* 2012;61(6):1616-1625. doi:10.2337/db11-1141
 146. Sun Y, Shi H, Yin S, et al. Human mesenchymal stem cell derived exosomes alleviate type 2 diabetes mellitus by reversing peripheral insulin resistance and relieving β -cell destruction. *ACS Nano.* 2018;12(8):7613-7628. doi:10.1021/acsnano.7b07643
 147. He Q, Song J, Cui C, et al. Mesenchymal stem cell-derived exosomal miR-146a reverses diabetic β -cell dedifferentiation. *Stem Cell Res Ther.* 2021;12(1):449.
 148. Mendicino M, Bailey AM, Wonnacott K, Puri RK, Bauer SR. MSC-based product characterization for clinical trials: An FDA perspective. *Cell Stem Cell.* 2014;14(2):141-145. doi:10.1016/j.stem.2014.01.013
 149. Kuljanin M, Bell GI, Sherman SE, Lajoie GA, Hess DA. Proteomic characterisation reveals active Wnt-signalling by human multipotent stromal cells as a key regulator of beta cell survival and proliferation. *Diabetologia.* 2017;60(10):1987-1998. doi:10.1007/s00125-017-4355-7
 150. Sabry D, Marzouk S, Zakaria R, Ibrahim HA, Samir M. The effect of exosomes derived from mesenchymal stem cells in the treatment of induced type 1 diabetes mellitus in rats. *Biotechnol Lett.* 2020;42(8):1597-1610. doi:10.1007/s10529-020-02908-y
 151. Cooper TT, Sherman SE, Bell GI, et al. Characterization of a Vimentinhigh/Nestinhigh proteome and tissue regenerative secretome generated by human pancreas-derived mesenchymal stromal cells. *Stem Cells.*

- 2020;38(5):666-682. doi:10.1002/stem.3143
152. Cooper TT, Sherman SE, Bell GI, et al. Ultrafiltration and injection of islet regenerative stimuli secreted by pancreatic mesenchymal stromal cells. *Stem Cells Dev.* 2021;30(5):247-264. doi:10.1089/scd.2020.0206
 153. Klerk E de, Hebrok M. Stem Cell-Based Clinical Trials for Diabetes Mellitus. *Front Endocrinol (Lausanne).* 2021;12:631463.
 154. Carlsson P-O, Schwarcz E, Korsgren O, Blanc K Le. Preserved b-Cell Function in Type 1 Diabetes by Mesenchymal Stromal Cells. *Diabetes.* 2015;64:587–592.
 155. Izadi M, Sadr Hashemi Nejad A, Moazenchi M, et al. Mesenchymal stem cell transplantation in newly diagnosed type-1 diabetes patients: a phase I/II randomized placebo-controlled clinical trial. *Stem Cell Res Ther.* 2022;13(1):1-20. doi:10.1186/s13287-022-02941-w
 156. Wang H, Strange C, Nietert PJ, et al. Autologous Mesenchymal Stem Cell and Islet Cotransplantation: Safety and Efficacy. *Stem Cells Transl Med.* 2018;7(1):11-19. doi:10.1002/sctm.17-0139
 157. Bell GI, Seneviratne AK, Nasri GN, Hess DA. *Transplantation Models to Characterize the Mechanisms of Stem Cell-Induced Islet Regeneration.* Vol 1.; 2013. doi:10.1002/9780470151808.sc02b04s26
 158. Kuljanin M, Elgamal RM, Bell GI, et al. Quantitative Proteomics Evaluation of Human Multipotent Stromal Cell for β Cell Regeneration. *Cell Rep.* 2018;25(9):2524-2536.e4. doi:10.1016/j.celrep.2018.10.107
 159. Takam Kamga P, Bazzoni R, Dal Collo G, et al. The Role of Notch and Wnt Signaling in MSC Communication in Normal and Leukemic Bone Marrow Niche. *Front Cell Dev Biol.* 2021;8(January). doi:10.3389/fcell.2020.599276
 160. Gordon MD, Nusse R. Wnt Signaling: Multiple Pathways, Multiple Receptors, and Multiple Transcription Factors. *J Biol Chem.* 2006;281(32):22429-22433.
 161. Kuljanin M, Elgamal RM, Bell GI, Xenocostas A, Lajoie GA, Hess DA. Human Multipotent Stromal Cell Secreted Effectors Accelerate Islet Regeneration. *Stem Cells.* 2019;37(4):516-528. doi:10.1002/stem.2976
 162. Zhou Q, Melton DA. Pancreas regeneration. *Nature.* 2018;557(7705):351-358. doi:10.1038/s41586-018-0088-0.Pancreas
 163. Domínguez-Bendala J, Qadir MMF, Pastori RL. Pancreatic Progenitors: There and Back Again. *Trends Endocrinol Metab.* 2019;30(1):4-11. doi:10.1016/j.tem.2018.10.002
 164. Spears E, Serafimidis I, Powers AC, Gavalas A. Debates in Pancreatic Beta Cell Biology: Proliferation Versus Progenitor Differentiation and Transdifferentiation in Restoring β Cell Mass. *Front Endocrinol (Lausanne).* 2021;12(August):1-16. doi:10.3389/fendo.2021.722250

165. Jennings RE, Berry AA, Strutt JP, Gerrard DT, Hanley NA. Human pancreas development. *Development*. 2015;142(18):3126–3137.
166. Bastidas-Ponce A, Scheibner K, Lickert H, Bakhti M. Cellular and molecular mechanisms coordinating pancreas development. *Dev*. 2017;144(16):2873-2888. doi:10.1242/dev.140756
167. Sharon N, Chawla R, Mueller J, et al. A Peninsular Structure Coordinates Asynchronous Differentiation with Morphogenesis to Generate Pancreatic Islets. *Cell*. 2019;176(4):790-804.e13. doi:10.1016/j.cell.2018.12.003
168. Collombat P, Xu X, Ravassard P, et al. The Ectopic Expression of Pax4 in the Mouse Pancreas Converts Progenitor Cells into α and Subsequently β Cells. *Cell*. 2009;138(3):449-462. doi:10.1016/j.cell.2009.05.035
169. Courtney M, Gjernes E, Druelle N, et al. The Inactivation of Arx in Pancreatic α -Cells Triggers Their Neogenesis and Conversion into Functional β -Like Cells. *PLoS Genet*. 2013;9(10):1-18. doi:10.1371/journal.pgen.1003934
170. Kopp JL, Dubois CL, Schaffer AE, et al. Sox9+ ductal cells are multipotent progenitors throughout development but do not produce new endocrine cells in the normal or injured adult pancreas. *Development*. 2011;138(4):653-665. doi:10.1242/dev.056499
171. Pan FC, Bankaitis ED, Boyer D, et al. Spatiotemporal patterns of multipotentiality in Ptf1a-expressing cells during pancreas organogenesis and injury-induced facultative restoration. *Dev*. 2013;140(4):751-764. doi:10.1242/dev.090159
172. Cnop M, Hughes SJ, Igoillo-Esteve M, et al. The long lifespan and low turnover of human islet beta cells estimated by mathematical modelling of lipofuscin accumulation. *Diabetologia*. 2010;53(2):321-330.
173. Rieck S, Kaestner KH. Expansion of β -cell mass in response to pregnancy. *Trends Endocrinol Metab*. 2010;21(3):151-158.
174. Skog O, Korsgren O. On the dynamics of the human endocrine pancreas and potential consequences for the development of type 1 diabetes. *Acta Diabetol*. 2020;57(4):503-511. doi:10.1007/s00592-019-01420-8
175. Sullivan BA, Hollister-Lock J, Bonner-Weir S, Weir GC. Reduced Ki67 Staining in the Postmortem State Calls Into Question Past Conclusions About the Lack of Turnover of Adult Human β -Cells. *Diabetes*. 2015;64(5):1698–1702.
176. Chakravarthy H, Gu X, Enge M, et al. Converting Adult Pancreatic Islet α Cells into β Cells by Targeting Both Dnmt1 and Arx. *Cell Metab*. 2017;25(3):622-634.
177. Tang X, Uhl S, Zhang T, et al. SARS-CoV-2 infection induces beta cell transdifferentiation. *Cell Metab*. 2021;33(8):1577-1591.
178. Afelik S, Rovira M. Pancreatic β -cell regeneration: Facultative or dedicated progenitors? *Mol Cell Endocrinol*. 2017;445:85-94. doi:10.1016/j.mce.2016.11.008

179. Dor Y, Brown J, Martinez OI, Melton DA. Adult pancreatic β -cells are formed by self-duplication rather than stem-cell differentiation. *Nature*. 2004;429(6987):41-46. doi:10.1038/nature02520
180. Teta M, Rankin MM, Long SY, Stein GM, Kushner JA. Growth and Regeneration of Adult β Cells Does Not Involve Specialized Progenitors. *Dev Cell*. 2007;12(5):817-826. doi:10.1016/j.devcel.2007.04.011
181. Bramswig NC, Everett LJ, Schug J, et al. Epigenomic plasticity enables human pancreatic α to β cell reprogramming. *J Clin Invest*. 2013;123(3):1275-1284. doi:10.1172/JCI66514
182. Xiao X, Guo P, Shiota C, et al. Endogenous Reprogramming of Alpha Cells into Beta Cells, Induced by Viral Gene Therapy, Reverses Autoimmune Diabetes. *Cell Stem Cell*. 2018;22(1):78-90.e4. doi:10.1016/j.stem.2017.11.020
183. Thorel F, Népote V, Avril I, et al. Conversion of adult pancreatic α -cells to B-cells after extreme B-cell loss. *Nature*. 2010;464(7292):1149-1154. doi:10.1038/nature08894
184. Chung CH, Hao E, Piran R, Keinan E, Levine F. Pancreatic β -cell neogenesis by direct conversion from mature α -cells. *Stem Cells*. 2010;28(9):1630-1638. doi:10.1002/stem.482
185. van der Meulen T, Mawla AM, DiGruccio MR, et al. Virgin Beta Cells Persist throughout Life at a Neogenic Niche within Pancreatic Islets. *Cell Metab*. 2017;25(4):911-926.e6. doi:10.1016/j.cmet.2017.03.017
186. Li W, Cavelti-Weder C, Zhang Y, et al. Long-term persistence and development of induced pancreatic beta cells generated by lineage conversion of acinar cells. *Nat Biotechnol*. 2014;32(12):1223-1230. doi:10.1038/nbt.3082
187. Cavelti-Weder C, Li W, Zumsteg A, et al. Hyperglycaemia attenuates in vivo reprogramming of pancreatic exocrine cells to beta cells in mice. *Diabetologia*. 2016;59(3):522-532. doi:10.1007/s00125-015-3838-7
188. Bensley RR. Studies on the pancreas of the guinea pig. *Am J Anat*. 1911;12(3):297-388.
189. Laguesse E. Le pancréas. *Rev Générale d'Histologie*. 1906;2:3.
190. Piper K, Brickwood S, Turnpenny LW, et al. Beta cell differentiation during early human pancreas development. *J Endocrinol*. 2004;181(1):11-23.
191. Bonner-Weir S, Taneja M, Weir GC, et al. In vitro cultivation of human islets from expanded ductal tissue. *Proc Natl Acad Sci U S A*. 2000;97(14):7999-8004. doi:10.1073/pnas.97.14.7999
192. Suarez-Pinzon WL, Lakey JRT, Brand SJ, Rabinovitch A. Combination therapy with epidermal growth factor and gastrin induces neogenesis of human islet β -cells from pancreatic duct cells and an increase in functional β -cell mass. *J Clin*

- Endocrinol Metab.* 2005;90(6):3401-3409. doi:10.1210/jc.2004-0761
193. Swartz FJ, Carstens PHB, Swartz FJ. Histology and Histopathology An islet of Langerhans located within the epithelium of a human pancreatic duct* " 1981;986(1):17. [https://digitum.um.es/xmlui/bitstream/10201/17813/1/An islet of Langerhans located within the epithelium of a human pancreatic duct.pdf](https://digitum.um.es/xmlui/bitstream/10201/17813/1/An%20islet%20of%20Langerhans%20located%20within%20the%20epithelium%20of%20a%20human%20pancreatic%20duct.pdf).
 194. Asfaha S, Hayakawa Y, Muley A, et al. Krt19+/Lgr5- Cells Are Radioresistant Cancer-Initiating Stem Cells in the Colon and Intestine. *Cell Stem Cell.* 2015;16(6):627-638. doi:10.1016/j.stem.2015.04.013
 195. Zhang L, Theise N, Chua M, Reid LM. The stem cell niche of human livers: Symmetry between development and regeneration. *Hepatology.* 2008;48(5):1598-1607.
 196. Bonner-Weir S, Baxter LA, Schuppin GT, Smith FE. A second pathway for regeneration of adult exocrine and endocrine pancreas: A possible recapitulation of embryonic development. *Diabetes.* 1993;42(12):1715-1720. doi:10.2337/diab.42.12.1715
 197. Li WC, Rukstalis JM, Nishimura W, et al. Activation of pancreatic-duct-derived progenitor cells during pancreas regeneration in adult rats. *J Cell Sci.* 2010;123(16):2792-2802. doi:10.1242/jcs.065268
 198. Martin-Pagola A, Sisino G, Allende G, et al. Insulin protein and proliferation in ductal cells in the transplanted pancreas of patients with type 1 diabetes and recurrence of autoimmunity. *Diabetologia.* 2008;51(10):1803-1813. doi:10.1007/s00125-008-1105-x
 199. Criscimanna A, Speicher JA, Houshmand G, et al. Duct cells contribute to regeneration of endocrine and acinar cells following pancreatic damage in adult mice. *Gastroenterology.* 2011;141(4):1451-1462. doi:10.1053/j.gastro.2011.07.003
 200. Rovira M, Scott S-G, Liss AS, Jensen J, Thayer SP, Leach SD. Isolation and characterization of centroacinar/terminal ductal progenitor cells in adult mouse pancreas. *Proc Natl Acad Sci U S A.* 2010;107(1):75-80.
 201. El-Gohary Y, Wiersch J, Tulachan S, et al. Intra-islet Pancreatic Ducts Can Give Rise to Insulin-Positive Cells. *Endocrinology.* 2016;157(1):166 –175.
 202. Zhang M, Lin Q, Qi T, et al. Growth factors and medium hyperglycemia induce Sox9+ ductal cell differentiation into β cells in mice with reversal of diabetes. *Proc Natl Acad Sci U S A.* 2016;113(3):650-655. doi:10.1073/pnas.1524200113
 203. Solar M, Cardalda C, Houbracken I, et al. Pancreatic Exocrine Duct Cells Give Rise to Insulin-Producing β Cells during Embryogenesis but Not after Birth. *Dev Cell.* 2009;17(6):849-860. doi:10.1016/j.devcel.2009.11.003
 204. Gribben C, Lambert C, Messal HA, et al. Ductal Ngn3-expressing progenitors contribute to adult β cell neogenesis in the pancreas. *Cell Stem Cell.*

- 2021;28(11):2000-2008.e4. doi:10.1016/j.stem.2021.08.003
205. Zhou Q, Law AC, Rajagopal J, Anderson WJ, Gray PA, Melton DA. A Multipotent Progenitor Domain Guides Pancreatic Organogenesis. *Dev Cell*. 2007;13(1):103-114. doi:10.1016/j.devcel.2007.06.001
 206. Al-Hasani K, Pfeifer A, Courtney M, et al. Adult duct-lining cells can reprogram into β -like cells able to counter repeated cycles of toxin-induced diabetes. *Dev Cell*. 2013;26(1):86-100. doi:10.1016/j.devcel.2013.05.018
 207. Sancho R, Gruber R, Gu G, Behrens A. Loss of Fbw7 Reprograms Adult Pancreatic Ductal Cells into α , δ , and β Cells. *Cell Stem Cell*. 2014;15(2):139-153.
 208. Chera S, Baronnier D, Ghila L, et al. Diabetes recovery by age-dependent conversion of pancreatic δ -cells into insulin producers. *Nature*. 2014;514(7253):503-507. doi:10.1038/nature13633
 209. Wang D, Wang J, Bai L, et al. Long-Term Expansion of Pancreatic Islet Organoids from Resident Procr+ Progenitors. *Cell*. 2020;180(6):1198-1211.e19. doi:10.1016/j.cell.2020.02.048
 210. Westphalen CB, Takemoto Y, Tanaka T, et al. Dclk1 Defines Quiescent Pancreatic Progenitors that Promote Injury-Induced Regeneration and Tumorigenesis. *Cell Stem Cell*. 2016;18(4):441-455.
 211. Qadir MMF, Álvarez-Cubela S, Klein D, et al. P2RY1/ALK3-Expressing Cells within the Adult Human Exocrine Pancreas Are BMP-7 Expandable and Exhibit Progenitor-like Characteristics. *Cell Rep*. 2018;22(9):2408-2420. doi:10.1016/j.celrep.2018.02.006
 212. Ananthan B. Developing a model to assess the contribution of cytokeratin 19-expressing cells during multipotent stromal cell-induced islet regeneration. *Electron Thesis Diss Repos*. 2020;7330.
 213. Means AL, Xu Y, Zhao A, Ray KC, Gu G. A CK19CreERT knockin mouse line allows for conditional DNA recombination in epithelial cells in multiple endodermal organs. *Genesis*. 2008;46(6):318-323. doi:10.1002/dvg.20397
 214. Madisen L, Zwingman TA, Sunkin SM, et al. A robust and high-throughput Cre reporting and characterization system for the whole mouse brain. *Nat Neurosci*. 2010;13(1):133-140. doi:10.1038/nn.2467
 215. Grant CW, Duclos SK, Moran-Paul CM, et al. Comparative Medicine Development of Standardized Insulin Treatment Protocols for Spontaneous Rodent Models of Type 1 Diabetes. *Orig Res*. 2012;62(5):381-390.
 216. Stammberger I, Bube A, Durchfeld-Meyer B, Donaubaue H, Troschau G. Evaluation of the carcinogenic potential of insulin glargine (LANTUS) in rats and mice. *Int J Toxicol*. 2002;21(3):171-179. doi:10.1080/10915810290096306
 217. Ramzy A, Mojibian M, Kieffer TJ. Insulin-Deficient mouse b-Cells do not fully

- mature but can be remedied through insulin replacement by islet transplantation. *Endocrinology*. 2018;159(1):83-102. doi:10.1210/en.2017-00263
218. Bankhead P, Loughrey MB, Fernández JA, et al. QuPath: Open source software for digital pathology image analysis. *Sci Rep*. 2017;7(1):1-7. doi:10.1038/s41598-017-17204-5
 219. Dorrell C, Grompe MT, Pan FC, et al. Isolation of mouse pancreatic alpha, beta, duct and acinar populations with cell surface markers. *Mol Cell Endocrinol*. 2011;339(1-2):144-150. doi:10.1016/j.mce.2011.04.008
 220. Kim A, Miller K, Jo J, Kilimnik G, Wojcik P, Hara M. Islet architecture. *Diabetes Syst Biol*. 2020;1(2):129-136. doi:10.1088/978-0-7503-3739-7ch4
 221. Kharouta M, Miller K, Kim A, Wojcik P, Kilimnik G. No mantle formation in rodent islets – the prototype of islet revisited. 2010;85(3):252-257. doi:10.1016/j.diabres.2009.06.021.No
 222. Szkudelski T. The mechanism of alloxan and streptozotocin action in B cells of the rat pancreas. *Physiol Res*. 2001;50(6):537-546.
 223. Bensellam M, Laybutt DR, Jonas JC. The molecular mechanisms of pancreatic β -cell glucotoxicity: Recent findings and future research directions. *Mol Cell Endocrinol*. 2012;364(1-2):1-27. doi:10.1016/j.mce.2012.08.003
 224. Choi BY. Targeting Wnt/ β -Catenin Pathway for Developing Therapies for Hair Loss. *Int J Mol Sci*. 2020;21(14):4915.
 225. Girardi F, Grand F Le. Wnt Signaling in Skeletal Muscle Development and Regeneration. *Prog Mol Biol Transl Sci*. 2018;153:157-179.
 226. Huch M, Bonfanti P, Boj SF, et al. Unlimited in vitro expansion of adult bi-potent pancreas progenitors through the Lgr5/R-spondin axis. *EMBO J*. 2013;32(20):2708-2721. doi:10.1038/emboj.2013.204
 227. Sakhneny L, Rachi E, Epshtein A, et al. Pancreatic pericytes support β -cell function in a Tcf7l2-dependent manner. *Diabetes*. 2018;67(3):437-447. doi:10.2337/db17-0697
 228. Daniels Gatward LF, Kennard MR, Smith LIF, King AJF. The use of mice in diabetes research: The impact of physiological characteristics, choice of model and husbandry practices. *Diabet Med*. 2021;38(12):1-12. doi:10.1111/dme.14711
 229. Shultz LD, Schweitzer PA, Christianson SW, et al. Multiple defects in innate and adaptive immunologic function in NOD/LtSz-scid mice. *J Immunol*. 1995;154(1):180-191. <http://www.ncbi.nlm.nih.gov/pubmed/7995938>.
 230. Furman BL. Streptozotocin-Induced Diabetic Models in Mice and Rats. *Curr Protoc Pharmacol*. 2015;70(1):5.47.1-5.47.20. doi:10.1002/0471141755.ph0547s70
 231. Fergusson G, Éthier M, Guévremont M, et al. Defective insulin secretory response

- to intravenous glucose in C57Bl/6J compared to C57Bl/6N mice. *Mol Metab.* 2014;3(9):848-854.
232. Ahn SH, Granger A, Rankin MM, Lam CJ, Cox AR, Kushner JA. Tamoxifen suppresses pancreatic β -cell proliferation in mice. *PLoS One.* 2019;14(9). doi:10.1371/journal.pone.0214829
 233. Keeley TM, Horita N, Samuelson LC. Tamoxifen-Induced Gastric Injury: Effects of Dose and Method of Administration. *Cmgh.* 2019;8(3):365-367. doi:10.1016/j.jcmgh.2019.06.007
 234. Kanayama T, Tomita H, Binh NH, et al. Characterization of a BAC transgenic mouse expressing Krt19-driven iCre recombinase in its digestive organs. *PLoS One.* 2019;14(8):1-16. doi:10.1371/journal.pone.0220818
 235. Kasper M, von Dorsche HH, Stosiek P. Changes in the distribution of intermediate filament proteins and collagen IV in fetal and adult human pancreas - I. Localization of cytokeratin polypeptides. *Histochemistry.* 1991;96(3):271-277. doi:10.1007/BF00271547
 236. Alam CM, Baghestani S, Toivola DM. Intermediate Filament Keratins in The Exocrine Pancreas. 2020. doi:10.3998/panc.2020.02
 237. Zhong B, Zhou Q, Toivola D, Tao G, Resurreccion E, Omary M. Organ-specific stress induces mouse pancreatic keratin overexpression in association with NF- κ B activation. *J Cell Sci.* 2004;117(9):1709-1719.
 238. Byrnes LE, Wong DM, Subramaniam M, et al. Lineage dynamics of murine pancreatic development at single-cell resolution. *Nat Commun.* 2018;9(1):1-17. doi:10.1038/s41467-018-06176-3
 239. Valdez IA, Dirice E, Gupta MK, Shirakawa J, Teo AKK, Kulkarni RN. Proinflammatory Cytokines Induce Endocrine Differentiation in Pancreatic Ductal Cells via STAT3-Dependent NGN3 Activation. *Cell Rep.* 2016;15(3):460-470. doi:10.1016/j.celrep.2016.03.036
 240. Hendley AM, Rao AA, Leonhardt L, et al. Single-cell transcriptome analysis defines heterogeneity of the murine pancreatic ductal tree. *Elife.* 2021;10:1-29. doi:10.7554/eLife.67776
 241. Qadir MMF, Álvarez-Cubela S, Klein D, et al. Single-cell resolution analysis of the human pancreatic ductal progenitor cell niche. *Proc Natl Acad Sci U S A.* 2020;117(20):10876-10887. doi:10.1073/pnas.1918314117
 242. Öström M, Löffler KA, Edfalk S, et al. Retinoic acid promotes the generation of pancreatic endocrine progenitor cells and their further differentiation into β -cells. *PLoS One.* 2008;3(7):1-7. doi:10.1371/journal.pone.0002841
 243. Vieira A, Vergoni B, Courtney M, et al. Neurog3 misexpression unravels mouse pancreatic ductal cell plasticity. *PLoS One.* 2018;13(8). doi:10.1371/journal.pone.0201536

Appendices

Appendix 1. Supplementary Figures

A [Confocal video 1](#)

B [Confocal video 2](#)

C [Confocal video 3](#)

Supplementary Figure 1. Confocal z-stack imaging of islets from mice treated with Wnt+ CdM at **(A)** Day 21 and **(B)** Day 42. **(C)** Small insulin+ cluster from mouse treated with Wnt+ CdM at Day 21. Direct co-localization of tdTomato in insulin+ islet cells was observed. Green = insulin; Red = tdTomato; White = glucagon; Blue = DAPI. To play the videos, please click on the viewable links provided above.

Appendix 2. Human Ethics Approval



Date: 17 December 2021

To: David Hess

Project ID: 4050

Study Title: Transplantation of human stem cells for the induction of angiogenesis and the regeneration of beta-cell function (REB #12934)

Application Type: Continuing Ethics Review (CER) Form

Review Type: Delegated

Date Approval Issued: 17/Dec/2021

REB Approval Expiry Date: 19/Dec/2022

Dear David Hess,

The Western University Research Ethics Board has reviewed the application. This study, including all currently approved documents, has been re-approved until the expiry date noted above.

REB members involved in the research project do not participate in the review, discussion or decision.

Western University REB operates in compliance with, and is constituted in accordance with, the requirements of the Tri-Council Policy Statement: Ethical Conduct for Research Involving Humans (TCPS 2); the International Conference on Harmonisation Good Clinical Practice Consolidated Guideline (ICH GCP); Part C, Division 5 of the Food and Drug Regulations; Part 4 of the Natural Health Products Regulations; Part 3 of the Medical Devices Regulations and the provisions of the Ontario Personal Health Information Protection Act (PHIPA 2004) and its applicable regulations. The REB is registered with the U.S. Department of Health & Human Services under the IRB registration number IRB 00000940.

Please do not hesitate to contact us if you have any questions.

Sincerely,

The Office of Human Research Ethics

Note: *This correspondence includes an electronic signature (validation and approval via an online system that is compliant with all regulations).*

Appendix 3. Animal Ethics Approval

2018-184:6:

AUP Number: 2018-184

AUP Title: Transplantation of Novel Stem Cells for the Regeneration of B-Cell Function

Yearly Renewal Date: 05/01/2023

The **annual renewal** to Animal Use Protocol (AUP) 2018-184 has been approved by the Animal Care Committee (ACC), and will be approved through to the above review date.

Please at this time review your AUP with your research team to ensure full understanding by everyone listed within this AUP.

As per your declaration within this approved AUP, you are obligated to ensure that:

1. This Animal Use Protocol is in compliance with:
 - [Western's Senate MAPP 7.12 \[PDF\]](#); and
 - [Applicable Animal Care Committee policies and procedures](#).
2. Prior to initiating any study-related activities—[as per institutional OH&S policies](#)—all individuals listed within this AUP who will be using or potentially exposed to hazardous materials will have:
 - Completed the appropriate institutional OH&S training;
 - Completed the appropriate facility-level training; and
 - Reviewed related (M)SDS Sheets.

Submitted by: McInnis, Jennifer on behalf of the Animal Care Committee

Dr. Rob Gros,
Animal Care Committee Chair

Curriculum Vitae

Name: Nazihah Rasiwala

Post-secondary Education and Degrees: University of Western Ontario
London, Ontario, Canada
2015-2020 Bachelor of Medical Sciences, Honours Specialization in Interdisciplinary Medical Sciences

The University of Western Ontario
London, Ontario, Canada
2020-2022 M.Sc. Physiology and Pharmacology

Honours and Awards: 2020 Physiology and Pharmacology Research Day
New Student Poster Award
The University of Western Ontario
London, Ontario, Canada

2021 Till and McCulloch Meetings
Poster Award in Basic Science Research

2020-2022 Western Graduate Research Scholarship

Related Work Experience Graduate Research Associate
Dr. David Hess's lab, Robarts Research Institute,
Physiology and Pharmacology
The University of Western Ontario
2020-2022

Teaching Assistant
Department of Physiology and Pharmacology
The University of Western Ontario
2020-2022

Student Research Intern (via Western Science Internship Program)
Analytical Chemistry R&D Department, Parmalat Canada Inc.
2018-2019